UNIVERSITY OF CALIFORNIA, IRVINE

Deciphering the mechanism of TDP2/VPg unlinkase activity during picornavirus infections

DISSERTATION

Submitted in partial satisfaction of the requirements for the degree of

DOCTOR OF PHILOSOPHY

in Biomedical Sciences

by

Autumn Candace Holmes

Dissertation Committee:

Dr. Bert L. Semler, Chair
Dr. Paul Gershon
Dr. Michael McClelland
Dr. Suzanne Sandmeyer

2019

TABLE OF CONTENTS

LIST OF FIGURES

LIST OF TABLES

ACKNOWLEDGMENTS

I would like to acknowledge my thesis advisor Dr. Bert L. Semler for his guidance, mentorship, intellectual rigor, and support during my time in the PhD program. Having an excellent mentor makes all the difference in graduate school.

I would like to also acknowledge my current and former lab mates, Dr. Alexis Bouin, Michelle Vu, Dr. Wendy Ullmer, Dr. Dylan Flather, Dr. Eric Baggs, and Dr. Sonia Maciejewski for their collegiality and camaraderie in the lab. I also appreciate our scientific discussions and their critical review of my work.

Additionally, I would like to thank my dissertation committee, Dr. Paul Gershon, Dr. Michael McClelland, and Dr. Suzanne Sandmeyer for their keen scientific insights, which helped to drive my thesis project forward.

I would also like to acknowledge my collaborators on this project, Dr. Keith Caldecott, Dr. George Belov, and Dr. Eckard Wimmer for critical reagents they generously provided.

Finally, I would like to acknowledge my mother, Carol, my sister, Cheyna, and my fiancée, Damen for their love and support on this journey. It has meant the world to me.

CURRICULUM VITAE

Autumn C. Holmes

EDUCATION:

2013-2019 PhD, Biomedical Sciences, University of California, Irvine (UC Irvine)

2008-2012 B.S., Microbiology, (Spanish minor), University of Michigan, Ann Arbor

HONORS AND AWARDS:

March 2018	American Society for Virology Travel Award
February 2018	UC Irvine School of Medicine Dr. Lorna Carlin Scholar Fellowship
June 2015	AAAS/Science Program for Excellence in Science
March 2015	National Institutes of Health (NIH) Diversity Supplement Award
March 2015	National Science Foundation Graduate Research Fellowship Program (Honorable Mention)
March 2015	Ford Foundation Fellowship Program (Honorable Mention)
October 2014	Initiative for Maximizing Student Development-Minority Biomedical Research Support Program Training Grant (NIH-funded)
March 2015	Ford Foundation Fellowship Program (Honorable Mention)
February 2013	UC Irvine Graduate Dean's Recruitment Fellowship
March 2011	University of Michigan University Honors
September 2008	University of Michigan Tradition Scholarship

PROFESSIONAL ASSOCIATIONS

2017-present	American Society for Virology
2015-2018	AAAS (General Membership)
2014-2016	American Society for Microbiology
2014-present	Graduate Women in Science (Orange County, CA Chapter)

RESEARCH EXPERIENCE

UC Irvine, Department of Microbiology and Molecular Genetics

June 2014 – September 2019

Principal Investigator: Bert L. Semler, PhD

University of Rochester Post-baccalaureate Research and Education Program (PREP), Department of Microbiology and Immunology

July 2012 – June 2013

Principal Investigator: Luis Martinez-Sobrido, PhD

Research Focus: Characterizing the interaction between the nucleoprotein and Z matrix protein of arenaviruses

University of Michigan Medical School, Department of Human Genetics and Internal Medicine

September 2011 – June 2012

Principal Investigator: David Ginsburg, MD

Research Focus: Testing small molecule inhibitors for the treatment of antibiotic-resistant Group A Streptococcus

PUBLICATIONS

Autumn C. Holmes and Bert L. Semler. Picornaviruses and RNA Metabolism: Local and Global Effects of Infection. *Journal of Virology.* (In press)

Autumn C. Holmes, Guido Zagnoli Vieira, Fernando Gomez-Herreros, Keith W. Caldecott, and Bert L. Semler. Post-translational effects of VPg unlinkase activity during picornavirus infections of human cells. (In prep)

Bryan D. Yestrepsky, Colin A. Kretz, Yuanxi Xu, **Autumn C. Holmes**, Hongmin Sun, David Ginsburg, Scott D. Larsen. Development of tag-free photoprobes for studies aimed at identifying the target of novel Group A Streptococcus antivirulence agents. *Bioorg. Med. Chem. Lett.* 24**,** 1538–1544 (2014).

PRESENTATIONS AND CONFERENCES

July 2019 American Society for Virology Meeting, University of Minnesota (Oral Presentation)
July 2018 American Society for Virology Meeting, University of Maryland, College Park (Oral Presentation)
July 2017 International Union of Microbiological Societies (IUMS), Marina Bay Sands Conference Center, Singapore (Poster)
March 2016 Models of Infectious Disease Agent Study Meeting
May 2013 PREP program, University of Rochester (Poster)
October 2012 The Institute on Teaching and Mentoring

ABSTRACT OF THE DISSERTATION

Deciphering the mechanism of TDP2/VPg unlinkase

activity during picornavirus infections

By

Autumn Candace Holmes

Doctor of Philosophy in Biomedical Sciences

University of California, Irvine, 2019

Dr. Bert L. Semler, Chair

Members of the *Picornaviridae* family are responsible for many highly prevalent human illnesses. These include: the common cold, hepatitis, myocarditis, and paralytic poliomyelitis, which are caused by human rhinoviruses, hepatitis A virus, coxsackieviruses, and poliovirus, respectively. Given their limited coding capacity, picornaviruses must repurpose host factors to carry out their replication cycles. One such host protein is the DNA repair enzyme, tyrosyl-DNA phosphodiesterase 2 (TDP2), also known as VPg unlinkase. Picornaviruses use TDP2 to cleave the bond between viral genomic RNA and VPg, the primer for RNA synthesis that is covalently linked to the 5' end of virion RNA. Notably, viral RNA destined for RNA packaging must be VPg-linked, while VPg is absent from polysome-associated viral mRNAs and positive-strand RNA templates used to prime negative-strand RNA synthesis. Previous studies in cultured murine cells have revealed a significant dependence on TDP2 during

infection by poliovirus, coxsackievirus, or human rhinovirus. However, the precise biological consequences of VPg removal during picornavirus infections of human cells are unknown.

To determine the impact of TDP2 removal of VPg during picornavirus infections of human cells, we first established a human retinal pigment epithelial (RPE) cell model for the study of viral replication in the absence of TDP2. We then determined if premature encapsidation occurs in the absence of TDP2 VPg unlinkase activity. Finally, we assessed virus translation in wild type (WT) and knock-out (KO) TDP2 RPE cells by polysome analysis. We found that titers of either poliovirus or coxsackievirus B3 are reduced by 1-2 log10 units in the absence of TDP2 in human RPE cells and that this effect is multiplicity of infection-dependent. We also demonstrated that premature encapsidation is not responsible for the virus growth defect observed in the absence of TDP2. Finally, we determined that viral RNA is actively translated in both WT and KO TDP2 RPE cells at early times of infection. Additionally, we found that TDP2 is relocalized from the nucleus to the cytoplasm in a panel of cell lines and colocalizes with poliovirus structural protein, VP1 in the nucleus of MCF7 cells. Finally, we found that virion RNA that has been treated with proteinase K (which degrades VPg), acts as a more efficient template for both positive and negative strand RNA synthesis. From these data, we conclude that TDP2 is an important host cell factor for picornavirus infections of human cells and that TDP2 removal of VPg from viral RNA at early times during infection is involved in step(s) other than translation or encapsidation, a likely candidate being RNA synthesis.

CHAPTER 1

Introduction

Summary

The *Picornaviridae* are a large family of viruses that infect both humans and wildlife. They are highly abundant and have a global distribution. As is typical for any virus, picornaviruses engage in complex interactions with their host cell in order to replicate, employing numerous strategies to commandeer the host's molecular machinery. Although the evolutionary arms race between virus and host is unremittent, the ways in which picornaviruses overtake the host cell, in turn, provide molecular targets to be exploited for the development of novel anti-viral therapeutics. For this undertaking to be carried out, however, it follows that the mechanisms which underpin these targets must be elucidated. This Introduction chapter puts into context the biological basis for the study of such a mechanism involving the cellular DNA repair enzyme, tyrosyl-DNA phosphodiesterase 2 (TDP2) during the picornavirus replication cycle, which is the focus of this thesis.

Significance: Diversity and severity of human illnesses caused by picornaviruses

Picornaviruses are responsible for many highly prevalent human diseases worldwide. These include but are not limited to: poliomyelitis, the common cold, hepatitis, and myocarditis, which are caused by poliovirus, human rhinoviruses (HRV), hepatitis A virus, and coxsackievirus (CVB), respectively. The family also contains several other members in addition to poliovirus (e.g., CVA group viruses, enterovirus D68 [EV-D68], enterovirus 71 [EV-71], and certain echovirus species) which are also neurovirulent and are responsible for additional neurological manifestations of disease such as meningitis and encephalitis. Although immunocompetent individuals typically experience self-limiting illnesses, children, the elderly, and those who are immunocompromised are at a higher risk for more severe disease. This observation is particularly important in the context of HRV and of the resurgent picornavirus, EV-D68, which will be discussed in further detail below.

Respiratory disease caused by HRV and EV-D68. The range of human illnesses caused by picornaviruses span from upper respiratory infections to neurological disease. In the case of the former, ~25-50% of the upper airway infections colloquially referred to as the "common cold" are caused by the picornavirus, HRV (6). As indicated above, infections with HRV usually result in relatively mild illnesses for otherwise healthy individuals. However, for those with pre-existing respiratory conditions such as asthma or chronic obstructive pulmonary disease, both of which are highly prevalent globally (World Health Organization and American Academy of Allergy, Asthma, and Immunology factsheets), infection with HRV can result in more serious health complications (165). Unfortunately, there are currently no vaccines or FDA-approved drugs available to treat HRV infections. This is due, in part, to the fact that HRV exists as hundreds of different serotypes within three different species classifications (HRV-A, HRV-B, and HRV-C). This feature of the virus results in a broad antigenic diversity within the proteins that are antibody-accessible (i.e. structural proteins),

thus making it difficult to generate a pan-HRV vaccine (60). Moreover, as mentioned previously, because HRV, like all viruses, uses its host's cellular machinery to carry out its replication cycle, designing treatments that inhibit the virus without off-target effects that harm the host also continues to be a challenge. Additionally, outside of the biological realm, the economic cost of missed work by individuals who contract upper airway infections caused by HRV or who must stay at home to care for a sick child cannot be understated. Indirect costs are estimated at a loss of ~$25 billion/year in sick time (22, 76).

In addition to the common cold, early-life infections with HRV have also been speculated to be a potential inciting stimulus for the development of asthma later in life (13, 45, 89, 155). HRV is postulated to contribute to the phenomenon of airway remodeling (AR), which is a key feature of asthma. AR is broadly defined by the following: abnormal mucus cell infiltration of the bronchial tube, increased bronchial smooth muscle thickness, subepithelial fibrosis, increased neurite sprouting, increased angiogenesis (104), and bronchial barrier dysfunction (44), all of which ultimately result in the diminished lung function observed in asthma patients. HRV is thought to contribute to AR in several ways. The first is that the virus has been shown stimulate the epithelial-to-mesenchymal transition (EMT) in bronchial epithelial cell culture (121). This observation is significant because EMT has also been associated with asthma *in vivo*, resulting in increased numbers of myofibroblasts and epithelial basement membrane thickening (107). Another way that HRV is suspected to trigger AR is through the activation of airway smooth muscle cells. Specifically, HRV-infected bronchial epithelial cell homogenates have been shown to induce chemotaxis of smooth muscle cells, a process which is likely mediated by the chemoattractant CCL5 (160). Finally, HRV infection has been shown to upregulate the production of AR-associated factors in human lung fibroblasts and airway epithelial cells, namely VEGF and TGF-β (98, 196), which are considered to be major contributors to the abnormal vascularization of the bronchial wall

(164). While the connection between HRV and the development of asthma is far from resolved, it is clear there is fertile ground for research in this area and understanding how the virus replicates and which factors are involved will help to continue shedding light on the putative connection.

HRV is not the only picornavirus that occurs as a co-morbidity with asthma. In recent years, there has been an upsurge of acute respiratory infections in children caused by EV-D68 (88, 119), a picornavirus that was previously detected with only sporadic incidence. During the highly publicized 2014 outbreak of the virus in the United States, a large-scale epidemiological study found that over half of the patients hospitalized for respiratory symptoms such as shortness of breath, wheezing, cough, and fever and who had a confirmed case of EV-D68, also had a history of asthma or other reactive airway disease (120). Notably, despite the consensus on the status of HRV as an exacerbator of asthma, compared with HRV-infected children, children infected with EV-D68 had an even higher likelihood of having prior asthma history (51). This suggests that there may be unique features of EV-D68 respiratory infection (either in the mechanisms of virus replication or immune responses to the virus) that might synergize with the airway hyperresponsiveness observed in asthmatics. However, given the previous obscurity of EV-D68, this question remains an active area of research.

One preliminary possibility is that EV-D68 has been shown to significantly increase the levels of IL-17 production by –RORγt+NKp46– type 3 innate lymphoid cells during infection of mice compared to HRV-A1B infection (144). Concordantly, in the same study, IL-17 mRNA expression was shown to be significantly upregulated in the nasopharyngeal swabs of EV-D68-infected patients, compared to the levels induced in those with HRV-A1B infection. Moreover, EV-D68 infection in mice also resulted in increased neutrophil infiltration in the lungs than did HRV-A1B infection. This observation is also consistent with the increase in IL-

17 production given that it is a neutrophil chemoattractant (144). Importantly, IL-17 has been associated with severe asthma, as a Th17-driven, steroid-resistant pathogenic pathway has been identified (33). Taken together, these data present a first glimpse into the immune response differences between EV-D68 and HRV and implicate EV-D68 as perhaps an even more significant contributor to the pathogenesis of asthma than HRV.

CVA/B and EV71 interactions with microRNA (miRNA): insights into mechanisms of pathogenesis. Both CVA group viruses and EV71 are significant causes of central nervous system (CNS) infections. One pathogenic mechanism that is becoming increasingly appreciated in the field is viral manipulation of host cell miRNA. For example, it was recently demonstrated that the miRNA, miR-1303, is likely involved in regulating blood-brain barrier permeability during CVA16 infection (166). Specifically, miR-1303 was shown to be downregulated during either CVA16 or EV71 infection compared to mock-infected controls, and that matrix metalloprotease 9 (MMP9) is a target of miR-1303. As such, using both *in vitro* experiments, and *in vivo* experiments with rhesus monkeys, these studies showed that CVA16 upregulates MMP9 during infection, which leads to the decreased expression of cell junction proteins, including claudin5, VE-cadherin, and ZO-1, increasing the permeability of the blood-brain barrier. This result was reversed *in vitro* by overexpressing miR-1303. Histological analysis also revealed damage to the thalamus of infected monkeys compared to mock-infected controls. Altogether, these results suggest that miR-1303 and MMP9 form a regulatory network that CVA16 (and perhaps EV71) exploits to invade the CNS. Other investigators have shown that several other miRNAs, including miR-3473a (201) and miR‑206 (207), may also be involved in modulating CNS injury during EV71 infection via control of focal adhesion assembly and leukocyte migration, and upregulation of the chemokine CCL2 promoting inflammation of the CNS, respectively.

The role of miRNAs in coxsackievirus pathogenesis is not limited to neurological disease. For example, coxsackieviruses have also been implicated in the development of type I diabetes (82). There are several prevailing hypotheses about the possible pathogenic mechanisms of the virus in this disease, and viral interactions with miRNAs have been identified as having potential roles. Engelmann and colleagues (42) showed that persistent CVB4 infection in human pancreatic cells results in the dysregulation of a panel of 81 miRNAs. Moreover, using miRNA target prediction software, the group identified 49 known type I diabetes risk genes as potential targets of one or more of the dysregulated miRNAs, suggesting a link between miRNA expression profile changes elicited by persistent CVB4 and the risk for developing type I diabetes. In support of this proposition, Kim *et al*. (93) reported that acute CVB5 infection results in the dysregulation of 33 miRNAs in infected human pancreatic β islet cells and that 57 putative type I diabetes risk genes were predicted targets for the identified miRNAs. Determining the key gene expression changes that are sustained after coxsackievirus infection and/or maintained during persistent infection will be critical for elucidating the mechanisms by which these viruses might contribute to the development of type I diabetes.

Persistent coxsackievirus infections are also a significant cause of viral myocarditis, and miRNA profiling has been carried out in this disease context as well to uncover how the virus damages the heart during infection. Several recent studies have identified miRNAs that are associated with the outcome of virus-induced cardiac injury, and these miRNAs involve both the innate and adaptive immune responses. MiR-214 was shown to be upregulated in tissues from the hearts of patients with CVB3-induced myocarditis. This miRNA represses the expression of ITCH, an E3 ligase and a repressor in its own right of NF-κB (32). MiR-214 repression of ITCH was shown to cause the upregulation of several cytokines activated by the NF-κB pathway, including TNF α and IL-6, suggesting that viral modulation of miR-214

might contribute to the inflammatory tissue microenvironment of acute myocarditis. Contrasting with these results, Bao and Lin (9) found that miR-155, which is also upregulated in patients with myocarditis caused by CVB3, acts as a negative regulator of the NF-κB pathway through the targeting of RelA, a subunit of NF-κB. Interestingly, miR-155 was also shown to have pro-inflammatory effects during CVB3 myocarditis in mice, resulting in the infiltration of macrophages and T lymphocytes to the infection site (35). Conversely, knockdown of miR-155 improved infected mice survival and cardiac function (35). TH-17 cells particularly have been shown to contribute to the pathology of viral myocarditis in mice (109), and Liu *et al*. found that inhibiting both miR-21 and miR-146b reduces the production of TH-17-associated markers such as IL-17, IL-6, TGF-β, and RORγt. Downregulating these two miRNAs reduced cardiac injury in CVB3-infected mice and a decrease in the proportion of TH-17 cells harvested from the spleens of CVB3-infected, miRNA inhibitor-treated mice.

As a key mediator of both innate and adaptive immunity, type I interferon has been shown to have interactions with miRNAs that have significant consequences for the outcome of picornavirus infections. Ho and colleagues showed that EV71 upregulates miR-146a through the activity of activating protein-1 (AP-1), a dimeric transcription factor consisting of Jun, Fos, or other factors (14) and that this upregulation reduces the expression of the Toll-like receptor signaling molecules IRAK1 and TRAF6 (80). Moreover, the authors demonstrated that treating both EV71-infected mouse embryonic fibroblast cell lines and live mice with a lnc-RNA-based miR-146a antagomir resulted in restored IRAK1 and TRAF6 expression, improved mouse survival, and importantly, restored IFN-β production (80). These data suggest a novel mechanism by which miR-146a expression is achieved by EV71 activation of the c-Jun kinase pathway, which consequently downregulates and weakens immune responses to viral infection, allowing for viral innate immune escape.

The above-described findings underscore the importance of understanding the mechanisms by which picornaviruses hijack host miRNA pathways and how this contributes to virus pathogenesis. Critically, the data also highlight the possibility of miRNA and/or antagomir-based antivirals to treat picornavirus infections.

Harnessing picornavirus pathogenesis: putative molecular mechanisms governing success of chimeric polio/HRV2 virus as a cancer therapeutic. PV1(RIPO) is a chimeric virus consisting of the poliovirus type 1 (Mahoney strain) coding region and the HRV2 non-coding region (NCR) that grows to high titers in grade IV malignant glioma-derived cell lines, but, importantly, is attenuated in normal neuronal tissues (69, 70). When injected into mice bearing glioma xenografts, PV1(RIPO) halted tumor progression or eliminated the tumor entirely (71). As such, a variant of this virus, PVS(RIPO), which utilizes the live, attenuated Sabin poliovirus type 1 coding region, has recently demonstrated promise in Phase I clinical trials for treatment of patients with recurrent glioblastoma (37).

Despite its success as a treatment, the exact molecular mechanisms governing the difference between the PVS/1(RIPO) growth phenotype in normal vs. malignant brain tissues have only recently begun to be elucidated. The growth-suppressive element of PV1(RIPO) was mapped to of the HRV2 5' NCR (70, 118) An RNA affinity chromatography screen identified double-stranded RNA binding protein, DRBP76, as a critical restrictive host factor for PV1(RIPO) exclusively in non-malignant neuronal cells (118). Intriguingly, the protein is also present in glioma-derived cells, although the subcellular distribution is distinct (118). These observations suggest that cell-type specific differences control the availability and/or capability of DRBP76 to bind to the HRV2 5' NCR (118).

Polypyrimidine tract binding protein (PTBP1) is a nuclear-cytoplasm shuttling protein that is hijacked by picornaviruses to carry out their replication cycles (176, 203) and is also a key determinant of viral neurovirulence (72, 139) and neurotropism (90). Particularly,

overexpression of PTBP1 in SK-N-MC neuroblastoma cell lines has been shown to enhance replication of PV1(RIPO).Therefore, since PTBP1 confers the ability of PV1(RIPO) to replicate in cells of neuronal origin and other non-permissive cell lines (i.e., mouse L20B cells) and is up-regulated in several cancers, including glioblastoma (3) , and given the status of DRBP76 as a restrictive host factor, it is tempting to speculate that PTBP1 might compete for binding with DRBP76 to the 5' NCR of HRV2. As such, competitive binding between DRBP76 and PTBP1 may be a potential mechanism for the growth-restricted phenotype observed for the PV1(RIPO) virus.

Additional studies have also demonstrated that PVS(RIPO) permissiveness is mediated by the activity of MAPK signal-integrating kinase 1 and the MAPK signaling pathway (23, 61), which is also frequently up-regulated in cancer (151), viral subversion of the innate immune response in cancer cells (189), and virus-induced antitumor T cell responses (24). Moreover, as PV1/S(RIPO) is increasingly being demonstrated to be an effective cytolytic agent against other types of cancer, including breast and prostate cancer (83), the importance of uncovering the underlying mechanisms of replication for this powerful chimeric virus cannot be overstated. Ultimately, the elucidation of these specialized mechanisms requires an understanding of the basic replication processes that are utilized by picornaviruses, which will be outlined in the following sections.

Picornavirus translation and RNA synthesis, role of VPg, and its differential linkage to viral RNA during the picornavirus replication cycle

Though relatively short in duration, the picornavirus replication cycle involves a series of highly complex and coordinated molecular events. The family has been classified into 29 genera (195) with the *Enterovirus* genus being the focus of this thesis. The picornavirus virion particle consists of a non-enveloped, icosahedral capsid with T=3 symmetry which encases

the positive-sense, single-stranded, linear RNA genome. The genome is monopartite and is between ~7 and 9 kb in length depending on the picornavirus species. The replication cycle begins as is typical for most positive-stranded RNA viruses, with immediate translation of the RNA into viral protein upon deposition of the genome into the cell cytoplasm. Translation occurs via an Internal Ribosome Entry Site (IRES)-mediated mechanism, as these viruses lack a 7-methylguanosine (7mG) cap structure at the 5' end of the genomic RNA. The viral RNA also encodes a poly(A) tract at the 3' end, which is thought to mediate ribonucleoprotein complex (RNP) complex formation and circularization of the RNA to facilitate both translation and RNA synthesis (78). As illustrated in Figure 1, the viral mRNA produces 3 polyprotein precursors termed P1, P2, and P3, which are proteolytically processed into both intermediate products and the mature viral proteins. Importantly, some precursor molecules also have their own specific functions in the viral life cycle. Highlights of the mature proteins that are produced include the RNA-dependent RNA polymerase (RdRp) $3D^{pol}$; the non-structural proteins, 2B and 3A, which are involved in replication complex formation; the viral proteinases, $2A^{pro}$ and $3C^{pro}$, which direct cleavage of the viral polyprotein in addition to cleavage of host cell proteins [most notably the $2A^{pro}$-mediated cleavage of the eukaryotic initiation factor, eIF4G, which induces a dramatic shut-off of host cap-dependent translation (12)]; the structural proteins, VP1-4, which make up the capsid; and, of particular relevance to the current thesis, the small polypeptide 3B, or VPg (Virus Protein, genome-linked).

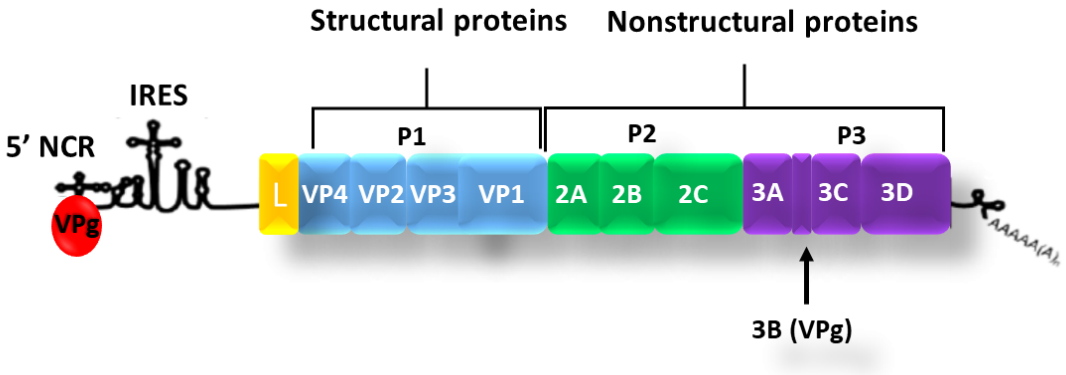

Figure 1.1: The picornavirus genome. Genome elements in order from left to right: 5' Non-coding region (NCR), which contains the cloverleaf structure which is essential for viral RNA synthesis; the Internal Ribosomal Entry Site (IRES) which drives cap-independent virus translation; L (leader) protein found in members of the *Cardiovirus* genus; Structural proteins, VP1-VP4 that form the capsid; Non-structural proteins, 2A-3D^{pol}; 3' NCR; virally-encoded poly(A) tail. VPg is bound at the 5' end of the viral RNA. The initial polyprotein is cleaved into 3 precursor proteins termed P1, P2, and P3.

Mechanisms of picornavirus translation and RNA synthesis: involvement of host cell factors, template usage switching, and replication organelle biogenesis. To carry out translation of the positive-sense RNA template, picornaviruses, including poliovirus, HRV, and CVA/B species take advantage of several key host proteins, namely the poly(rC)-binding proteins 1 and 2 (PCBP1 and PCBP2, also known as hnRNP E1 and hnRNP E2). These proteins normally function in RNA stability, regulation of translation, and transcriptional regulation in uninfected host cells (114). Picornaviruses hijack PCBP1/2 and use them as IRES trans-acting factors (ITAFs) to promote virus translation in a non-canonical, 7mG cap-independent manner. PCBP1/2 forms an RNP complex with a major stem-loop (SL) structure, called SL-IV, within the viral IRES (19, 20). PCBP1 and PCBP2 also bind to two C-rich sequences within the first ~100 nucleotides of the 5' NCR to promote viral RNA replication (54, 56, 132, 175) However, there are differences in the affinities of PCBP1 and 2 for poliovirus SL-IV, with PCBP2 having a 50-fold higher binding affinity than PCBP1 (158, 188). This differential affinity was shown to be mediated by the linker region between the second and third K-homologous (KH) domains of PCBP2 (158). Moreover, it has been demonstrated that only PCBP2, and not PCBP1, can rescue *in vitro* translation of poliovirus genomic RNA in PCBP-depleted HeLa S10 extracts (188). This result, together with the observation that several other picornavirus IRESs including those of EV71 (106) bovine enterovirus (173), CVB3 (187), HRV (187), and hepatitis A virus (206), either require PCBP2 to drive translation and/or the protein has been shown to bind to the IRES, supports the conclusion that PCBP2 plays a critical role in facilitating picornavirus IRES translation.

As noted above, PCBP2 (as well as PCBP1) also binds to sequences within the first ~100 nucleotides of the poliovirus 5' NCR that form a cloverleaf-like structure also called SL-I (56, 132). The viral proteinase-polymerase precursor protein 3CD binds to a distinct sequence element within SL-I to form a ternary complex with PCBP1/2 and a shift in the

occupancy of PCBP2 from SL-IV to SL-I, which reduces the levels of virus translation and promotes negative strand RNA synthesis (52, 54, 55, 163, 188) This is important to note because a crucial challenge of any positive-stranded RNA virus, including the picornaviruses, is to balance the use of the positive-strand RNA for translation versus negative strand RNA synthesis, as both processes cannot occur simultaneously on the same RNA template (10, 55). One possible activity that resolves this biological challenge is the cleavage of PCBP2 by the viral 3CD proteinase during poliovirus infection, which has been proposed as a mechanism to mediate the switch between virus translation and RNA replication in this family of viruses (30, 138). Specifically, the protein is cleaved between the KH2 and KH3 domains, producing a truncated form of PCBP2 lacking the KH3 domain. Cleaved PCBP2 does not bind to the viral IRES but retains its ability to form the replication-competent, ternary complex with the 5' cloverleaf RNA structure, suggesting that removal of this key RNA binding domain facilitates the switch. In addition, the critical interactions that occur between PCBP1/2 at the 5' end and poly(A) binding protein (PABP) at the 3' end suggest a possible mechanism in which circularization of the positive-strand RNA is required to facilitate viral translation and subsequently, negative strand RNA synthesis (11, 78). Once the switch is achieved, ribosomes clear from the positive sense RNA template and the primer for RNA synthesis, a uridylated VPg substrate (which will be discussed in further detail in the upcoming section), forms an RNP complex at the 3' end of the RNA to initiate the synthesis of negative strand RNA. This process results in the formation of what is known as the replicative form (RF) of the RNA, which consists of a double-stranded intermediate of plus-sense RNA template and the newly synthesized minus strand RNA (135).

Circularization of viral RNA has also been proposed to function in the priming of positive-strand RNA synthesis on the negative-strand template for picornaviruses, albeit via a different repertoire of host cell proteins than for negative-strand RNA synthesis (43, 152,

153). A critical factor involved in this mechanism is hnRNP C (25, 26). In the uninfected cell, hnRNP C functions as a splicing regulator, most notably acting to suppress the deleterious inclusion of Alu elements into mature gene transcripts (204). For picornaviruses, hnRNP C has been shown to bind separately to both the 5' and 3' terminal sequences of the negative strand RNA template, and binding may be dependent on multimerization of the protein (43). Accordingly, replication of viral RNA *in vitro* is enhanced by the addition of recombinant hnRNP C, and depletion of the protein in HeLa cells results in a decrease in positive strand RNA synthesis (25, 43). Replication kinetics are also delayed for poliovirus in cells expressing lower relative endogenous levels of hnRNP C, compared to those expressing higher endogenous levels (25). Collectively, these studies suggest a mechanism by which hnRNP C facilitates interactions between the 5' and 3' termini of viral RNA that are critical for positive strand RNA synthesis. While this is a proposed model, an important caveat to note is that binding of hnRNP C to both termini simultaneously has not yet been demonstrated. The difficulty in observing simultaneous binding of hnRNP C to the ends of viral RNA suggests that the interactions of hnRNP C with the RNA may be transient, are only needed to facilitate initiation of RNA synthesis, and do not need to be sustained throughout the elongation process. This would make the protein available to initiate the synthesis of multiple positive-strand RNAs on a single negative strand template, generating the well-characterized picornavirus replicative intermediate. Further studies in this area are needed to characterize the nature and composition of the hnRNP C-mediated protein complex. Furthermore, the formation of what is known as the replicative intermediate (RI) occurs during positive-strand RNA synthesis for picornaviruses. RI consists of one negative-strand RNA molecule templating the production of 6-8 molecules of nascent positive-sense strand RNA (135). This mechanism leads to the characteristic skewed ratio of positive:negative strand RNA (~40-70:1) that is observed during picornavirus infections, and ultimately contributes to the

exponential increase in virus particle production that occurs at mid-times during the infectious cycle.

Picornaviruses, like other positive-sense RNA viruses, remodel host cell membranes to form cytoplasmic replication organelles upon which both positive and negative-strand RNA synthesis occurs (41, 146). These membranous structures have been thought to serve at least two purposes: to concentrate viral and host proteins necessary for RNA biogenesis, and to prevent viral RNA detection by the host innate immune system. The viral non-structural proteins 2B and 3A, along with the precursor 2BC re-purpose autophagic, ER, and Golgi membranes for replication complex formation, in addition to anchoring the viral RNA to the complex (16). Recently, it was demonstrated that there is a conversion of global lipid synthesis pathways from the production of neutral lipids to negatively charged phospholipids during poliovirus infection and that this is a major driver of replication complex formation (183). This observation was shown to be dependent on the nuclear-cytoplasmic re-localization of the lipid biogenesis enzyme, CTP:phosphocholine cytidylyltransferase α.

Belov and colleagues demonstrated that blocking the phospholipid-based generation of replication organelles does not, in fact, lead to reduced RNA synthesis but does lead to increased activation of type I interferon signaling (183). This study introduces the paradigm-shifting idea that the main purpose of membranous replication complex formation might be to shield the double-stranded RNA intermediates that occur during picornavirus infection (RF and RI) from innate immune detection, rather than to (necessarily) promote the mechanics of RNA synthesis. Conflicting results in earlier studies also hinted at this idea in that one group demonstrated that CVB3 $3D^{pol}$ is recruited to replication organelles by the phospholipid PI4P (85) while another group challenged this observation describing replication-competent CVB3 mutants that can bypass the requirement for PI4P (180).

VPg uridylyation, *its role in both positive and negative strand RNA synthesis, and the unlinking of VPg from positive sense RNA*. VPg is a 22 amino acid polypeptide that plays an important role in the viral life cycle by acting as the primer for both positive and negative strand RNA synthesis. The RdRp $3D^{pol}$ uridylylates VPg at a highly conserved tyrosine residue in the third position of the polypeptide. Initial experiments demonstrated that *in vitro* uridylation of VPg and subsequent RNA synthesis could be achieved with a minimal reaction containing VPg, ^{32}P-labeled UTP, high (micromolar) concentrations of purified $3D^{pol}$, and a poly(A) template, suggesting that both VPg uridylation and RNA synthesis occurred at the 3' poly(A) tract of the RNA template (134). However, the RNA yield from these reactions was very low and poly(A) templating of VPg uridylylation did not account for the specificity of the reaction on viral RNAs, given that cellular mRNAs also contain 3' poly(A) tracts. Therefore, these observations eventually led researchers in a different direction to determine the mechanism responsible for VPg uridylyation and ultimately to the discovery that this process involves an indispensable templating RNA structural element termed the *cre*, or *cis*-acting replication element in picornaviruses.

The *cre* is found in highly divergent locations within the genomes of different picornaviruses even though the function appears to be identical for each virus. For example, while the *cre* for poliovirus and CVB3 is located within the 2C coding region, it is found in the VP1 coding region for HRV3, HRV14, and HRV 76, and in the VP2 coding sequence for C group HRVs and for several members of the *Cardiovirus* genus (135). The *cre* within 2C for poliovirus and CVB3 [*cre*(2C)] is the most well-characterized of this class of RNA structures. *Cre*(2C) consists of a 14-nucleotide stem-loop in which the templating portion for VPg uridylyation contains the conserved motif $R_1NNNA_5A_6R_7NNNNNNR_{14}$, where N is any base, the bases at positions 1, 7, and 14 are purines (R), and the adenosines at positions 5 and 6 act as the templating residues for addition of uridine monophosphate (UMP) to VPg (133,

150). The reaction results in two substrates, VPgpU, and VPgpUpU, in which either one or two UMP residues are added. For the latter substrate, A_5 and A_6 are thought to participate in a "slide-back" mechanism (136), in which A_5 acts as the template for the addition of the first UMP residue, which slides "backward" to hydrogen bond with A_6. A_5 then templates the addition of the second UMP. Because the viral RdRp does not have a proof-reading function, this slide-back mechanism is thought to ensure specificity of the reaction such that only UMPs are added to VPg because it is the only monophosphate that is able to hydrogen bond to A_6. Moreover, it is noteworthy to mention that while this reaction has been shown *in vitro* to occur on VPg itself, it is not known if the mature protein or one of its precursors (3AB, 3ABC, 3BC, 3BCD, or P3) is uridylated *in vivo* (135). Additionally, the uridylation reaction *in vitro* at the *cre* requires the dimerization and binding of the precursor $3CD^{pro}$. Once the uridylated VPg substrate is produced, the RdRp $3D^{pol}$ elongates it into either full-length negative or positive-strand RNA. Importantly, as a result of this priming mechanism, all nascent viral RNA, regardless of polarity, is linked to VPg via an O4-(5' uridyly)tyrosine bond (171).

An historical conundrum presented itself when the Wimmer, Baltimore, and Darnell groups demonstrated that poliovirus RNAs found on polysomes contain neither a 7mG cap nor VPg at their 5' ends (46, 79, 125, 126). These results subsequently led to the conclusion that, although nascently transcribed viral RNAs are linked to VPg, either a viral or cellular enzymatic activity must be active during the infectious cycle to account for the removal of VPg from viral mRNA transcripts, and, given that translation and RNA synthesis occur in *cis* (127), from the positive-sense strand of the RF as well. The various VPg-linked or unlinked forms of the viral RNA that are produced during infection are depicted in **Figure 1.2**. The Baltimore group followed up these studies and determined that a cellular activity found in both the nucleus and cytoplasm of uninfected cells was responsible for hydrolyzing the

phosphotyrosyl bond between VPg and the viral RNA. This activity was termed VPg unlinkase (2).

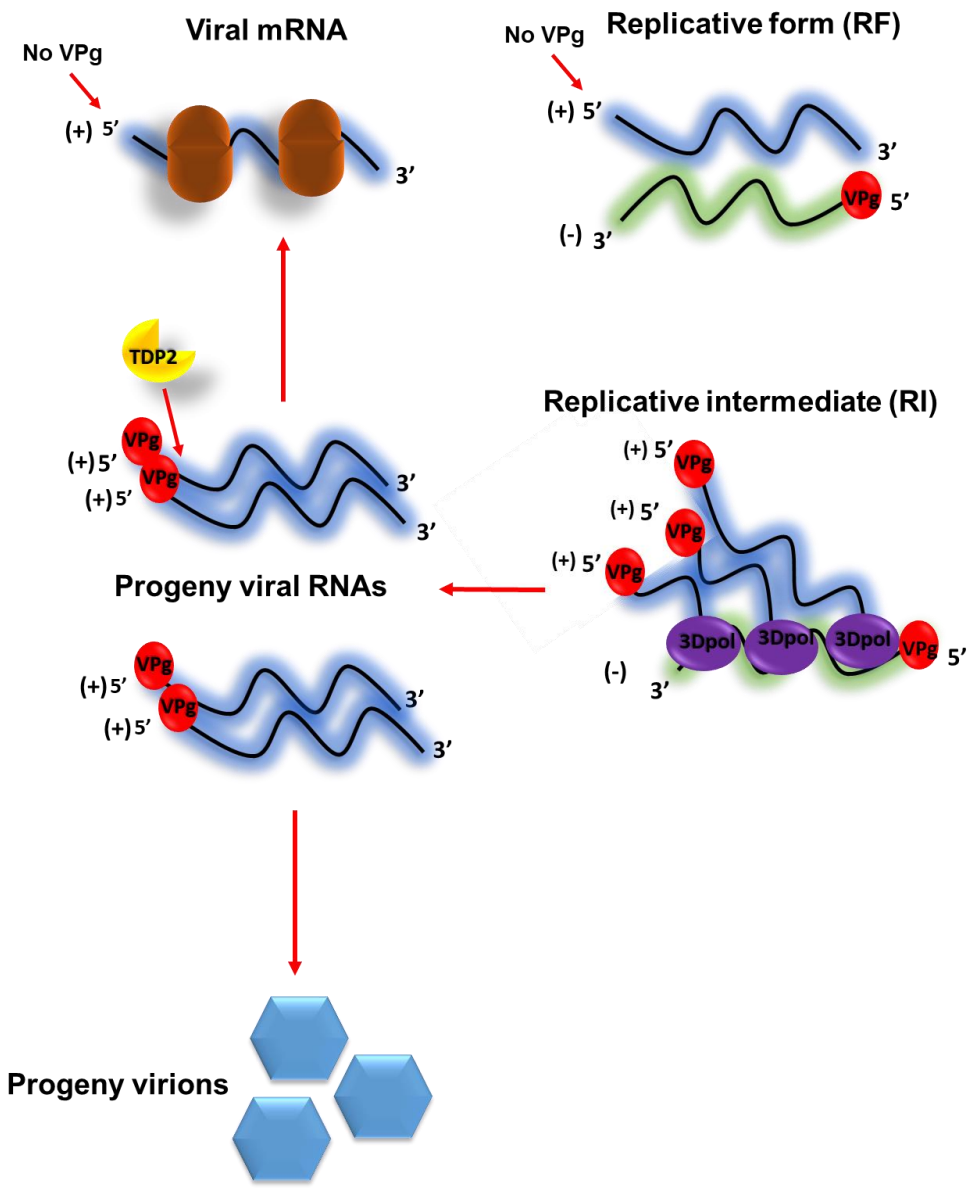

Figure 1.2. Forms of the viral RNA that arise during picornavirus infections and their linkage to VPg. TDP2 cleaves VPg from positive sense viral RNA destined to be used for translation or as a template for negative strand RNA synthesis. Negative sense RNA and nascent positive strand RNA retains the VPg linkage. Nascent VPg-linked positive-sense RNA can be used for further rounds of replication and translation or be packaged into progeny virions.

TDP2 as VPg unlinkase: roles in the uninfected cell hijacked by picornaviruses

Several studies aimed at characterizing VPg unlinkase demonstrated that VPg linked to, at minimum, an RNA heptanucleotide fragment or the full-length viral RNA is the most efficient substrate for the enzyme (73, 154), but that VPg linked to one, two, or three UMPs cannot be cleaved by unlinkase. This result makes sense given that, as mentioned above, VPgpUpU acts as the primer for RNA synthesis. It stands to reason that the phosphodiester bond of VPgpUpU should be protected to ensure that appropriate levels of the substrate are maintained throughout virus infection for the initiation of RNA synthesis. Under conditions of proteinase K digestion of VPg, it was determined that pUp is the minimal portion of the viral RNA that is required for unlinkase (73).

Despite these initial studies characterizing the activity of the enzyme, the cellular identity of VPg unlinkase remained enigmatic until only recently. Using a multi-step purification scheme, Virgen-Slane and co-workers (185) isolated a 38 kDa polypeptide that was demonstrated to have VPg unlinkase activity in an *in vitro* assay developed by Rozovics *et al*. (154). Mass spectrometry analysis expertise contributed by Gershon and co-workers at UC Irvine determined that this protein was the DNA repair enzyme, TDP2 (185), revealing the identity of the VPg unlinkase that had eluded the field for over three decades.

In the uninfected cell, TDP2 is a member of the Mg(2+)/Mn(2+)-dependent family of endonucleases (36). Three isoforms of the protein have been described in the literature, including a nuclear-localized, DNA-associated isoform, and a shorter, mitochondria-associated isoform, which is produced via an alternative transcription site and (87) repairs mitochondrial DNA damage mediated by the drug doxorubicin (87). The mRNA also was recently shown to possess an IRES element at the second in-frame AUG of the TDP2 coding sequence (34), producing a third cytoplasmic isoform with a truncated N-terminus compared to the full-length nuclear TDP2. This observation is intriguing given that picornaviruses shut-

down host cap-dependent translation during infection, leading to the speculation the virus might have evolved to take advantage of TDP2 because levels of the protein can remain abundant during the infectious cycle. In its nuclear DNA repair capacity, the enzyme acts to hydrolyze the 5' phosphotyrosyl bond linking stalled topoisomerase II (TOP2) cleavage complexes (cc) to cellular DNA (140), which is the cellular activity that picornaviruses "hijack" for removal of VPg from the viral RNA. Normally, TOP2 forms transient double-stranded breaks in the DNA to allow for strand passage (that is, the passage of one DNA duplex) through the break in order to facilitate the relaxation of DNA supercoiling (140). However, if TOP2 encounters any lesions (e.g., abasic sites) or is in the presence of what are known as "TOP2 poisons" (e.g., etoposide), the enzyme can become irreversibly bound to the DNA, which can ultimately lead to downstream genome instability and the activation of cellular apoptosis pathways (8). Therefore, TDP2 resolution of the TOP2cc has been demonstrated to play an indispensable role in many biological processes including neuronal maintenance (63) and cell cycle regulation (99), cellular events that involve high levels of topological stress to the DNA vis a vis gene transcription and/or DNA replication. To this end, TDP2 has recently been shown to directly reduce the chromosome translocations that occur as a result of abortive TOP2 activity during gene transcription (64).

TDP2 structure and DNA repair function. Several key studies aimed at elucidating the structural and molecular basis of the mechanism by which TDP2 acts on stalled TOP2cc have been carried out in the ten years since its landmark discovery as the first eukaryotic 5' phosphodiesterase (36). The active site of the enzyme spans amino acid residues 120-369, which corresponds to the C-terminal two-thirds of the enzyme, and can be classified as a canonical endonuclease_exonuclease_phosphodiesterase domain that includes the conserved catalytic residues E152, G261, D262, N264, D350, and H351 (99). There is also structural homology between the TDP2 active site and other related endonucleases (e.g.,

DNAse I and apurinic- or apyrimidinic-site endonuclease 1) in that the protein fold within the site consists of a double layer of β-sheets inserted between two α-helices (162). However, despite these similarities, the DNA binding groove of TDP2 has been shown to be deep and narrow, compared to that of the previously mentioned endonucleases, which have broader and more shallow binding grooves (162). When TDP2 is co-crystalized with single-stranded DNA, the latter binds to TDP2 such that the first two 5'-terminal bases occupy the narrow binding groove, while the following three bases are stacked on top of each other, resembling double-stranded DNA (162). Altogether, this structural information fits with the observed function of TDP2, in which the enzyme binds to the 5' 1-4 nucleotides in the single-stranded DNA overhang of the double-stranded break that results from TOP2cc formation. Importantly, binding of TDP2 to the DNA has also been shown to occur in a sequence-independent manner (156), thereby allowing the enzyme to act at stalled TOPcc and repair DNA damage broadly, irrespective of the gene locus.

With respect to the 5' phosphotyrosyl linkage, TDP2 has been shown to engage this moiety within a hydrophobic groove created by L134, Y188, and M214 of the protein, whose conformation is stabilized by the adjacent residues M204, M205, L124, and Y178 (156). Moreover, until recently, the prevailing thought in the field was that in order for TDP2 to access the 5' linkage, TOP2, which is a relatively large protein (~180 kDa) must be degraded and that this step was likely proteasome-dependent (58, 115, 205). Gao *et al*. demonstrated that trypsin-mediated proteolysis of a 48-nucleotide TOP2-linked substrate resulted in significantly more efficient hydrolysis of the phosphotyrosyl bond by TDP2 *in vitro* (58) as compared to untreated, intact TOP2. However, Schellenberg and co-workers recently challenged this assertion and reported that a novel TDP2-interacting protein termed ZATT, or zinc finger protein associated with TDP2 and TOP2 promotes removal of TOP2cc by TDP2 via a proteasome-independent mechanism (157). ZATT is a SUMO2 E3/E4 ligase (27) and the

authors demonstrated that ZATT binds to and SUMOylates TOP2 which acts to facilitate TDP2 phosphodiesterase activity. Importantly, the authors demonstrated that the resolution of SUMOylated TOP2cc was only impaired by proteasome inhibition in the *absence* of TDP2. This suggests the existence of an alternative ZATT-mediated repair pathway that requires degradation of SUMOylated TOP2 but is independent of TDP2 (157). Furthermore, in the same study, small angle X-ray analysis revealed that TDP2 interacts with SUMO via a noncanonical "split-SUMO interacting motif" that is formed by the N-terminal and C-terminal portions of the TDP2 catalytic domain. The authors propose an alternative model of TOP2cc resolution in which the binding of ZATT to SUMOylated TOP2, as opposed to proteolysis, changes the conformation of TOP2 in such a way that TDP2 is able to access and hydrolyze the 5' phosphotyrosyl linkage.

In addition to SUMO binding, TDP2 also contains a ubiquitin-associated protein-like domain at its N-terminus, which has also recently been shown to interact directly with both mono- and poly-ubiquitin substrates (with a distinct preference for binding the latter) and that mutation of this domain impairs TDP2 enzymatic activity (145). This suggests that ubiquitination of TOP2 might act as a signal to TDP2 that the cc has stalled and thus stimulate its hydrolysis activity on the 5' TOP2-DNA linkage. Altogether, these findings reveal the mechanism of TDP2 phosphodiesterase activity on TOP2cc, and, pertinent to the current thesis, provide a starting molecular framework for understanding how TDP2 might engage the VPg-linked RNA substrate of the picornavirus genome, especially given that there is currently no structural information available for the latter.

Functions of TDP2 beyond DNA repair. Notwithstanding the DNA repair function of the enzyme, TDP2 is also a highly pleiotropic protein, and has multiple cellular roles outside of genome maintenance, although these roles are less well-characterized. They include signal transduction, transcriptional regulation, and involvement in the innate immune

response (100). As a signal transduction factor, TDP2 has been shown to bind to CD40, a TNF receptor which mediates Nf-κB signaling, and to several TNF receptor-associated factors (TRAFs), with an especially high affinity for TRAF6 (143). TDP2 inhibits CD40 signaling in a dose-dependent manner, likely through these protein-protein interactions. Conversely, TDP2 overexpression in non-small cell lung cancer cells activates the MAP-ERK signaling pathway via Raf-1 and ERK1/2 (99), which is important to note given that both CVB3 and EV71 replication is promoted by this signaling pathway (57, 199). Furthermore, ERK3, an atypical ERK family kinase, has been shown to phosphorylate TDP2, which stimulates the enzyme's phosphodiesterase activity (17). ERK3 and TDP2 were demonstrated to interact by co-immunoprecipitation assays and to act synergistically to protect lung cancer cells from TOP2 poison-induced apoptosis (17). As a transcriptional regulator, TDP2 interacts with the transcription factor, Ets1, and represses Ets1 transactivation of its target promoters, including those of genes involved in cell cycle progression (137, 159). In fact, this was the first characterized activity of TDP2, as one of the protein's aliases is EAP2 or Ets-associated protein 2.

TDP2 has been demonstrated to be a component of PML (promyelocytic leukemia protein) nuclear bodies, and its expression is upregulated in response to interferon-γ (200) (as is typical for PML bodies-associated proteins), which is noteworthy given that interferon signaling is activated during virus infection. The protein has also been implicated in neurodegenerative disorders such as Parkinson's (184, 209), and Alzheimer's disease (198). For the former, TDP2 was shown to bind the Parkinson's disease-associated protein DJ-1 and in doing so protected neuroblastoma cells from apoptotic cell death, suggesting that TDP2 might play a protective role in the disease. However, DJ-1 proteins containing mutations that are thought to contribute to the disease phenotype overrode the cytoprotective effect of TDP2. These proteins bound with higher affinity to TDP2 than did the wild type

versions which subsequently led to the activation of the c-jun N-terminal kinase JNK - and p38-MAPK apoptosis pathway (209). Furthermore, the same group found that DJ-1 with the same mutations as the previous study re-localizes TDP2 from the nucleolus to the cytoplasm, where it is recruited to cytoplasmic aggregates (184) and that this alters ribosomal RNA biogenesis, a phenomenon that is associated with several other neurodegenerative disorders.

Given the neuroprotective role of TDP2, both in its DNA repair capacity *in vivo* (63) and via the protein-protein interactions observed in cultured cells mentioned previously, as well as the neurotropism of picornaviruses, it begs the question of whether viral manipulation of TDP2 [i.e., re-localization of TDP2 from the nucleus to the cytoplasm during infection (185)] might contribute directly to the neuropathogenesis elicited by these viruses. While several host factors that determine tissue tropism have been identified (195), the cellular implications that specifically underlie picornaviral hijacking of TDP2 have not been examined. However, understanding the functional significance of TDP2 usage by picornaviruses during their replication cycle is an important first step in answering this question.

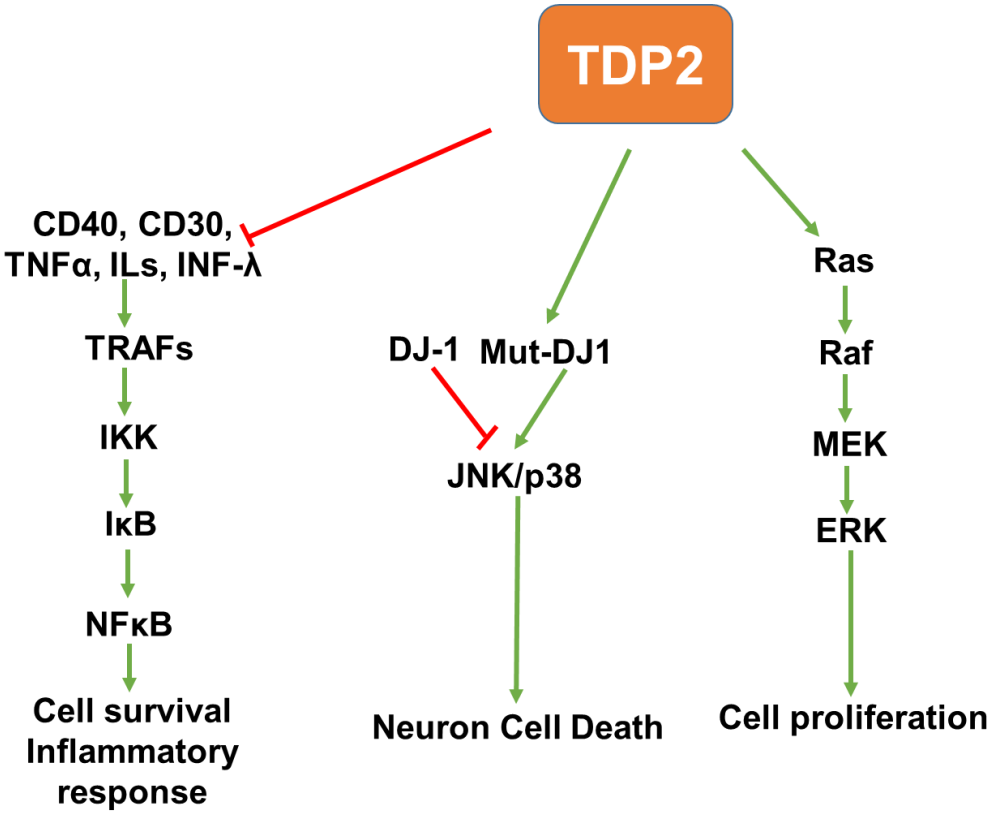

Figure 1.3 TDP2: beyond DNA repair. TDP2 is a highly pleiotropic enzyme that has been demonstrated to have a role in several cell signaling pathways outside of its role in the repair of stalled TOP2 cleavage complexes. TDP2 antagonizes the NFκB pathway via interactions with the TNF family receptor, CD40, and the TNF receptor-associated factor, TRAF6. TDP2 has also been shown to stimulate the activation of the p38/JNK pathway in neurons expressing a mutated DJ-1 protein, which is associated with neurodegeneration in Parkinson's disease. Moreover, overexpression of TDP2 activates the MAPK-ERK signal cascade in non-small cell lung cancer cells, leading to an increase in cell proliferation. As such, TDP2 has been implicated as a putative target for cancer therapeutics (147).

Biological significance of TDP2-mediated unlinking of VPg from picornavirus RNA: what we know and questions remaining

Although the discovery that TDP2 acts as VPg unlinkase shed light on a decades-old quandary in the field, the biological consequences of VPg removal from the viral RNA during the picornavirus replication cycle remain unclear. Prior to this discovery, it was thought that VPg is released from the viral mRNA template to facilitate efficient polysome association *in vivo* (125). However, follow up studies revealed that a VPg-linked RNA can form a functional translation initiation complex *in vitro* (62). Others have since elaborated on this observation to elucidate if TDP2-mediated hydrolysis of VPg from the RNA is important for virus replication, and if so, for which step(s) in the replication cycle is it required.

Using an "uncleavable" VPg-linked RNA template, Langereis and colleagues determined that release of VPg from input viral RNA is not required for the initial round of viral translation or RNA synthesis (95). The template was generated via click chemistry-mediated attachment of VPg to poliovirus RNA resulting in a 5' VPg-triazole-RNA bond, which cannot be hydrolyzed by TDP2. The non-cleavable VPg-linked RNA contained a luciferase reporter gene and was transfected into HeLa cells in the presence or absence of guanidine HCl (GuHCl, a potent inhibitor of picornavirus RNA synthesis), to test the effect of blocking the removal of VPg on viral translation and RNA synthesis separately. Subsequent luciferase assays were carried out 8 hours post-transfection on the transfected cells. The authors found that luciferase expression levels generated from the RNA containing VPg-triazole linkage were comparable to those generated from the wild type poliovirus RNA.

As indicated above, the study by Langereis *et al*. demonstrates that removal of VPg is not required to initiate translation and/or RNA synthesis upon deposition of the picornavirus RNA into cell cytoplasm. However, the implications of this work are limited in that they only apply to the input viral RNA, given that the non-hydrolyzable linkage is not encoded in the

viral genome. This means that after subsequent rounds of translation and replication, the normal linkage is produced on the nascent viral RNA and the uncleavable linkage is not maintained throughout the remainder of the replication cycle. Therefore, conclusions about the requirement of VPg removal by picornaviruses in steps that occur *after* initiation of the virus infection (during the switch from translation to RNA synthesis or during the exponential amplification of the latter) cannot be made from these data.

Maciejewski *et al*. followed up this study and determined that picornaviruses require TDP2 to efficiently carry out their replication cycles, and that the extent of the requirement is virus-specific (111). In this study, mouse embryonic fibroblasts (MEFs) that were ablated of TDP2, in addition to their wild type counterparts, were infected with either poliovirus, CVB3, or HRV1A and single cycle growth analyses were carried out (111) on the infected cells. The authors found that while there was an approximate 1-2 $\log_{10}$ reduction in virus titers produced in the absence of TDP2 for poliovirus and HRV1A, there was a severe impairment in CVB3 virus production and virtually no virus progeny was produced throughout the course of infection. Western blot analysis and luciferase assays also revealed that CVB3 protein production is substantially reduced in TDP2 knock-out (KO) MEFs (111) compared to wild type, consistent with the results obtained from the virus growth kinetics experiments. It is important to note, however, that the experiments carried out in this study utilized a mouse cell model, but the picornaviruses that were examined normally infect human cells. Therefore, the ways in which host species variability might affect virus replication, irrespective of the role of TDP2, must also be taken into consideration.

Altogether, these data suggest that although removal of VPg is not necessary to initiate the virus infection, there is(are), in fact, step(s) beyond initiation of the picornavirus replication cycle that require TDP2. However, the *exact* step(s) and the overall picture of how the presence of VPg on the viral RNA might interfere remains to be determined. Therefore,

taking into consideration the evidence presented above, we hypothesize that either viral mRNA translation and/or RNA synthesis requires the removal of VPg from the RNA to proceed efficiently.

Conclusions

Picornaviruses are masters of molecular manipulation and, therefore, remain critically important human pathogens. Moreover, as picornaviruses such as EV-D68 begin to re-emerge, particularly with both striking and unanticipated sequalae (172), it will become even more important to continue deciphering the mechanisms by which picornaviruses hijack their host. In doing so, this allows for the potential to develop novel, anti-picornaviral therapeutics, which are particularly important for picornaviruses for which we still do not have a vaccine (i.e., HRV). While the virus family has indeed been extensively studied, there is much that we still do not know, and thus, there are still many unexplored avenues to introduce countermeasures to virus replication. Finally, by examining and studying picornaviruses in greater depth, we can extend our knowledge of the virus family and of RNA virus biology in general, allowing us to continue to retool the virus to *our* advantage, as oncolytic therapeutics, drug delivery systems, and beyond.

CHAPTER 2

Post-translational effects of TDP2 VPg unlinkase activity during picornavirus infections in human cells

Summary

In the experiments described in this chapter, we set out to characterize the role of TDP2/VPg unlinkase activity during picornavirus infections in a human cell model of infection. We utilized a CRISPR/Cas-9-generated TDP2 KO human retinal pigment epithelial-1 (hRPE-1) cell line, in addition to the wild type (WT) counterpart (64) for our studies. We determined that in the absence of TDP2, virus growth kinetics for poliovirus and CVB3, were delayed by approximately 2 hours and virus titers were reduced by ~2 $\log_{10}$ and 0.5 $\log_{10}$ units, respectively, starting at 4 hours post-infection (hpi), and by ~1 $\log_{10}$ unit at 6 hpi for poliovirus. However, virus titers were indistinguishable from those of control cells by the end of the infectious cycle. Moreover, we determined that this was not the result of an alternative source of VPg unlinkase activity being activated in the absence of TPD2 at late times of infection. Protein production in TDP2 KO cells was also substantially reduced at 4 hpi for poliovirus infection, consistent with the observed growth kinetics delay, but reached normal levels by 6 hpi. Interestingly, this result contrasts with what has been reported previously for the TDP2 KO mouse cell model (111), suggesting that either cell type or species-specific differences might also be playing a role in the observed phenotype. Furthermore, we determined that catalytically inactive TDP2 does not rescue the growth defect, confirming that TDP2 5' phosphodiesterase activity is required for efficient virus replication.

Importantly, we show for the first time that polysomes can assemble efficiently on VPg-linked RNA after the initial round of translation in a cell culture model, but both positive and negative strand RNA production is impaired in the absence of TDP2 at mid-times of infection, indicating that the presence of VPg on the viral RNA affects a step in the replication cycle

downstream of translation (e.g., RNA synthesis). Concordantly, we found that double-stranded RNA production (a marker of viral RNA synthesis) is delayed in TDP2 KO RPE-1 cells. Additionally, we demonstrated that encephalomyocarditis virus (EMCV, a member of the *Cardiovirus* genus) is insensitive to KO of TDP2 in hRPE cells; however, the IRES of EMCV driving P2 and P3 protein expression within a bicistronic polio/EMCV chimera does not rescue virus particle production or RNA synthesis in the absence of TDP2. This result suggests that the reduced protein production observed in TDP2 KO RPE-1 cells is likely due to the failure of the RNA to amplify at mid-times of infection, rather than a defect in translation itself, consistent with the results we obtained from the polysome analysis. Moreover, we show that premature encapsidation of nascent, VPg-linked RNA is not responsible for the observed virus growth defect. Finally, we demonstrate that virion RNA in which the VPg has been degraded can partially rescue the defect in RNA production that occurs in the absence of TDP2. Altogether, we present the first lines of evidence to suggest that either positive or negative-sense RNA synthesis are likely candidates for the step that requires the removal of VPg from the RNA to proceed efficiently.

Introduction

The *Picornaviridae* comprise a diverse family of viruses that includes both circulating and re-emerging human pathogens. While the most well-studied among them is poliovirus, for which there is an effective vaccine, other members such as human rhinovirus (HRV), enterovirus (EV) D68, EV-71, coxsakieviruses (CV), and hepatitis A still represent major health threats worldwide, particularly for those who have are immunocompromised or who have pre-existing conditions (165). Of particular concern is the resurgence of EV-D68, which was the cause of the 2014 outbreak in North America and Europe of severe lower respiratory illness (119), mainly in children. The virus has also been implicated as the infectious agent responsible for

the recent incidence of non-polio acute flaccid paralysis (31, 40). Furthermore, several other picornaviruses also have a distinct neurotropism (e.g., EV71 and CVA group viruses), making them major causes of aseptic meningitis and encephalitis globally (96).

As their name suggests, picornaviruses are small, positive-sense RNA viruses. There are 29 genera currently described in the family and the genome size ranges from ~7 to 9 kb. The RNA is uncapped at the 5' end and, as such, viral translation is mediated by an internal ribosome entry site (IRES) within the 5' noncoding region (NCR). Compared to the *de novo* initiation of RNA synthesis employed by most RNA viruses, picornaviruses utilize a unique mechanism to copy their genome. RNA replication involves the use of the protein primer, VPg (Virus Protein genome-linked). Two uridine monophosphate residues are added to VPg at Tyr3 of the polypeptide by the viral RNA-dependent RNA polymerase (RdRp), $3D^{pol}$, to form the substrate VPgpUpU (134). This uridylylation reaction is templated by an RNA structure called the *cre,* or *cis*-acting replication element, located at different positions within the picornavirus coding sequence depending on the virus species, (59, 66, 117, 134), or in the case of foot-and-mouth disease virus, within the 5' NCR (116). VPgpUpU is then elongated by $3D^{pol}$ and, as a result, all nascent picornavirus RNAs, both positive- and negative-sense, are linked to VPg via a 5' phosphotyrosyl bond. Interestingly, however, VPg uridylylation at the *cre* has been shown to be dispensable for negative-strand synthesis (67, 122) and that the 3' poly(A) tract is likely the template for this reaction when UTP levels are not limiting (168).

It has been well-appreciated in the field for several decades that the different forms of the viral RNA which arise during the picornavirus replication cycle have differential linkages to VPg (1, 46, 125, 126). Specifically, VPg was shown to be removed from positive-sense RNA destined for translation and subsequent negative-strand RNA synthesis by a cellular enzymatic activity termed "VPg unlinkase" based on its function (2). More than thirty years

later, the identity of unlinkase was determined to be the cellular DNA repair enzyme, tyrosyl-DNA phosphodiesterase 2 (TDP2) (185). Picornaviruses hijack the 5' phosphodiesterase function of TDP2, which, in the uninfected cell, is normally involved in the resolution of stalled topoisomerase 2 cleavage complexes on cellular DNA (36).

Several questions emerged upon the discovery of TDP2 as VPg unlinkase. Chief among them is whether removal of VPg from the RNA by TDP2 is necessary for efficient virus replication. Previous studies addressed this question using a mouse embryonic fibroblast (MEF) cell model of picornavirus infection and found that in the absence of TDP2, poliovirus, HRV1A, and CVB3 virus production is either significantly reduced or completely abolished (111). Concordantly, protein accumulation for both poliovirus and CVB3 is also severely diminished in TDP2 KO MEFs (111). These findings suggested that picornaviruses indeed require the presence of TDP2 to efficiently carry out their replication cycles in a mouse cell model of virus infection. However, it is remains unclear which step in the cycle requires the removal of VPg by TDP2. Unlinking of VPg has been shown not to be necessary for the initial round of translation and replication of the incoming RNA template (95), indicating that the requirement for TDP2 occurs at a later step during infection. It has been suggested that removal of VPg might prevent the premature encapsidation of nascent positive-sense RNA (185) based on the pattern of TDP2 redistribution observed during infection and the fact that only nascent VPg-linked RNA has been shown to be packaged; however, this has not yet been demonstrated directly. Other studies have shown that VPg-linked RNA can efficiently form a translation complex *in vitro* (62), but whether this is true *in vivo* after the initiating round of translation is unknown.

To replicate their genomic RNA, picornaviruses must generate an antisense template from which copies of positive-sense RNA are produced. Negative-strand RNA synthesis in picornaviruses involves the assembly of two key viral and host cell proteins into a

ribonucleoprotein complex (RNP) at a 5' terminal RNA structure called the cloverleaf (4). These proteins include the host factor, PCBP2, and the viral protein 3CD proteinase ($3CD^{pro}$) (187). PCPB2 binds to stem-loop (SL) "b" located within the first 30 nucleotides of the 5' end and to a C-rich region 10 nucleotides downstream of SL "d" of the cloverleaf, adjacent to the IRES (129), while $3CD^{pro}$ binds within SL "d" (116). The PCBP2/$3CD^{pro}$ 5' RNP complex is thought to act as a scaffold to recruit factors required for RNA synthesis and to facilitate circularization of the RNA, allowing synthesis of the antisense template to initiate at the 3' poly(A) tract (78). The structure of the cloverleaf and binding of the complex is illustrated in **Figure 2.1**. Somewhat surprisingly, The PCBP2/$3CD^{pro}$ complex has also recently been shown to be required for positive-strand RNA synthesis (186) along with the host protein, hnRNP C (26). The proposed model predicts that the binding of the complex at the 5' end of nascent positive sense strands acts to reinitiate the synthesis of subsequent copies of positive-sense RNA on the same negative-strand template (186). Additionally, the PCBP2/$3CD^{pro}$ RNP complex also has been shown to stabilize the viral RNA (92, 123, 161), given that picornavirus RNA is uncapped and, as such, is subject to degradation by host exonucleases (178).

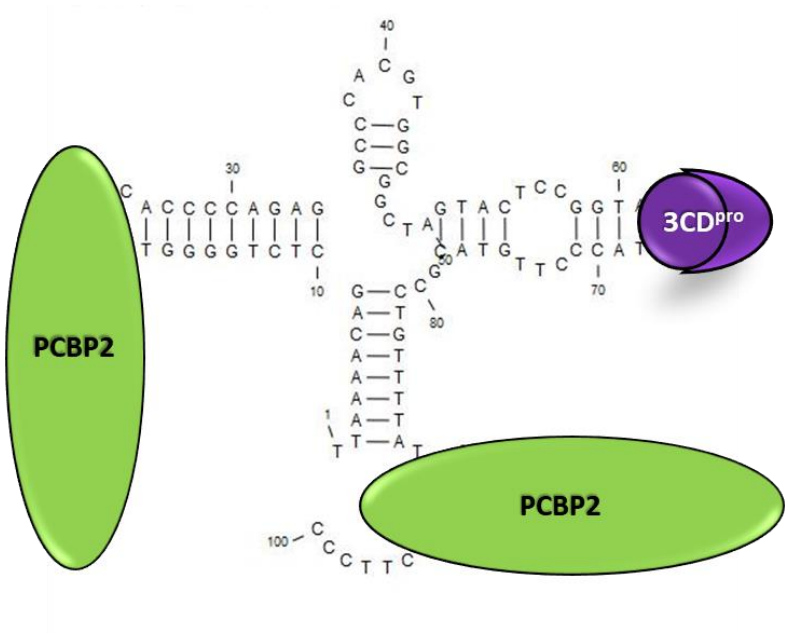

Figure 2.1 Binding of PCBP2 and 3CD^{pro} to the poliovirus 5' cloverleaf structure. Host RNA binding protein PCBP2 (green orbs) and viral 3CD proteinase (3CD^{pro}, purple orb) form a ternary complex with the 5' cloverleaf structure of the viral RNA to initiate positive- and negative-sense RNA synthesis. Formation of this complex is postulated to facilitate circularization of the RNA template which is thought to be important for the synthesis process. Image of the structure was generated with CLC Main Workbench Version 7.7.3. using the DNA sequence of the cloverleaf within the plasmid, pT7-PV1. Plasmid is used to *in vitro* transcribe viral RNA.

It was demonstrated that while the addition of a 5' 7-methylguanisine cap also stabilizes poliovirus RNAs containing mutations which disrupt the cloverleaf structure, doing so abolishes negative-strand RNA synthesis *in vitro* (11). This result was also observed when the cap was added to wild type RNA, albeit, the effect was modest (11). Furthermore, it is known that a precise 5' end of the poliovirus RNA is required for efficient positive-strand RNA synthesis (77), and the addition of one or two extra nucleotides which are not encoded by the genome results in diminished positive strand RNA production *in vitro* and delayed overall RNA replication in transfected cells (77). In contrast, Langereis *et a*l. showed that small chemical modifications to the 5' end (i.e. the addition of a biotin molecule, a Cy5 adduct, or an amine group) did not affect the initiating round of translation or replication of the RNA (95). Altogether, these data suggest that there may be certain classes of alterations to the 5' end of picornavirus positive-sense RNA which might disrupt viral RNA synthesis, possibly as a result of destabilization of the 5' cloverleaf structure and/or a decrease in the binding efficiency of the 5' PCPB2/3CD^{pro} RNP complex. This raises the possibility that TDP2-mediated removal of VPg from the 5' end of the positive-sense RNA template might be important for efficient RNA synthesis after the initiating round (that is, during the exponential amplification phase of the replication cycle).

Results

TDP2 protein expression and VPg unlinkase activity is absent in TDP2 knock-out hRPE-1 cells

To determine the effect of maintaining VPg on viral RNA during the picornavirus replication cycle, we utilized a hRPE-1 cell model of infection. While previous studies used mouse embryonic fibroblast cells (MEFs) to elucidate if TDP2 is required for virus replication (111), there are certain aspects of this model that do not faithfully recapitulate human infections with

picornaviruses. Specifically, it was observed that host cap-dependent translation is not shut off during CVB3 infection of MEFs (Ullmer and Semler, unpublished observations); however, this is a canonical feature of picornavirus infection of human cells (28). Thus, to circumvent any potential species-specific differences that might confound interpretation of the results, we chose to use hRPE-1 cells. hRPE-1 are differentiated from neuroectoderm and are therefore of the neuronal cell lineage (97) making them a suitable human cell model given that our viruses of interest are neurotropic. Furthermore, it has been shown that in the presence of certain transcription factors, hRPE-1 can differentiate into neuron-like cells (86, 103, 190). Moreover, hRPE-1 cells express all three isoforms of TDP2 (Gomez-Herreros and Caldecott, unpublished observations), allowing us to determine if there are any isoform-specific effects of TDP2 on virus infection.

We carried out an initial characterization of the TDP2 WT and KO RPE-1 cell lines to confirm that both VPg unlinkase activity and TDP2 protein expression are absent in the KO cells (**Figure 2.2**). To test the former, we used a rapid, *in vitro* VPg unlinkase assay developed by Rozovics *et al* (154) that relies on a $^{[35]}$S-methionine ($^{[35]}$S-met)-labelled virion RNA substrate. Poliovirus engineered to contain two extra methionine residues in the VPg polypeptide sequence (94) was grown in the presence of $^{[35]}$S-met, allowing the VPg to be radiolabeled. The labelled RNA was isolated and subsequently incubated with a of a source of TDP2/VPg unlinkase (either recombinant protein or whole cell lysates). The entire reaction mix was then loaded onto a 13.5% tris-tricine gel and analyzed by autoradiography. Released VPg can be observed as radioactive signal migrating towards the bottom of the gel. As expected, we observed that cell lysates generated from WT TDP2 hRPE-1 cells possess VPg unlinkase activity (**Figure 2.2 A, lane 2**), while those generated from KO TDP2 cells do not (**Figure 2.2 A, lane 4**). As positive and negative controls, we used either recombinant WT TDP2 or a catalytically inactive version of the enzyme containing an alanine substitution at

His351 (**Figure 2.2 A lanes 1 and 3**), which has been shown previously to abolish TDP2 5' phosphodiesterase activity (58). To control for non-specific, non-phosphodiesterase-mediated release of VPg, we treated the radiolabeled substrate with RNAse A (**Figure 2.2 A, lane 1**), which generates VPgpU and therefore migrates with a higher molecular mass than VPg alone. We also determined by Western blot analysis that TDP2 protein expression is absent in hRPE-1 TDP2 KO cells compared to WT (**Figure 2.2 B**). Altogether, these data confirm that hRPE1 TDP2 KO cells are discernably devoid of TDP2 VPg unlinkase activity and protein expression.

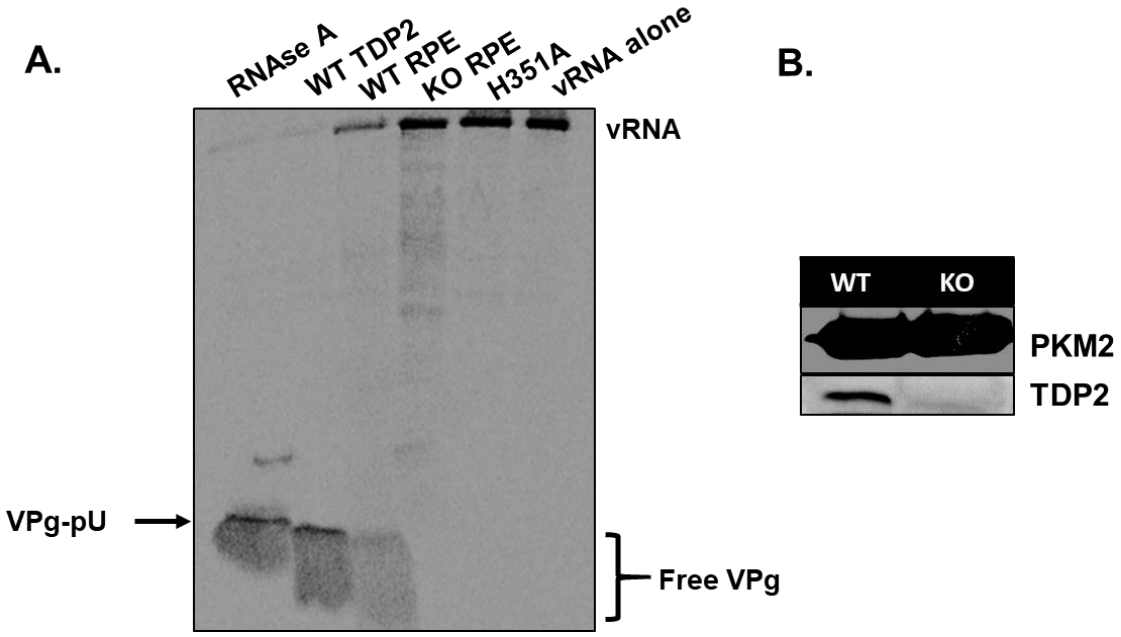

Figure 2.2 TDP2 protein expression and VPg unlinkase activity is absent in KO RPE cells. A) Lysates from WT and KO TDP2 hRPE cells (WT and KO RPE) were generated and used as source of VPg unlinkase to determine unlinkase activity on a radiolabeled VPg-linked RNA substrate. Release of VPg from the RNA is indicated by the free VPg signal at the bottom of the gel. Recombinant WT (WT TDP2) and catalytically inactive TDP2 (H351A) were used as positive and negative controls, respectively. RNAse A was used as a control for non-phosphodiesterase-mediated unlinking of VPg. vRNA alone was also used as a negative control. B) Western blot analysis was carried out on WT and KO TDP2 hRPE cell lysates. PKM2 was used as a loading control.

Virus growth kinetics are delayed in the absence of TDP2 for poliovirus and CVB3 in hRPE-1 cells, and the effect is MOI-dependent

We infected the WT and KO TDP2 hRPE-1 cells with either poliovirus or CVB3 at a multiplicity of infection (MOI) of 3 and carried out single cycle growth analyses to determine virus growth kinetics. As depicted in **Figure 2.3, panels A and B**, we observed an approximate 2 $\log_{10}$ and 0.5 $\log_{10}$ unit reduction in virus titer at 4 hpi for poliovirus and CVB3, respectively, and ~1 $\log_{10}$ reduction at 6 hpi for poliovirus. The growth defect was enhanced for CVB3 when the cells were infected at a lower MOI of 0.1 (**Figure 2.3, panel C**). From these data, we concluded that virus growth is delayed in the absence of TDP2 and this effect is both virus and MOI-dependent.

Poliovirus titers are comparable in WT and KO RPE cells after multiple replication cycles

We observed that virus titers reach normal levels in TDP2 KO cells at the end of the infectious cycle (8 hpi) and are indistinguishable from those obtained from WT cells. Moreover, it appeared that for poliovirus, the rate of virus production was increased in the TDP2 KO cells between 4 to 6 hpi based on the slope of the line and the titer at 6 hpi, compared to that of the equivalent time points in WT cells. Thus, we considered whether an early delay in growth kinetics in the absence of TDP2 might lead to higher overall virus production after multiple replication cycles. This would suggest that the presence of VPg on the RNA might slow down virus replication in a way that is advantageous to the virus specifically in contexts where TDP2 is limiting. However, we found this not to be the case, and virus titers from WT and KO TDP2 cells are comparable after 1 or 2 replication cycles (**Figure 2.4**).

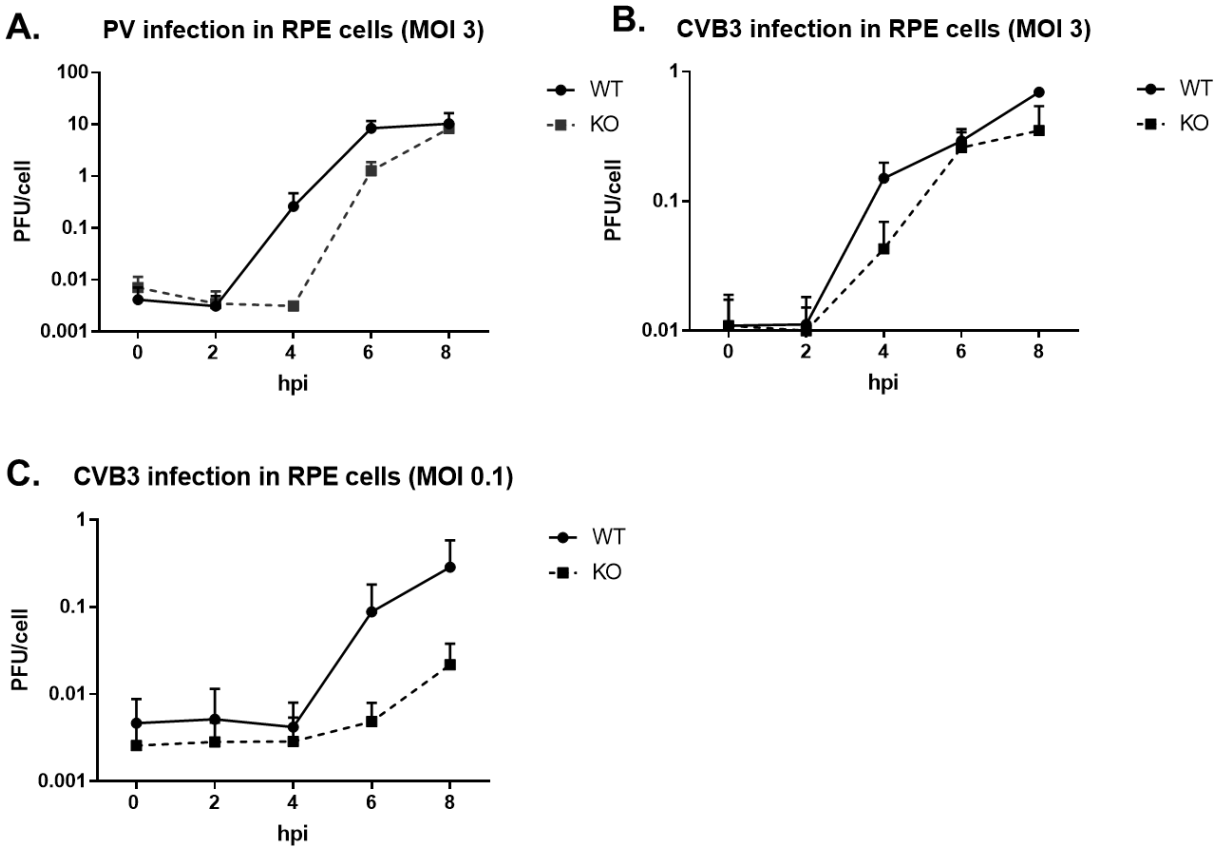

Figure 2.3 Virus growth kinetics are delayed in the absence of TDP2 for poliovirus and CVB3 in hRPE-1 cells and the effect is MOI-dependent. A-C) Single cycle growth analyses were carried out on either poliovirus- or CVB3-infected WT and KO TDP2 hRPE cells ($2.5x10^5$) over an 8-hour infection time course. Cells were infected either at a MOI of 3 (poliovirus and CVB3) or 0.1 (CVB3). Infected cells and supernatant were harvested at the indicated time points, subjected to 4 freeze-thaw cycles, and the virus titer was determined by plaque assay. Infectious particle production is represented as plaque forming units (PFU) per cell. Error bars indicate the standard deviation of the results. Experiments were performed in biological triplicate.

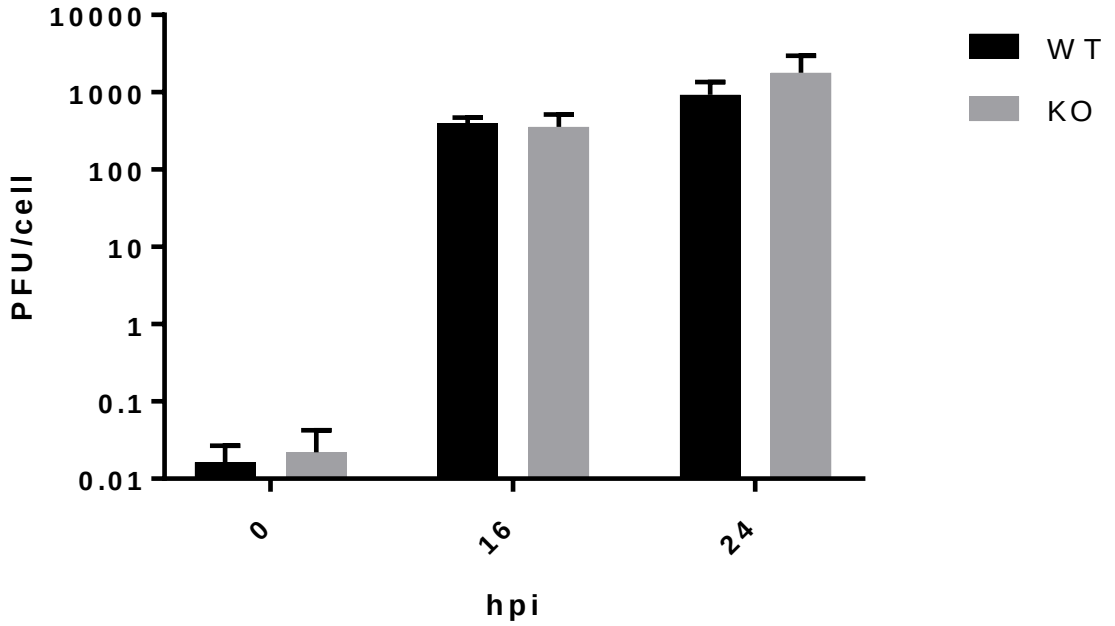

Figure 2.4 Poliovirus titers are comparable in WT and KO RPE cells after multiple replication cycles. WT and KO TDP2 hRPE cells were infected with poliovirus at a MOI of 3. Cells and supernatant were harvested at 0, 16, or 24 hpi and plaque assays were carried out to determine the virus titer. Infectious particle production as well as statistical error are represented as indicated in Figure 2.3. Data are the average of three biological replicates.

eIF4G is cleaved in both WT and KO TDP2 RPE cells during poliovirus infection

As mentioned in the preceding section, it has been demonstrated that host cap-dependent translation is not shut off during CVB3 infection of MEF cells. This is noteworthy because ongoing host translation during the virus infection increases the competition between virus and host mRNAs for ribosomes and other translation initiation factors (68), which has the potential to make the overall virus replication cycle inefficient. As such, it could be difficult to parse out the effect of TDP2 KO on virus replication vs. the inherent inefficiency of picornavirus translation in mouse cells. This was a key factor in our decision to develop the hRPE-1 cell model of infection. Therefore, we wanted to determine if host translation is shut off during picornavirus infection of hRPE-1 cells and that the growth defect we observed was not due to an indirect effect of host competition for translation resources. To test this, we either mock- or infected the WT and KO TDP2 cells with poliovirus and generated extracts at 0, 4, or 8 hpi. Using Western blot analysis, we assayed for the cleavage of the eukaryotic initiation factor, eIF4G. Picornavirus $2A^{pro}$-mediated proteolysis of eIF4G is required for host translation shut-off (182) and is routinely used as a read-out for this step. As predicted, eIF4G cleavage products could be detected as early as 30 minutes post-infection (0 hpi time point) and were the most prominent at 8 hpi for both the WT and KO TDP2 cell lines (**Figure 2.5**).

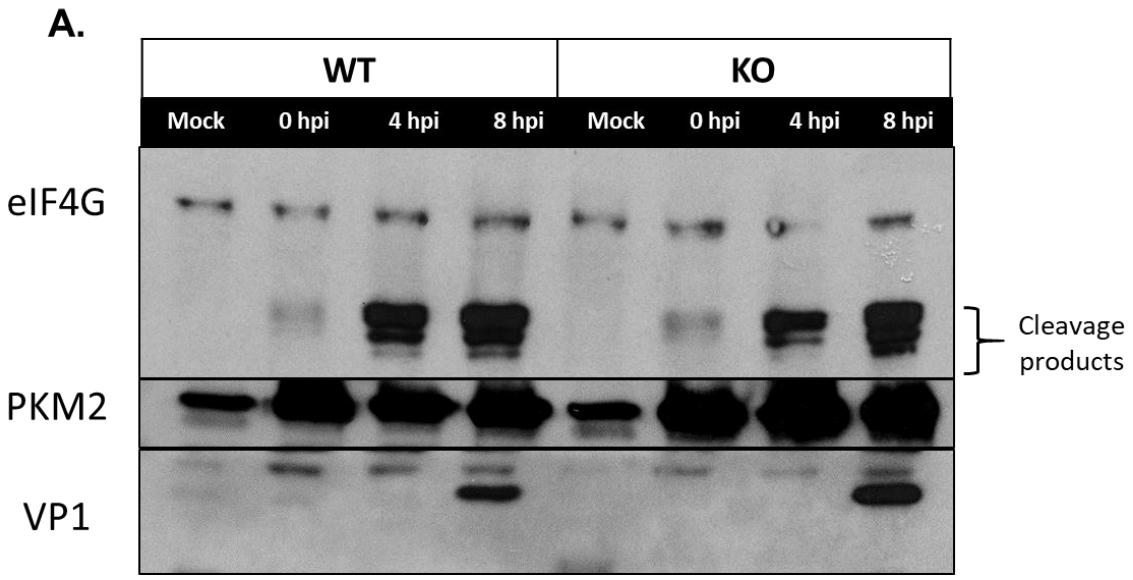

Figure 2.5 eIF4G is cleaved in both WT and KO TDP2 RPE cells during poliovirus infection. WT and KO TDP2 hRPE cells were infected at a MOI of 3 and incubated at 37°C for the indicated time periods. Cells were harvested, washed once with 1X PBS, and centrifugated at 15,000 RPM in a benchtop Eppendorf centrifuge. Cell pellet was resuspended in 1% NP-40 lysis buffer and incubated on ice for 15 minutes. Debris was removed and protein concentration was determined. 50 µg of protein from each sample was loaded onto a 12.5% SDS-PAGE gel and resolved for 2 hours at 200 V. Proteins were transferred overnight to a PVDF membrane and Western blot analysis was carried out. PKM2 expression was used as a loading control. Poliovirus structural protein VP1 expression was used as a control for virus infection. eIF4G cleavage products are indicated.

An alternative source of VPg unlinkase activity is not activated at late times of infection in TDP2 KO hRPE-1 cells

In our single cycle growth analysis studies, we noted that, while virus production was hampered at mid-times of infection, this delay was recaptured later during the infection cycle (6-8 hpi). As such, we reasoned it was possible that the activation of an alternative source of VPg unlinkase activity in the absence of TDP2 could account for this increase in virus titers. In fact, several other cellular enzymes in addition to TDP2 have recently been reported to participate in the resolution of stalled TOP2 cleavage complexes, including FEN1 (91) and MRE11 (81). To determine if an alternative source of VPg unlinkase activity was activated at late times of infection, we generated lysates from either WT or KO TDP2 mock- or poliovirus-infected hRPE-1 cells that were collected at 6 hpi and used them to carry out a VPg unlinkase assay. We determined that, in contrast to the WT TDP2 cells, the virus-infected KO cells did not possess any discernable VPg unlinkase activity (**Figure 2.6,** compare lanes 2 and 4), demonstrating that the activation of a redundant 5' phosphodiesterase is not responsible for the recovered virus growth observed late during poliovirus infection.

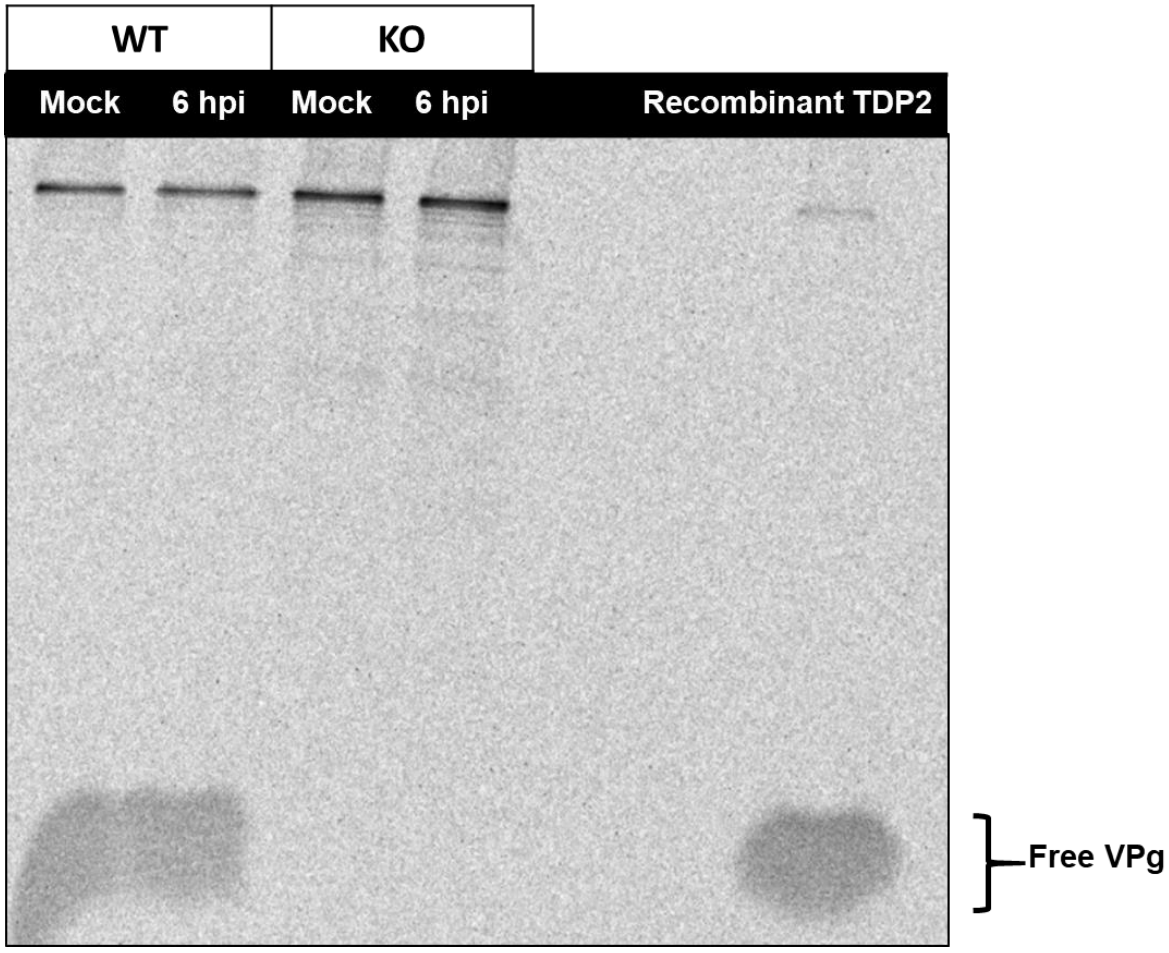

Figure 2.6 An alternative source of VPg unlinkase activity is not activated at late times of infection in TDP2 KO hRPE-1 cells. WT and KO TDP2 hRPE cells were infected or mock-infected at a MOI of 3 and harvested at 6 hpi. Cell lysates were prepared and VPg unlinkase assay was carried out as indicated in the legend to Figure 2.2. Recombinant WT TDP2 was used as a positive control.

All isoforms of TDP2 can be used by picornaviruses during their replication cycle

Given the fact that there are three different isoforms of TDP2 described in the literature which all possess 5' phosphodiesterase activity (34, 36, 87), that hRPE cells express all three (Gomez-Herreros and Caldecott, unpublished observations), and that three species of TDP2 VPg unlinkase with varying levels of activity have been reported (185), we wanted to determine if picornaviruses preferentially use a specific isoform of TDP2 to release VPg from the viral RNA during replication. To this end, our collaborator, Keith Caldecott at the University of Sussex generously provided us with CRISPR TDP2 KO hRPE cell lines that were individually complemented with GFP-tagged versions of either the α (nuclear), β (mitochondrial), or γ (cytoplasmic) TDP2 isoforms, or GFP alone (negative control) for our studies. We characterized the localization pattern of each isoform in either mock-infected or poliovirus infected cells. Consistent with previous reports (185), the nuclear α isoform relocalizes from the nucleus to the cytoplasm during poliovirus infection (**Figure 2.7, panel A, top right)**. The β isoform appears to aggregate in punctate-like structures in infected cells (**Figure 2.6, panel A, top left**), which we thought might be representative of membranous virus replication complexes and therefore, possibly indicative of a specific virus interaction with this isoform. The localization of the γ isoform, however, did not change over the course of the infection and remained distributed throughout the cytoplasm (**Figure 2.7, panel A, bottom left**). We also confirmed that each of the isoform-complemented cell lines possessed VPg unlinkase activity (**Figure 2.7, panel B**), albeit to varying degrees. Finally, we then went on to infect each cell line with poliovirus and carry out single cycle growth analysis.

Consistent with what was observed in the WT and total KO TDP2 cells (**Figure 2.3**) there was a growth kinetics delay that manifested starting at 4 hpi in the negative control cells complemented with empty GFP plasmid. However, all three isoforms of TDP2 were able to rescue the growth defect, suggesting that each isoform individually can be used by

picornaviruses to efficiently carry out their replication cycles (**Figure 2.7, panel C**). However, a caveat to this experiment is that it does not take into account the relative abundance and/or accessibility of each isoform when all three are present, which, if limiting, might put pressure on the virus to preferentially use one or the other. Nevertheless, from these data we can conclude that picornaviruses are able to harness each isoform of TDP2 to hydrolyze VPg from their genomic RNA.

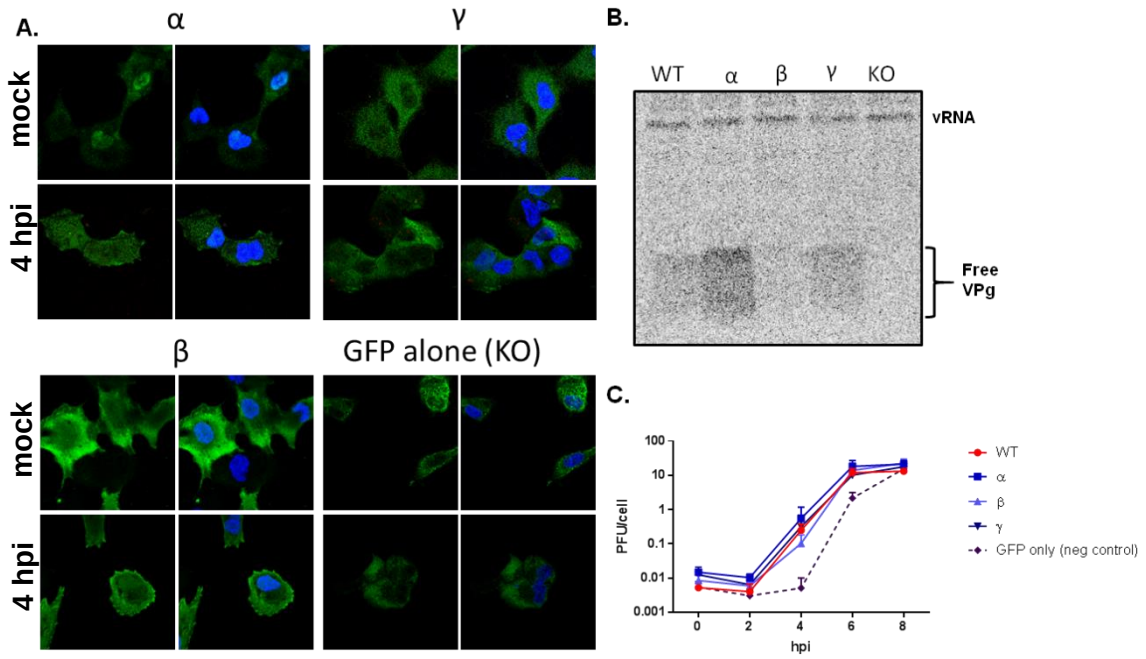

Figure 2.7 All isoforms of TDP2 can be used by poliovirus during the replication cycle. A) Immunofluorescence assay of hRPE-1 cells individually expressing the three isoforms of TDP2 in either mock- or poliovirus-infected cells. hRPE cell lines expressing either GFP-tagged versions of the α, β, or γ isoform of TDP2 or empty GFP plasmid (negative control) were seeded onto coverslips in 6-well plates. Cells were either mock-infected or infected with poliovirus at a MOI of 3 and fixed at 4 hpi in 3.7% formaldehyde. Cells were permeablized and immunofluorescence assay was performed. Coverslips were mounted onto microscope slides and imaged using a Zeiss confocal fluorescence microscope at 63x magnification. B) VPg unlinkase activity of the three isoforms of TDP2. Lysates were prepared from isoform- or GFP only-expressing cells and VPg unlinkase assay was performed as described the legend to Figure 2.2. C) Indicated cell lines were infected with poliovirus at a MOI of 3 and single cycle growth analysis was carried out. Data and error bars were plotted as described in the legend to Figure 2.3. Data are the composite of three biological replicates.

TDP2 5' phosphodiesterase activity is required for efficient poliovirus replication

In addition to DNA repair, TDP2 has other roles in the uninfected cell ((100), **Figure 1.3**). Critically, several of the pathways in which TDP2 is involved have been shown to also be involved in picornavirus replication. For example, overexpression of TDP2 has been demonstrated to activate the MAPK-ERK signal cascade resulting in an increase in cell proliferation (99). Additionally, it is known that efficient CVB3 replication is dependent on the activation of the MAPK-ERK pathway (105, 110) and is also influenced by the cell cycle (47, 192). Furthermore, TDP2 blocks the activation of the NF-κB pathway via its interactions with the CD40 receptor and TRAF6 (143), and several picornaviruses including poliovirus, HRV14, echovirus 1 (124) and EV71 (102) have also been shown to downregulate NF-κB signaling by targeting either the p65-RelA subunit of the NF-κB complex for $3C^{pro}$-mediated degradation, or by blocking IKKβ activation through interactions with 2C to promote virus replication (102).

Thus, it is conceivable that a function of TDP2 which is independent of its 5' phosphodiesterase activity might be involved in picornavirus replication and could therefore be responsible for the growth defect we observed in TDP2 KO hRPE cells. To determine if this is the case, we generated hRPE cell lines that constitutively express FLAG-tagged versions of either WT TDP2 (FLAG-TDP2) or the catalytically inactive protein containing the H351A mutation (FLAG-H351A) described previously (**Figure 2.1)**. These cell lines were created using the CRISPR TDP2 KO cells as the backbone. We determined the relative protein expression level of FLAG-TDP2 and FLAG-H351A in the complemented cells by Western blot analysis (**Figure 2.8, panel A**) and chose clones which had comparable protein levels for the remainder of our studies. We then went on to assess the level of VPg unlinkase activity in both cell lines. As expected, lysates of FLAG-TDP2-expressing cells were able to hydrolyze VPg from the RNA similarly to lysates from WT cells (**Figure 2.8, panel B**, compare

lanes 3 and 4), while those from FLAG-H351A-expressing cells were not, and VPg unlinkase activity was comparable to that of KO TDP2 cells. (**Figure 2.8, panel B**, lanes 6 and 7). We next infected either cell line with poliovirus, along with either the WT or KO TDP2 cells as positive and negative controls, respectively. We then carried out single cycle growth analysis to determine if catalytically inactive TDP2 is able to rescue the delay in virus production observed in TDP2 KO cells. If so, this would suggest that other functions of TDP2 aside from its DNA repair activity may be playing a role in the virus replication cycle. However, we observed that the catalytically inactive version of TDP2 is unable to rescue virus replication (**Figure 2.8 panel C**, dashed red line) and growth kinetics are comparable to those in the negative control. In contrast, consistent with previously published results (111), FLAG-TDP2 can rescue the virus growth defect (**Figure 2.8 panel C**, dashed blue line), and titers are similar to those from WT TDP2 cells.

Our data demonstrate that TDP2 5' phosphodiesterase activity is important for efficient poliovirus replication and most likely acts directly on VPg-linked RNA. However, it is important to note that this experiment does not rule out the possibility that there are other cellular pathways which are activated by TDP2 enzymatic activity that picornaviruses also require to carry out their replication cycles. Such putative pathways have yet to be described and the signal cascades mentioned above rely only on TDP2 activation via protein-protein interactions and not its enzymatic activity. Moreover, given the unique DNA/RNA-protein linkage upon which TDP2 acts, it is unlikely that this activity is used to activate a signaling pathway directly.

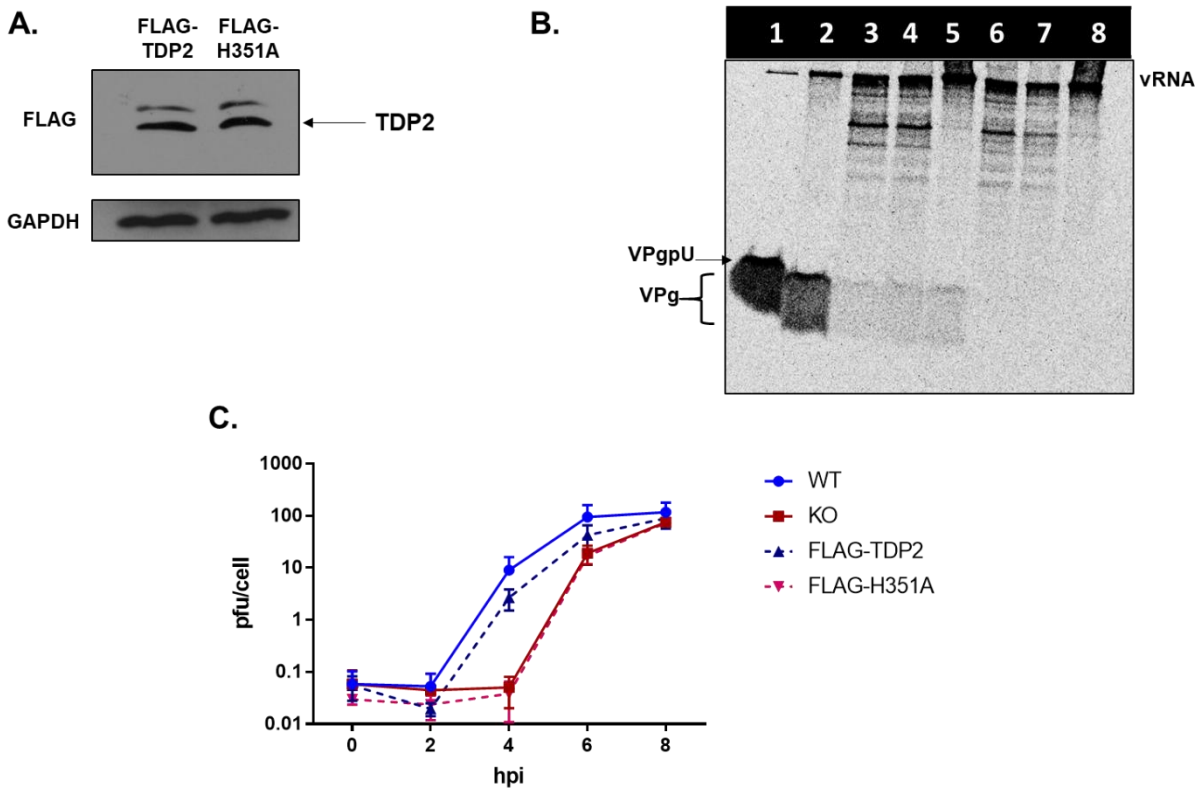

Figure 2.8 TDP2 5' phosphodiesterase activity is required for efficient poliovirus replication. A) Western blot analysis was carried out on FLAG-tagged WT or H351A catalytically inactive TDP2-expressing hRPE-1 cells as described in Figure 2.5. B) VPg unlinkase assay was carried out using the following sources of unlinkase activity: Lane 1, RNAse A; Lane 2, recombinant GST-tagged TDP2; Lane 3, WT TDP2 hRPE-1 cell lysate; Lane 4, FLAG-TDP2 hRPE-1 cell lysate; Lane 5, recombinant His-tagged TDP2; Lane 6, KO TDP2 hRPE-1 cell lysate; Lane 7, FLAG-H351A hRPE-1 cell lysate; Lane 8, vRNA alone (negative control). Lysates were prepared as in Figure 2.5. C) Single-cycle growth analysis of poliovirus infection in WT TDP2, KO TDP2, FLAG-TDP2, or FLAG-H351A-expressing hRPE-1 cells lines. Bands at the top the gel are non-specific degradation products.

Poliovirus protein production is delayed in the absence of TDP2 in hRPE-1 cells.

Our initial characterizations of picornavirus infection in the absence of TDP2 revealed that infectious virus particle production was delayed. However, as mentioned in the introduction, there are several steps at which TDP2 VPg unlinkase could act during the replication cycle that would result in a decrease in total virus yield. To further dissect the mechanism underlying this observation, we first assessed virus protein production in the absence of TDP2 in hRPE-1 cells to determine if this was also impaired. If protein production was impaired, this would suggest a defect in either virus translation and/or RNA synthesis mediated by the presence of VPg on the viral RNA, given that protein accumulation during infection is the aggregate of both activities.

We tested if virus protein production was impaired in the absence of TDP2 both qualitatively by Western blot analysis, and quantitatively using a *Renilla* luciferase-expressing poliovirus reporter (7) termed PV-PPP, which is depicted in **Figure 2.9 panel B**. We infected the WT and KO TDP2 hRPE-1 cells with either WT poliovirus or the luciferase reporter virus and harvested infected cells at 2-hour intervals throughout the 8-hour time course of infection. We then carried out Western blot analysis on the infected cell lysates which we probed for the viral protein 3AB, or luciferase assays to quantify virus protein accumulation. Consistent with our previous observations of infectious particle output, there was a substantial delay in the virus protein production in the TDP2 KO cells that could be observed in both assays at 4 hpi but was recovered between 6 and 8 hpi (**Figure 2.9 panels A and C**). Overall, this confirms that the growth delay that occurs in the absence of TDP2 is likely an effect on virus translation and/or RNA synthesis, but importantly, this putative mechanism includes an “escape hatch” for the virus, which can be used to overcome the deleterious effect at late times during the replication cycle.

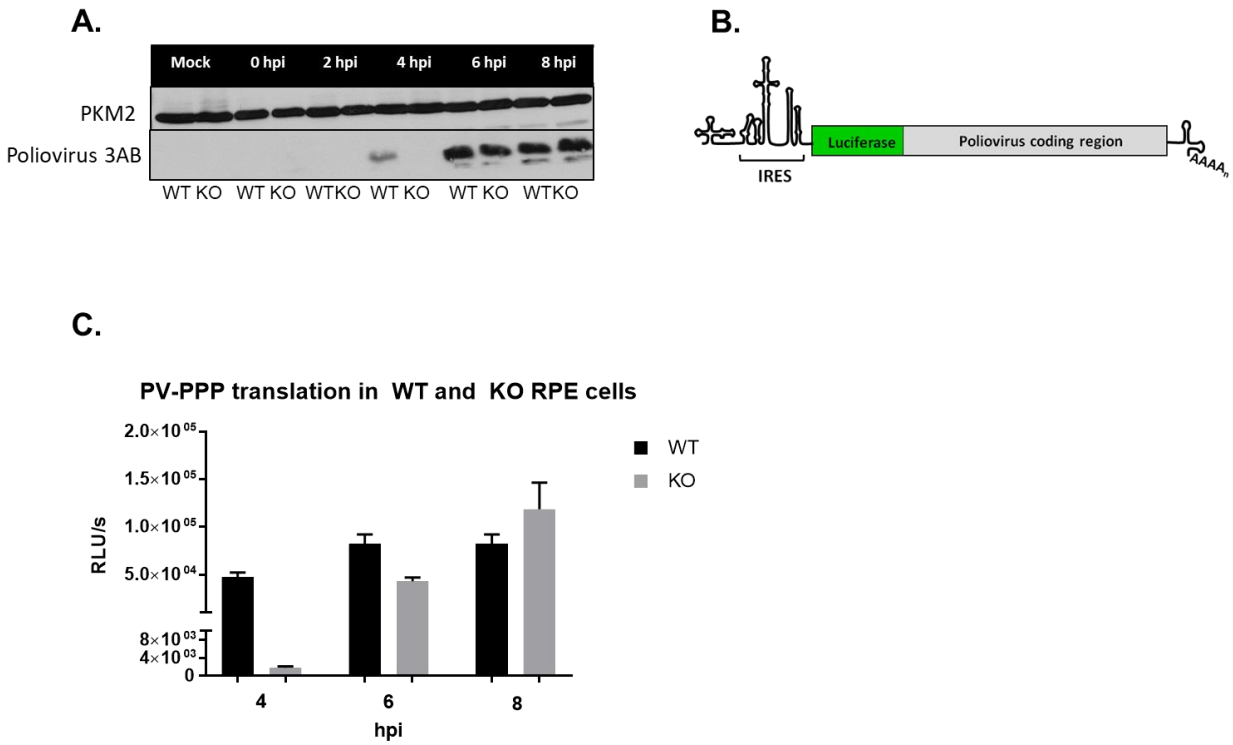

Figure 2.9 Poliovirus protein production is delayed in the absence of TDP2 in hRPE-1 cells. A) Western blot analysis of poliovirus-infected WT and KO hRPE-1 cells. Cells were infected with poliovirus and harvested at the indicated time points. Lysates were prepared as described in the legend to Figure 2.5. Poliovirus 3AB protein expression was detected using a mouse monoclonal antibody against 3A (which also recognizes the precursor protein). PKM2 expression was determined and used as a loading control. B) Schematic of the *Renilla* luciferase reporter virus construct, PV-PPP. C) Quantitation of luciferase production by PV-PPP in WT and KO TDP2 hRPE-1. Cells were infected with 200 µl of inoculum containing PV-PPP (MOI 0.01) and incubated at 37°C for the indicated time periods. Cells were lysed using Passive Lysis Buffer (Promega) and luciferase activity was determined using a luminometer. Values are presented as Relative Luminometer Units (RLU) per second. PV-PPP construct was generously provided by Eckard Wimmer, Stony Brook University. Error bars represent the standard deviation of the results obtained from three biological replicates.

Polysomes can assemble efficiently on VPg-linked RNA after the initial round of translation and replication in cultured cells in the absence of genome amplification at mid-times of infection

To tease apart the contribution of a potential defect in either virus translation or RNA synthesis to the growth phenotype observed, we set out to examine virus translation directly by polysome profile analysis. As mentioned previously, the prevailing hypothesis in the field regarding the removal of VPg from viral RNA during picornavirus infections has been that this allows for efficient polysome association (46, 126) *in vivo*, although it has been demonstrated *in vitro* that VPg-linked RNA can form translation-competent RNP complexes (62). To test if the presence of VPg hampers polyribosome loading onto viral RNA during picornavirus infection of cultured cells, we infected WT and KO TDP2 RPE cells with poliovirus and treated the cells with cycloheximide to pause the actively translating ribosomes on the RNA. We collected the samples at 2 or 4 hpi, generated lysates from the infected cells and fractionated them through a 10-50% sucrose gradient, after which we carried out polysome profile analysis on the fractionated lysates. We then purified the total RNA in each fraction by phenol-chloroform extraction and quantified the viral RNA content by qRT-PCR. Viral RNA content in the fractions was normalized to GAPDH expression and is represented as a ratio of the total, unfractionated cytoplasmic viral RNA content in an equivalent sample volume generated from either WT or KO cells.

If VPg acts as an impediment to polysome formation, we would expect that a majority of the viral RNA obtained from the KO TDP2 cells would appear in the lower monosome fractions which are indicative of free RNP complexes, or in the 40 or 60S fractions, suggesting a block in ribosome assembly. However, as depicted in **Figure 2.10, panels A-C**, the majority of the poliovirus RNA detected in both WT and KO TDP2 cells falls into either the 80S (5-6) or the low polysome (7-10) fractions at 2 hpi, indicating that polyribosomes can, in fact, load

efficiently onto VPg-linked RNA after the initial round of translation and replication. Moreover, the ratio of polysome-associated viral RNA to total WT or KO cytoplasmic viral RNA content is comparable, demonstrating that early virus translation is not impaired in the absence of TDP2.

To our surprise, however, when we quantified the viral RNA content of the fractions at 4 hpi, we found that, although the polysome profile was comparable in WT and KO TDP2 RPE cells, in which most of the viral RNA was observed to be in the low polysome fraction (7-8) (**Figure 2.10, panels D and E**), the total levels of virus RNA obtained from the KO cells were substantially lower than those from WT cells, which is depicted as the ratio between KO polysome-associated viral RNA and WT total cytoplasmic viral RNA (**Figure 2.10, panel F**). This indicates that although viral translation can proceed normally on VPg-linked RNA, the RNA fails to amplify at mid-times of infection (i.e., 4 hpi) in the absence of TDP2.

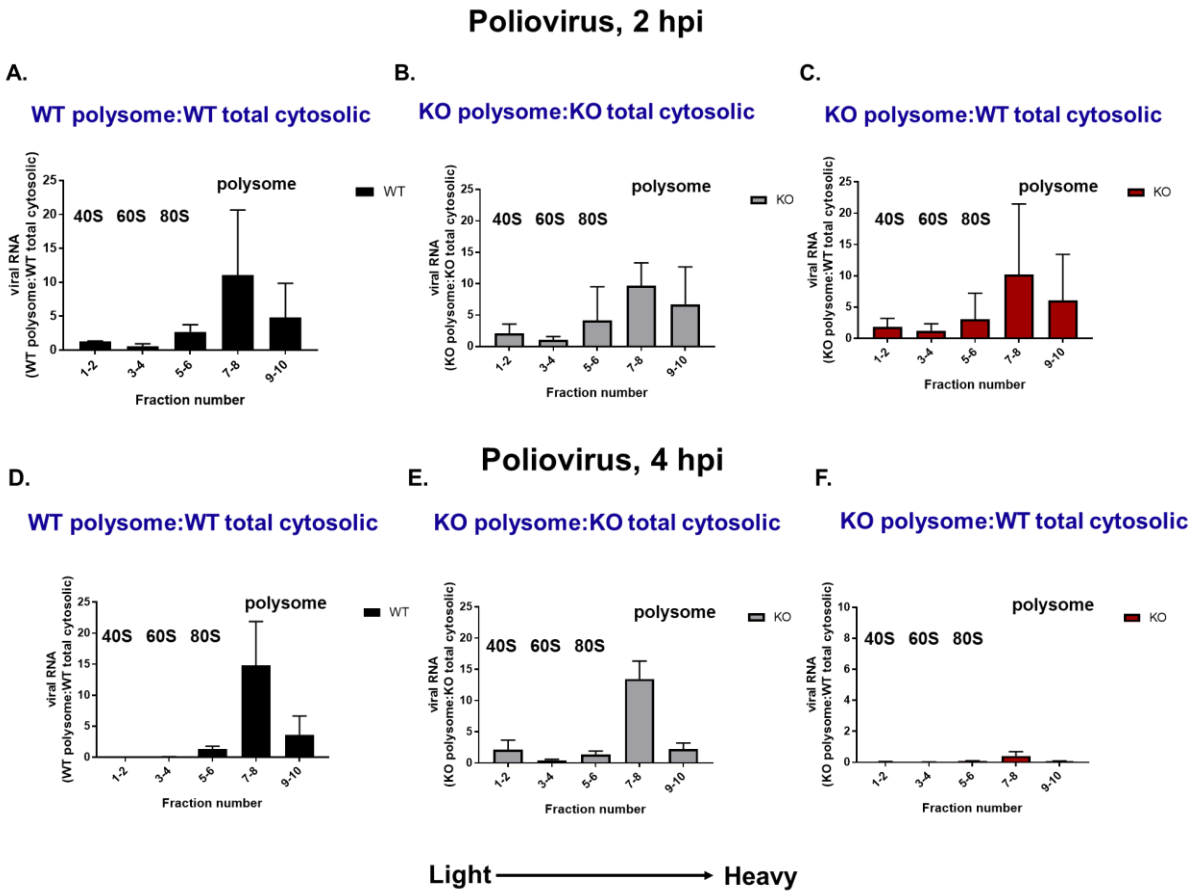

Figure 2.10 Polysomes can assemble efficiently on VPg-linked RNA after the initial round of translation in cultured cells but fails to amplify at mid-times of infection. Polysome analysis of WT or KO TDP2 hRPE-1 cells infected with poliovirus at a MOI of 3 collected at 2 hpi (A-C) or 4 hpi (D-F). Infected cells were treated with 30 mg/ml of cycloheximide for 3 minutes then lysed in polysome lysis buffer on ice for 30 minutes. Lysate was then layered onto a continuous 10-50% sucrose gradient. Gradients were centrifugated at 30,000 RPM in an SW41 swinging bucket rotor for 2 hours at 4°C and subjected to polysome fractionation at 4°C. RNA was purified, and qRT-PCR analysis was carried out to quantitate viral RNA present in each fraction. Values obtained for each set of pooled fractions are standardized to GAPDH mRNA levels and are represented as the normalized value relative to viral RNA present in the total unfractionated, cytoplasmic sample generated from WT (A, C, D, and F) or KO (B and E) TDP2 hRPE-1 cells.

Viral RNA synthesis is delayed in the absence of TDP2 in hRPE cells

We followed up the results obtained from the polysome analysis experiments to validate the observed decrease in virus RNA levels at 4 hpi. To do this, we carried out an 8-hour infection time course for poliovirus in WT and KO TDP2 RPE cells, collected cell lysates at 2-hour intervals, TRIzol-extracted the total cellular RNA, and quantified the viral RNA content by qRT-PCR. In this experiment, we quantified both positive- and negative-strand RNA production.

Corroborating what we observed in the polysome experiments and consistent with our growth kinetics data, we saw a ~2 or 3 $\log_{10}$ unit reduction in positive and negative-strand RNA production at 4 hpi, respectively, in TDP2 KO cells compared to WT, and a ~1-2 $\log_{10}$ reduction at 6 hpi (**Figure 2.11, panels A and B**), suggesting that viral RNA synthesis is impaired on VPg-linked RNA. Unlike infectious particle output, RNA production does not reach WT levels at the end of the infectious cycle, indicating either that fewer positive-sense RNA strands are synthesized in KO RPE cells or that the positive-sense RNA at this time during the infection is being immediately packaged, has egressed from the host cell, and therefore cannot be quantified in our analysis.

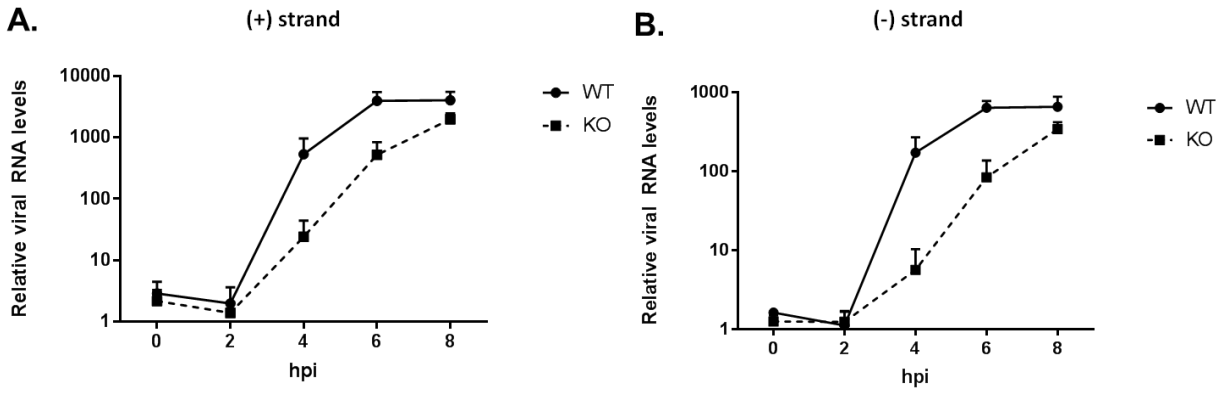

Figure 2.11 Viral RNA synthesis is delayed in the absence of TDP2 in hRPE cells. Positive- A) or negative- B) strand RNA production was quantitated for poliovirus over an 8-hour infection time course in WT and KO TDP2 hRPE-1 cells. Cells were infected with poliovirus at a MOI 3. RNA was extracted from the infected cells at the indicated times post-infection using TRIzol reagent. qRT-PCR analysis was carried out as described in the legend to Figure 2.10 and Materials and Methods. Relative expression values for viral RNA production are standardized to those of GAPDH mRNA levels at each time point.

RF and/or RI formation is delayed in TDP2 KO hRPE-1 cells

Picornavirus RNA replication results in the formation of two double-stranded RNA (dsRNA) intermediates. These are termed the replicative form (RF), which consists of nascent negative-sense RNA duplexed to a positive-sense RNA template and occurs during negative-strand RNA synthesis, and the replicative intermediate (RI), which is comprised of multiple nascent positive-strands being synthesized from the same negative-sense template and forms during positive-strand RNA synthesis. RF and RI are detected by host innate immune sensors (e.g., RIG-I and MDA5), and the virus has developed mechanisms to antagonize these pathways (39, 208). Important to the current study is that an antibody has been developed (denoted “J2”) which also recognizes dsRNA above 40 base pairs in length (21) and is frequently used to detect virus replication. We used this antibody to determine the relative dsRNA production in virus-infected WT and KO TDP2 cells. If the abundance of dsRNA is decreased in the absence of TDP2, this would indicate that either RF or RI formation is impaired, further suggesting that either positive or negative-strand RNA synthesis (or both) is inefficient on VPg-linked viral RNA. To test this, we seeded WT and KO TDP2 RPE cells onto coverslips, mock-infected or infected them with poliovirus, and fixed the cells at 2, 4, or 6 hpi. We then carried out immunofluorescence assays on the infected cells to visualize dsRNA using the J2 antibody. We found that, consistent with the time course analysis of viral RNA production, the signal for double-stranded RNA appears to be lower in virus-infected KO TDP2 cells at both 2 and 4 hpi (**Figure 2.12**), compared to WT, indicating that the generation of the RF and/or RI is also delayed in the absence of TDP2.

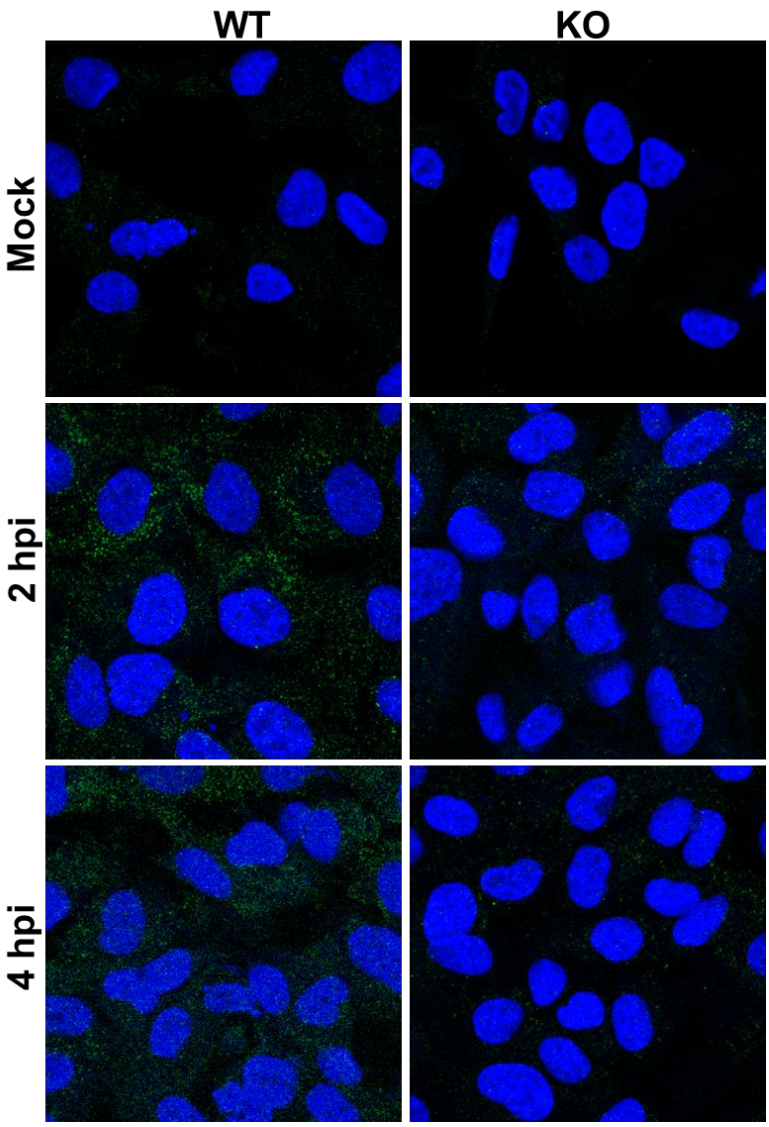

Figure 2.12 RF and/or RI formation is delayed in TDP2 KO hRPE-1 cells. Immunofluorescence assays of poliovirus-infected WT and KO TDP2 hRPE-1 cells. Mock-infected or poliovirus-infected cells were fixed and treated as described in Figure 2.7. J2 antibody was used to detect dsRNA. Goat anti-mouse DyLight 488 (Bethyl) fluorescent antibody was used to detect J2. Cells were counterstained with DAPI to detect nuclei. Coverslips were mounted onto microscope slides and imaged as described in the Materials and Methods.

The EMCV IRES driving non-structural protein expression does not rescue virus particle production or RNA synthesis

As mentioned above, picornavirus protein production is a composite of the contribution from both translation and RNA synthesis. The exponential amplification of positive-sense RNA that occurs during virus replication, in turn, amplifies the number of templates available for translation, or depending on the timeframe during infection, RNA synthesis. We demonstrated that polysomes can efficiently associate with viral RNA in the absence of TDP2 (**Figure 2.10**), which should presumably lead to normal protein levels. However, this is not what we have observed (**Figure 2.9**). The data therefore suggest that a step after of translation (i.e., RNA synthesis) is affected by the presence of VPg on the viral RNA and that this could account for the observed delay in virus protein production. However, we wanted to validate this result using an alternative approach. To do so, we utilized a bicistronic polio/EMCV virus which has previously been used to uncouple effects on translation from RNA synthesis (188). The DNA construct from which the virus was generated is comprised of the entire poliovirus coding region and its 5' NCR, including the IRES, which drives expression of the P1 structural proteins. The EMCV IRES is positioned just downstream of P1 and is separated from the end of the VP1 sequence by a 7-nucleotide spacer (188) and drives P2 and P3 non-structural protein expression (**Figure 2.13, panel A**).

For this approach to be informative, EMCV translation cannot be sensitive to KO of TDP2. EMCV has recently been demonstrated to be dependent on TDP2 for efficient virus replication in a MEF cell model (112). However, in the hRPE cell model, we show that EMCV can replicate similarly either in the presence or absence of TDP2 (**Figure 2.13, panel B**), further suggesting that there are likely species-specific differences which underlie the observed differences in growth phenotype. To generate the polio/EMCV virus, we linearized the plasmid containing the bicistronic nucleotide sequence. We then *in vitro*-transcribed RNA

from the linearized DNA template and transfected this RNA into HeLa cells. Virus isolates were plaque-purified and subsequently passaged 3 times. After the third passage, cells were harvested, debris was removed, and the virus titer was determined. We then used the resulting virus stock to infect either WT or KO TDP2 hRPE-1 cells.

As seen in **Figure 2.13, panel C**, the polio/EMCV bicistronic virus grows comparably to both WT poliovirus (**Figure 2.3**) and EMCV (**Figure 2.13 panel B**) in WT hRPE-1 cells, and the endpoint titer is ~10-20 $\log_{10}$ units. However, we observed a similar growth kinetics lag at 4 and 6 hpi for the bicistronic virus in the absence of TDP2 (**Figure 2.13, panel C**), indicating that the presence of EMCV IRES is unable to rescue virus particle production. Significantly, RNA synthesis was also not rescued by EMCV IRES-driven expression of the P2 and P3 proteins (which include the RdRp $3D^{pol}$ and other virus proteins necessary for replication complex formation), depicted in **Figure 2.13, panel D**, which confirms that the delay in RNA synthesis (and infectious virus production for that matter) in the absence of TDP2 is not likely due to a decrease in the proportion of virus protein accumulation contributed by translation to the replication cycle.

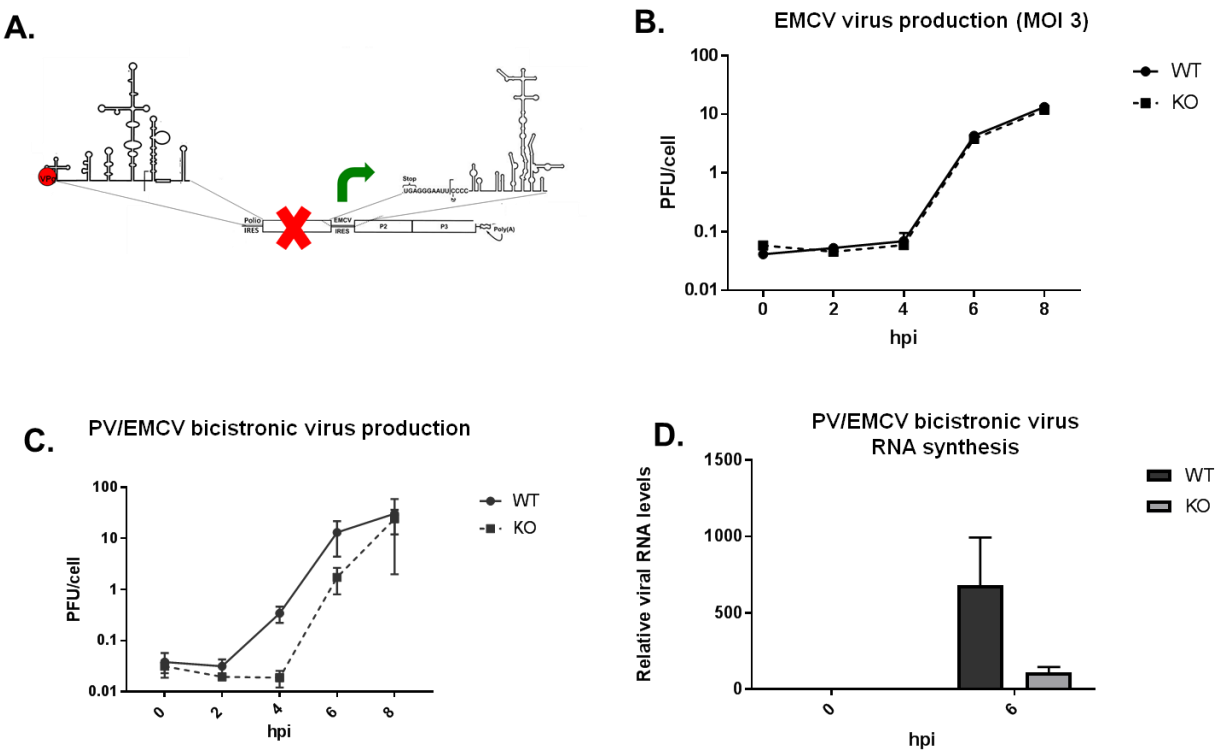

Figure 2.13 The EMCV IRES driving P2 and P3 protein expression does not rescue virus particle production or RNA synthesis. A) Schematic of the polio/EMCV bicistronic virus. Poliovirus IRES drives P1 expression, while EMCV IRES drives P2 and P3 expression. If poliovirus translation is impaired due to the presence of VPg on the RNA (red orb), P1 expression should be diminished (represented by the red X). On the other hand, if EMCV translation is not affected, IRES activity should result in the P2 and P3 proteins being produced (represented by the green forward arrow). B) Single cycle growth analysis of EMCV infection in WT and KO TDP2 hRPE-1 cells. C) Single cycle growth analysis of the polio/EMCV bicistronic virus in WT and and KO TDP2 hRPE-1 cells. Infectious particle production for B) and C) was quantified by plaque assay as described in the legend to Figure 2.2. D) qRT-PCR analysis of WT and KO TDP2 hPRE-1 cells infected with polio/EMCV bicistronic virus. Cells were collected at 0 or 6 hpi and treated as described in the Materials and Methods.

Premature encapsidation of viral RNA is not responsible for observed growth phenotype in the absence of TDP2

Implicit in the idea that RNA synthesis is impaired in the absence of TDP2 is that there are fewer positive and/or negative-strand RNA templates available upon which RNA synthesis can occur, thereby delaying the virus replication cycle. Another possibility to account for this phenomenon, however, is the premature encapsidation of nascent, positive-sense VPg-linked RNA. Virgen-Slane *et al*. initially proposed that the presence or absence of VPg acts as a "mark" for the virus to distinguish RNA destined for translation, RNA synthesis, or encapsidation (185), and that hydrolysis of VPg early on during the infectious cycle precludes the packaging of viral RNA too soon, which would truncate the infection. This hypothesis is based on the fact that poliovirus has been demonstrated to re-localize TDP2 from the nucleus to the cytoplasm at mid times of infection. Moreover, the TDP2 forms a distinctive pattern in HeLa cells late during the infection, whereby the protein is localized adjacent to but does not colocalize with markers of virus replication complexes (185). The interpretation of this is that TDP2 may be excluded from sites of replication when VPg unlinkase activity is no longer required at late times of infection. Furthermore, it is known that only nascent, VPg-linked RNA is encapsidated (128) and that, although VPg does not function as a packaging signal per se, the protein does interact with the viral precursor 3CD which is thought to promote packaging (53).

To test if the growth defect we observed in the absence of TDP2 was due to premature packaging of the viral RNA, we used a known picornavirus encapsidation inhibitor called hydantoin (181), which at low concentrations (<50 µg/mL), blocks virion maturation but leaves both virus translation and RNA synthesis unaffected. At concentrations >50 µg/mL, however, RNA synthesis is also diminished (174). Therefore, we set out to titrate the drug in RPE cells to determine the appropriate concentration to use such that only viral RNA packaging was

affected. The logic underlying this experiment is that if the RNA is packaged too soon during the replication cycle in the absence of TDP2 and if this is responsible for the growth kinetics delay, then blocking encapsidation should be able to rescue the delayed virus replication phenotype. We infected WT TDP2 hRPE cells in the presence of increasing concentrations of hydantoin (0 µg/mL-100 µg/mL), harvested the cells at 6 hpi, and determined the virus titer by plaque assay. In concurrent experiments, we TRIzol-extracted RNA from drug-treated, poliovirus-infected WT hRPE cells and quantified the positive-sense viral RNA content by qRT-PCR. **Figure 2.14, panels A and B** demonstrate that while virus production is reduced starting at the 25 µg/mL concentration, viral RNA production is not affected until the highest concentration of the drug is reached (100 µg/mL), consistent with previously published data demonstrating a divergence in the concentration of the drug required to achieve a block in packaging vs. in RNA synthesis. We chose to proceed with the 25 µg/mL concentration for the remainder of our experiments.

Since these experiments entail blocking encapsidation infectious particle production cannot be used as a read-out. Instead, we utilized the *Renilla* luciferase-expressing reporter virus described earlier (**Figure 2.9**). We treated WT and KO TDP2 hRPE-1 cells with either DMSO or 25 µg/mL of hydantoin, infected these cells with the reporter virus, harvested the cells at 6 hpi, and carried out luciferase assays on the cell lysates. As observed previously, luciferase expression is reduced in TDP2 KO cells compared to WT in the vehicle-treated condition (**Figure 2.14 panel C**). Importantly, however, this reduction is not rescued in the presence of hydantoin (**Figure 2.14 panel C**), indicating that premature encapsidation of the viral RNA is not responsible for the growth phenotype.

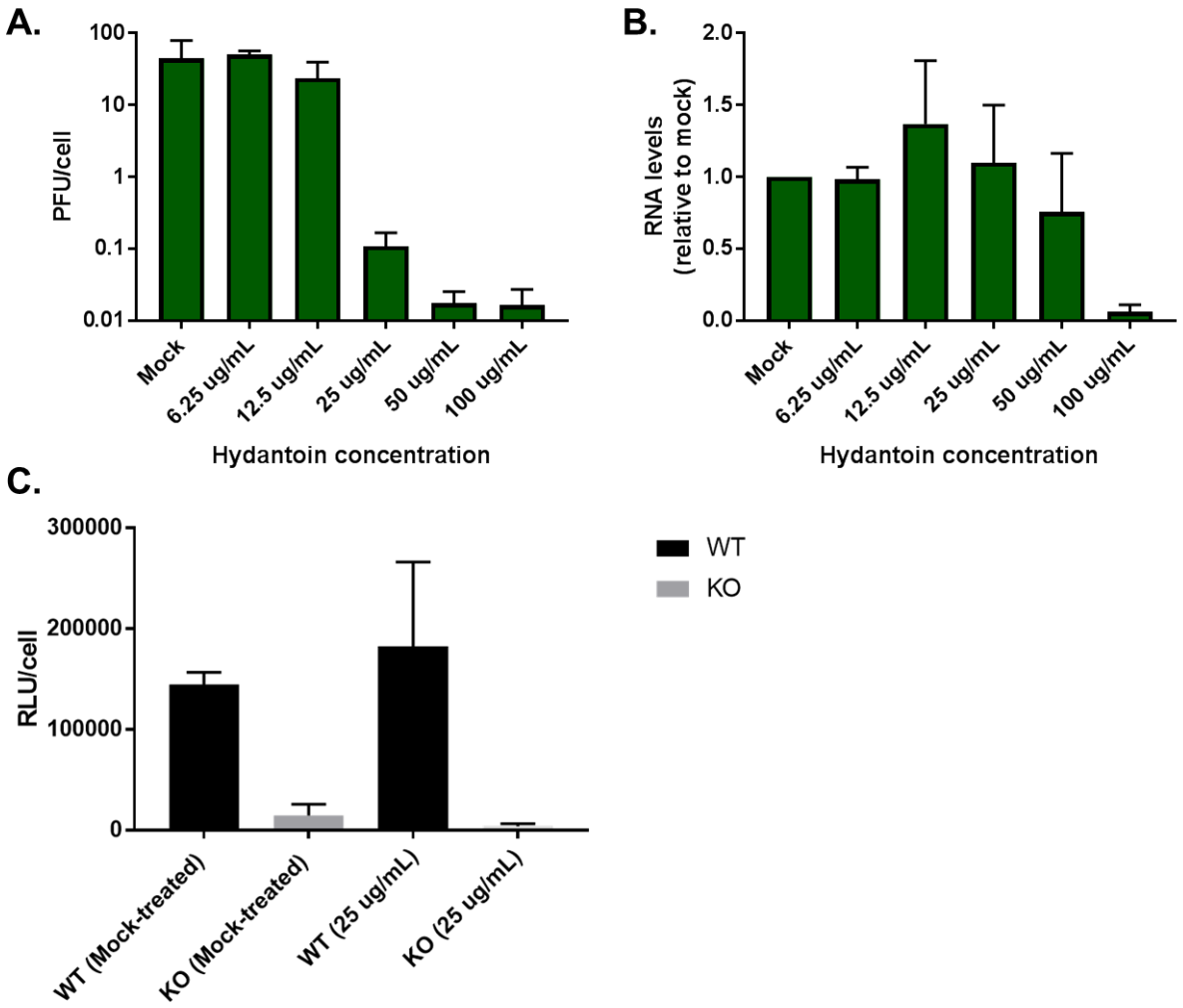

Figure 2.14 Premature encapsidation is not responsible for observed growth phenotype in the absence of TDP2. A) Encapsidation inhibition assay. WT and KO TDP2 hRPE-1 cells were infected with poliovirus in the presence of 6.25, 12.5, 25, 50, or 100 µg/ml of the encapsidation inhibitor, hydantoin, or DMSO (mock) as a negative control. Cells were harvested at 6 hpi and virus particle production was determined by plaque assay and represented as described in Figure 2.2. B) qRT-PCR analysis of hydantoin-treated, poliovirus infected WT and KO TDP2 hRPE-1 cells. C) Infection of WT and KO TDP2 hRPE-1 with PV-PPP treated with 25 µg/ml hydantoin or mock-treated with DMSO. Luciferase assays were carried out as described in the legend to Figure 2.9.

Proteinase K treatment of viral RNA partially rescues both positive- and negative-strand RNA production in TDP2 KO cells and boosts RNA production in WT cells

It has been suggested that the presence of VPg on picornavirus RNA might act to prevent activation of host innate immune sensors such as RIG-I (65). This is given the fact that the protein-primed mechanism of RNA synthesis employed by picornaviruses prevents the formation of 5' triphosphates during replication, which is the ligand that is recognized by RIG-I (84). Additionally, VPg-linked RNA is also protected from the host mRNA decay pathway mediated by the exoribonuclease, XRN1, which is responsible for degrading uncapped cellular mRNAs bearing a 5' monophosphate (178). However, because VPg is removed from the RNA during virus replication, it is thought that the PCBP2/3CD RNP complex acts as a functional "cap" to stabilize viral RNA and prevent degradation by XRN1 (11). As mentioned in the Introduction, the formation of this complex with the picornavirus cloverleaf structure is also essential for both positive- and negative-strand RNA synthesis. However, it is unclear if the presence of VPg on the viral RNA specifically impairs this step in the replication cycle. Therefore, we sought to determine if degradation of VPg from the viral RNA could rescue either positive or negative-strand RNA production in KO TDP2 cells. We treated poliovirus virion RNA with proteinase K (K) to degrade VPg, leaving behind a minimal number (<5) of undigested amino acid residues (73). We then purified the RNA by phenol-chloroform extraction and transfected the purified RNA into WT and KO TDP2 hRPE-1 cells. We harvested the transfected cells at 4, 5, or 6 hours post-transfection (hpt) and quantified both positive and negative-strand RNA synthesis by qRT-PCR. We also included mock-treated virion RNA-transfected cells (WT and KO) as negative controls. At the earliest time points (4 and 5 hpt) we observed that positive and negative-strand RNA levels were reduced in the TDP2 KO cells transfected with either mock-treated or K-treated RNA, albeit we did observe a trend in that RNA levels were slightly higher for cells transfected with K-treated virion RNA

compared to those transfected with mock-treated virion RNA at each timepoint (**Figure 2.14, panels A and B**).Critically, we observed that positive- and negative-sense RNA production is partially rescued at the 6 hpt time point (**Figure 2.14 panels C and D**), suggesting that maintaining VPg on the viral RNA does (at least minimally) impede picornavirus RNA synthesis.

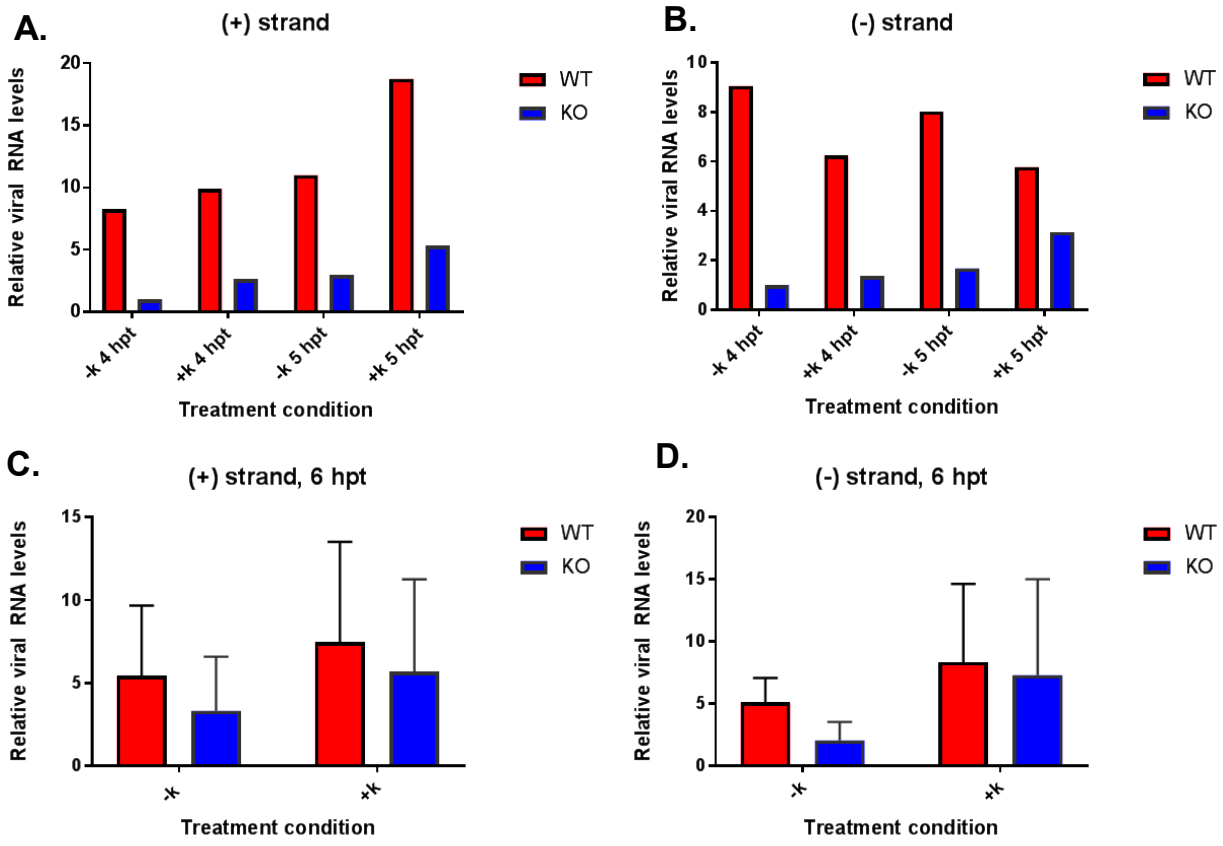

Figure 2.15 Proteinase K treatment of viral RNA partially rescues both positive- and negative-strand RNA production in TDP2 KO cells at 6 hpt. Positive- A) and C) or negative- B) and D) sense RNA production in WT and KO TDP2 cells transfected with proteinase K-treated or mock-treated vRNA. vRNA was incubated in the presence of 20 mg/ml proteinase K for 30 minutes at 37°C. RNA was phenol-chlorform extracted. 20 ng of either K-treated or mock-treated, purified virion RNA was then used to transfect WT and KO TDP2 RPE cells (density=$4.0x10^5$). Cells were harvested at the indicated times post-transfection and cellular RNA was extracted using TRIzol. qRT-PCR analysis was carried out on total cellular RNA to determine relative positive- or negative-sense RNA levels. Viral RNA expression is standardized to GAPDH mRNA levels.

Discussion

In this chapter, we demonstrated that the DNA repair enzyme, TDP2, is required for efficient picornavirus replication in human RPE cells and that this is dependent on its 5' phosphodiesterase activity. Furthermore, we showed that removal of VPg is not necessary for polysome association with the viral RNA after the initiating round of translation, but that viral RNA production is impaired in the absence of TDP2. Finally, we found that viral RNA production can be partially rescued by transfecting TDP2 KO hRPE-1 cells with an RNA template that had been treated with proteinase K to remove VPg, suggesting that the presence of VPg on the RNA is, in part, an impediment to viral RNA synthesis.

While our findings are overall in agreement with previously published work on the role of TDP2 during picornavirus infections (111), they diverge in the degree to which the enzyme is observed to be required for virus replication. Maciejewski *et al*. reported a striking reduction in virus titers for CVB3 infection in TDP2 KO MEF cells, whereby virtually no new infectious particles were produced over the course of one infectious cycle (10 hpi) or after multiple replication cycles (24 hpi) (111). Additionally, the authors reported that for poliovirus infection in the absence of TDP2, although virus titers do increase over the infection time course, they do not reach the level of those obtained from WT TDP2 MEF cells by the end of the infectious cycle (111). In contrast, we observed only a modest decrease (~0.5 $\log_{10}$ units) in virus production for CVB3 at 4 hpi in TDP2 KO hRPE-1 cells. Only when we infected cells at a lower MOI of 0.1 did we see a more substantial reduction (1-1.5 $\log_{10}$ units) in virus titers. Furthermore, while we observed a considerable growth kinetics delay at 4 hpi for poliovirus (~2 $\log_{10}$ units), virus production was fully recovered by the end of the infectious cycle.

As alluded to previously, we suggest that this difference in phenotype may be due to the cell models used. While we demonstrated that the eukaryotic initiation factor eIF4G is cleaved in both WT and KO TDP2 hRPE-1 cells during poliovirus infection, indicating that

host cap-dependent translation is shut-off by the virus, host translation continues to occur throughout CVB3 infection of MEFs (Ullmer and Semler, unpublished). Therefore, it is possible that the apparent competition between host and viral mRNAs for ribosomes/translation resources in MEFs might amplify the defect in virus replication precipitated by the presence of VPg on the viral RNA, thus leading to the more dramatic growth phenotype observed in MEFs. This could explain why picornaviruses have evolved to remove VPg from their RNA in the first place. While the virus might be able to recover from a relatively minor delay in virus production during infection of cultured cells, this delay might become more deleterious to the progression of the virus infection in an *in vivo* context. This is because: 1) the virus would have to contend with the host immune system; and 2) the MOI of a natural infection is orders of magnitude lower than what is routinely used in cell culture. In support of this proposition, we have demonstrated that the growth delay in the absence of TDP2 is augmented at a lower MOI. Because picornaviruses infect multiple cell types during an *in vivo* infection, all of which might not be ideal to the same degree for virus replication, it would make sense for the virus to employ a mechanism to ensure that a small defect inherent to its replication strategy could be overcome. In fact, it has been demonstrated that SK-OV-3 cells express lower endogenous levels of the protein hnRNP C (an important host factor for picornavirus replication), which leads to a delay in poliovirus RNA synthesis (25). This is a defect which could synergize with the delay observed due to the presence of VPg on the RNA, leading to a major loss of virus infectivity, similar to what was observed for CVB3 in MEF cells. Ultimately, any intrinsic disadvantage to virus replication should be selected against, and, regardless of the extent (which may be context-dependent) it is clear that picornaviruses depend on TDP2 carry out their replication cycles efficiently.

In this study, we showed for the first time that not only do picornaviruses require the presence of TDP2 for efficient virus replication, but they specifically rely on the 5’

phosphodiesterase activity of the enzyme. This finding is not trivial given that TDP2 has other cellular roles aside from its DNA repair function which have also been shown to be involved in the replication cycle for several picornaviruses (102). Moreover, we determined that a redundant 5' phosphodiesterase is not activated at late times of picornavirus infection to account for the increase in virus replication observed. This suggests that the step in the replication cycle affected by the presence of VPg on the RNA is only inefficient but not completely defective, and by virtue of either a feature inherent to the mechanism itself or another parallel facet of the virus infection, the defect can eventually self-correct. We also determined that poliovirus can utilize all three isoforms of TDP2 to carry out efficient virus replication.

Given that the magnitude of the growth delay phenotype observed in TDP2 KO hRPE cells is dependent upon the amount of input virus in the inoculum, and is recovered at mid- to late times of infection (during the phase in which RNA is amplified exponentially), this makes RNA synthesis an attractive candidate as the step which requires the removal of VPg from the RNA. Consistent with this idea, we found that polysome association with viral RNA is unaffected in the absence of TDP2 and that the majority of viral RNA was recovered from the low polysome fraction for both WT and KO TDP2 cells at 2 and 4 hpi. Previous work showed that a functional translation initiation complex can be formed on VPg-linked RNA *in vitro* (62), and our data from cell culture infections are consistent with this observation. Although earlier studies found that polysome-associated viral RNA isolated from whole cell lysates is not linked to VPg, our findings suggest that there is likely a pool of VPg-linked RNA that is also translated, even in the presence of TDP2/VPg unlinkase. The proportion of total polysome-associated viral RNA that this pool might occupy, however, remains to be determined.

In contrast to the effect on translation, the overall levels of viral RNA recovered from the polysome fractions were reduced in the absence of TDP2 at 4 hpi, compared to what was recovered from WT cells. This suggests that although VPg-linked RNA can be translated efficiently, it fails to amplify at mid-times of infection. This result was validated by a time course analysis of both positive and negative-sense RNA production, as well as by immunofluorescence assays demonstrating that dsRNA formation (representative of viral RI and RF from positive- and negative-strand RNA synthesis, respectively) is reduced in TDP2 KO cells at 2 and 4 hpi. Additionally, we determined that virus protein production is also diminished at 4 hpi. As mentioned above, viral protein accumulation is an amalgamation of the output from both translation and RNA synthesis. Putting these results in the context of our findings from the polysome profiling experiments, the observed delay in protein production is most likely explained by the failure of the RNA to amplify. This conclusion is supported by results obtained from infecting WT and KO TDP2 cells with a bicistronic polio/EMCV virus in which the poliovirus IRES drives P1 structural protein expression while the EMCV IRES drives P2 and P3 non-structural protein expression. Although WT EMCV infection was unaffected in the absence of TDP2, the bicistronic virus could not replicate efficiently in TDP2 KO cells. This indicates that although translation can proceed normally in the absence of TDP2, this still does not rescue the growth delay phenotype, further suggesting that a step downstream of translation is affected by the presence of VPg on the viral RNA.

At the time when TDP2 was discovered as VPg unlinkase, it was proposed that removal of VPg early on during the replication cycle might act to prevent nascent RNA from being packaged prematurely (111, 185). If this were the case, we would expect to see an early boost in virus particle production in TDP2 KO cells compared to WT followed by an immediate plateau (i.e., logarithmic growth). This growth pattern has never been observed; however, one reason to account for this is that resolution of this difference at early time points

might not be achievable by plaque assay. The growth kinetics data obtained from TDP2 KO MEFs for poliovirus and CVB3 infection fit better with this explanation than do our results in hRPE-1 cells. Still, it is possible that a delay in virus particle production caused by premature encapsidation might also eventually be overcome in the absence of TDP2, leading to the phenotype that we observe in hRPE-1 cells. However, we demonstrated that the delay in protein production that occurs at mid-times of infection in the absence of TDP2 is not rescued by blocking RNA packaging using the inhibitor hydantoin, suggesting that encapsidation of VPg-linked RNA is not responsible for the phenotype.

We directly tested if the presence of VPg on the RNA impairs the step of RNA synthesis. We observed that transfection of proteinase-K treated virion RNA resulted in a partial rescue of the decrease in both positive and negative-strand RNA production that occurs in TDP2 KO cells. Moreover, there was a slight increase in RNA production that was observed at 4 and 5 hpt in KO TDP2 cells transfected with proteinase K-treated virion RNA compared to those transfected with the mock-treated RNA. This demonstrates that the removal of VPg is at least minimally required for efficient RNA synthesis. We propose that the presence of VPg at the 5' end of the RNA might hinder the formation of the PCBP2/3CD RNP complex at the cloverleaf structure, a step that is required for both positive and negative-strand RNA synthesis. Our model for this scenario is depicted at the end of **Chapter 4**.

Another possibility to explain the growth phenotype we observed and why VPg is removed is that the presence of VPg on the RNA may act as a mark for viral RNA degradation/sequestration as opposed to protecting the RNA from being targeted by host mRNA decay machinery. It is known that, although the 5' monophosphate that is revealed upon hydrolysis of VPg from the RNA is likely shielded by the binding of the PCBP2/3CD RNP complex and that this prevents degradation of the viral RNA (11). Poliovirus has been shown to antagonize the 5'-3' exoribonuclease decay pathway by accelerating the rate of

proteasome-mediated degradation of XRN1 and by $3C^{pro}$ cleavage of the de-capping enzyme, DCP1 (178). This begs the question of why the virus would evolve to downregulate this pathway if it should ultimately have no effect on the viral infection. Moreover, poliovirus has been demonstrated to disrupt the formation of both stress granules and P bodies (38), two types of cytoplasmic foci that are involved in the sequestration, degradation, and/or silencing of cellular mRNAs (38). Additionally, the mRNA decay protein AUF1 has been shown to act as an antiviral factor, whereby KO of the protein enhances picornavirus replication (177).

Given that RNA-protein 5' phosphotyrosyl bonds similar to that which links VPg to the viral RNA have not yet been described in the uninfected cell and that the presence of DNA linked to protein by 5' phosphotyrosyl bonds in the cytoplasm is likely a signal for the activation of innate immune pathways (202), it is conceivable that picornaviruses might have evolved to ensure that this bond is not recognized by the host. One way that this could be accomplished is by hydrolyzing VPg from the RNA immediately upon infection. However, given the existence of the mRNA decay pathways mentioned above, any putative deleterious effects of maintaining the VPg on the viral RNA would have to be counterweighed with the risk of exposing the 5' monophosphate. Overall, picornaviruses must manage a fine balance between the multitudinous, and at times, opposing activities that they undertake in order to wrest control of the host cell, which is no small feat for these small (but mighty) RNA viruses.

Materials and methods

Cell culture and virus stocks

Wild type (WT) and knock-out (KO) TDP2 hTERT RPE-1 (hRPE-1) cell lines were generated as described by Gomez-Herreros, *et al*. (64). WT, KO, GFP-tagged, and FLAG-tagged TDP2-expressing hRPE-1 cells were grown as monolayers in Ham's F-12 media containing 10% fetal bovine serum. The latter two cell lines were also grown in the presence of 800 µg/ml G418. HeLa cells used for plaque assays were grown as monolayers in Dulbecco's modified Eagle's medium (DMEM) containing 8% newborn calf serum (NCS). HeLa cells used for the purpose of generating virus stocks were grown in suspension culture in suspension minimal essential medium containing 8% NCS and subsequently in methionine-free DMEM.

Poliovirus-1 (Mahoney strain), coxsackievirus B3-0, and EMCV were used to infect WT and KO TDP2 hRPE cells or tagged TDP2-expressing cells. Radiolabeled poliovirus virion RNA was generated using the W1-VPg31 virus (94). EMCV/polio bicistronic virus was generated from the construct pT7RibPVE2A(MluI) (188). Luciferase-expressing poliovirus was generated from the construct pT7R-Luc-PPP (7). All virus stocks except PV-PPP were expanded by three serial passages in HeLa cells.

Generation of ^{35}S-Methionine-labeled VPg-linked RNA substrate and VPg unlinkase assay

W1-VPg31 virus was used to generate the ^{35}S-methionine (^{35}S-met)-labeled VPg-linked RNA substrate as described by Rozovics *et al*. (154). Briefly, ~8x10^9 HeLa cells were grown in suspension culture and subsequently infected with W1-VPg31 at a MOI of 20. The infected cells were methionine-starved for 2 hours, after which 2.5 mCi of ^{35}S-met was added to the infected cell suspension in a dropwise fashion. The cells were then incubated for 3.5 additional hours. Virion RNA (vRNA) was then purified from the infected, radiolabeled cells as previously described (154).

The rapid *in vitro* VPg unlinkase assay was carried out as described (154). In brief, 1 µl of radiolabeled vRNA substrate (equivalent to 1000-5000 CPM) was incubated with recombinant TDP2, whole cell lysates, or RNAse A in unlinkase buffer (20 mM Tris-HCl, pH 7.5, 1 mM DTT, 5% (v/v) glycerol) and in the presence of 2 mM for a total of 30 minutes at 30°C. Reactions mixtures were preincubated without the vRNA for 10 minutes after which time the RNA was added. Reactions were then incubated further for 20 minutes at the indicated temperature. The reactions were subsequently loaded onto an SDS-containing, 13.5% polyacrylamide gel in Tris-tricine and resolved by electrophoresis for 3.5 hours. The gel was dried for 1 hour and visualized by autoradiography using a phosphor screen. TDP2 recombinant proteins used included GST-tagged TDP2 that was expressed from the pGEX-2TK2-GST-EAPII plasmid kindly provided by Runzhao Li, formerly of Emory University; 6x histidine-tagged WT, or catalytically inactive TDP2 that was expressed from the pET-15b vector. Lysates included those generated from the follow cell lines: WT or KO TDP2 hRPE-1; FLAG-tagged WT or catalytically inactive TDP2-expressing hRPE-1; GFP-tagged TDP2 isoform-expressing hRPE-1.

Generation of tagged TDP2-expressing hRPE cell lines

Flag-tagged TDP2-expressing hRPE-1 cells were generated using the hTERT RPE-1 cell line ablated of TDP2 by CRISPR/Cas9 targeting exon 4 (KO hRPE-1). WT TDP2 or TDP2 containing an alanine point mutation at position 351 in the polypeptide (H351A) was excised from the pET-15b plasmid with XbaI and EcoRI and purified by gel extraction. The purified product was amplified by PCR using forward 5’ GGAAGTCTAGAATTTGGGGAGTTGCC and reverse 5’ GGAAGGAATTCTTATTATATCTAAGT 3’ primers, subsequently digested with EcoRI and KpnI, and ligated into the N-terminal pCMV-FLAG vector (Sigma) which was also digested with EcoRI and KpnI and treated with alkaline phosphatase. Products of the ligation

reaction were sequenced and purified using a cesium chloride gradient. KO TDP2 hRPE-1 cells were seeded onto 10 cm^2 plates and were subsequently transfected with the pCMV-FLAG-TDP2, FLAG-H351A, or empty FLAG vector as a negative control using jetPRIME transfection reagent (Polyplus transfection). G418-resistant colonies were isolated and expanded. Clones were maintained in Ham's F12 medium containing 10% FBS and 2 mg/ml G418. FLAG-TDP2 expression was verified by Western blot analysis.

GFP-tagged TDP2 isoform-expressing cells were generated similarly on the KO hRPE-1 cell line. KO hRPE-1 cells were transfected with plasmids containing GFP-tagged versions of the α, β, or γ TDP2 isoforms using the Neon transfection system (Thermo-Fisher). Clones were selected using G418. The GFP-tagged TDP2-expressing hRPE-1 cell lines were kindly provided by Keith Caldecott at the University of Sussex.

Virus infections and single cycle growth analysis

hRPE-1 cells were grown in monolayer in 6-well plates at a density of $4.0x10^5$ cells/well. Media was removed and cells were washed twice with 1X PBS and subsequently infected with either poliovirus or CVB3 at a MOI of 3 or, where indicated, 0.1. Virus adsorption was carried out at room temperature for 30 minutes for poliovirus and 45 minutes for CVB3. The cells were then washed once with 1X PBS, serum-containing media was added back to the cells, which were incubated at 37°C for the indicated time periods. Cells and supernatant were harvested and subjected to 4 freeze-thaw cycles. Infectious particle production was quantified by plaque assay. Virus yields are represented as plaque forming units per cell and plotted on a logarithmic scale. Experiment was done in biological triplicate. Error is reported as standard deviation of the mean.

Preparation of lysates from uninfected and infected cells and Western blot analysis

Cells were collected and centrifugated at 15,000 RPM in 1.5 ml Eppendorf tubes. The cell pellet was washed once with 1X PBS and resuspended in 1% NP-40 lysis buffer (50 mM Tris-HCl, pH 7.5, 150 mM NaCl, 1% (v/v) NP-40. Cell suspension was incubated on ice for 15 minutes. Debris was pelleted and protein concentration of the lysate was determined by Bradford assay. For Western blot analysis of eIF4G cleavage and poliovirus 3AB expression in WT and KO TDP2 cells, 50 µg of protein was loaded onto a 12.5% polyacrylamide-containing SDS gel, subjected to electrophoresis, and transferred onto a PVDF membrane. Membrane was blocked in 5% milk for 1 hour and incubated with the primary and secondary antibodies for 1 hour and 45 minutes, respectively. The membrane was washed 4 times in 0.01% PBS-tween in between primary and secondary antibody incubations. Anti-poliovirus 3A antibody (which also recognizes 3AB) was used at a dilution of 1:2000. The mouse monoclonal against 3A was kindly provided by George Belov, University of Maryland. The rabbit monoclonal antibody against eIF4G was purchased from Cell Signaling Technologies and was used at a dilution of 1:2000. Anti-pan enterovirus VP1 antibody (Dako) was used at a dilution of 1:1000; Anti-PKM2 (Bethyl) was used at a concentration of 1:5000 to detect endogenous PKM2 as protein a loading control. Anti-FLAG (Agilent) and anti-GFP (Abcam) were used at a dilution of 1:1000 to detect FLAG- and GFP-tagged proteins, respectively. Protein bands were visualized by ECL Western Blotting Substrate (Life Technologies).

Generation of *Renilla* luciferase reporter virus and luciferase assays

For the generation of *Renilla* luciferase-expressing polio reporter virus, Rluc-PV-PPP, RNA was *in vitro*-transcribed and subsequently transfected into HeLa cells. The construct pT7-Luc-PPP was linearized using PvuI prior to *in vitro* transcription. pT7-Luc-PPP was generously provided by Eckard Wimmer, Stony Brook University. Reactions were carried out using the MEGAscript T7 transcription kit (Thermo Fisher). Transfected cells were collected

24 hours post-transfection and subjected to 4 freeze-thaw cycles to release infectious virus. Cell debris was pelleted and supernatants were used to infect WT and KO TDP2 hRPE-1 cells.

Polysome profile analysis and quantitation of viral RNA production

Polysome analysis was carried out as described (48). WT and KO TDP2 hRPE cells were seeded onto five 10 cm^2 plates at a density of $7x10^5$ cell/plate. Cells were infected with poliovirus as described above and incubated for the indicated times at 37°C. The infected cells were then incubated with cycloheximide diluted in 50% ethanol at a concentration of 30 mg/ml for 3 minutes. Media was removed and cells were subsequently washed once with 1X PBS containing 30 mg/ml cycloheximide. Cells were scraped into 10 ml of 1X PBS containing cycloheximide and centrifugated at 1,500 RPM for 5 min. PBS was removed and cells were resuspended in 1.6 ml of polysome lysis buffer (300 mM NaCl, 15 mM $MgCl_2$, 10 mM Tris-HCl, pH 7.5, 1% (v/v) Triton-X) with 10 µg/ml cycloheximide for 30 min on ice. Cell suspension was centrifugated at 14,000xg, debris was removed, and the lysates were frozen at -80°C. The samples were subsequently thawed on ice, 800 µl of which was applied to a continuous 10-50% sucrose gradient, and centrifugated at 30,000 RPM in a SW41 swinging bucket rotor for 2 hours at 4°C. The remaining 800 µl of lysate was used to represent the total viral RNA content. Samples were removed and subjected to polysome profile analysis on a in which twenty 500 µl fractions were generated. The first 10 fractions were recovered for analysis as viral RNA was not observed in fractions beyond number 10 (data not shown). The fractions were subsequently frozen at -80°C until further analysis.

Samples were thawed on ice and RNA content from each fraction was purified by phenol-chloroform extraction. Samples from fractions 1-2, 3-4, 5-6, 7-8, and 9-10 were pooled. In parallel, RNA was extracted from the equivalent volume of unfractionated sample

using the TRIzol reagent (Invitrogen). RNA concentration was measured in the pooled fractions and the unfractionated sample, and cDNA was prepared from 1 µg of total cellular RNA. One-step, real-time quantitative PCR (qRT-PCR) using SYBR green (Thermo-Fisher) was then carried out to quantitate poliovirus RNA levels. qRT-PCR analysis was done in technical duplicate. GAPDH mRNA levels were used as an internal control. RNA levels for the polysome analysis experiments were recorded as the relative expression value of polivorus RNA obtained from either the fractionated or unfractionated sample and are normalized to that of GAPDH. RNA production is plotted as the ratio of the normalized values obtained from the fractionated sample to those of the unfractionated sample. Time course analysis of RNA production followed the same steps as the preparation of polysome-associated RNA except that the levels of RNA are represented only as the normalized relative expression value.

Immunofluorescence assays

WT, KO TDP2, or TDP2 isoform-expressing hRPE-1 cells ($2.5x10^5$ cells/well) were seeded onto coverslips placed into 6-well plates. Cells were infected with poliovirus as indicated and fixed in 3.7% formaldehyde at room temperature at the indicated time points for 10 minutes. Formaldehyde was removed and fixed cells were washed twice in 1x PBS and subsequently stored at 4°C. The cells were subsequently permeabilized in 0.5% NP-40 in PBS for 5 min and were then washed 3 times with 1% NCS in 1X PBS. Cells were blocked in 1% donkey serum in 200 µl of 1% bovine serum albumin (BSA) for 30 minutes at room temperature. The cells were washed again 3 times with 1% NCS and incubated with the primary mouse monoclonal antibody against double-stranded RNA (J2, Scions) for 2 hours at a concentration of 1:200. The J2 antibody was diluted in 1% BSA. After incubation, the coverslips were washed 3 times with 1% NCS and then incubated with the fluorescent secondary anti-mouse

antibody (Dylight 488, Bethyl) for 30 minutes. Coverslips were then washed 3 times with 1% NCS and counterstained with DAPI to label nuclei. GFP-expressing cells were directly incubated with DAPI and were not treated with primary or secondary antibody. Coverslips were mounted onto microscope slides using Fluoro-gel (Electron Microscopy Sciences) and imaged using a Zeiss LSM700 confocal fluorescence microscope at 63x magnification.

Encapsidation inhibition assays

WT TDP2 hRPE cells were seeded into 6-well plates at a density of $2.5x10^5$. Virus infections were carried out as previously described in "Virus Infections and Single Cycle Growth Analysis" section in the presence of 6.25, 12.5, 25, 50, or 100 µg/mL of Hydantoin or DMSO alone as a negative control. Cells were subsequently harvested 6 hours post-infection and analyzed for infectious particle production by plaque assay or for RNA production by qRT-PCR.

Proteinase K treatment of virion RNA and transfections of hRPE-1 cells

Virion RNA was prepared from HeLa suspension cells as described. vRNA (1 µg) was either treated or mock-treated with 20 mg/ml of proteinase K in buffer (10 mM Tris-HCl, pH 7.5, 100 mM NaCl, 25 mM EDTA, 0.5% SDS) for 30 minutes at 37°C. The RNA was phenol-chloroform extracted from the reaction mixture and 20 ng of either treated or mock-treated RNA was subsequently transfected into WT and KO hRPE-1 cells (density=$4.0x10^5$/well in a 6-well plate). Cells were collected at 4, 5, or 6 hours post-transfection and RNA was extracted using TRIzol for subsequent qRT-PCR analysis.

CHAPTER 3

Differential patterns of TDP2 and VP1 subcellular localization during picornavirus infections of multiple human cell lines

Summary

In this chapter, we sought to characterize the localization pattern of TDP2 VPg unlinkase and the picornavirus structural protein, VP1, during poliovirus or CVB3 infection in a panel of human cell lines. Specifically, we aimed to determine if the previously reported expression patterns of both proteins were consistent across multiple cellular contexts. We found that TDP2 is relocalized from the nucleus to the cytoplasm during both poliovirus and CVB3 infection in HeLa cells, albeit with different kinetics. Moreover, the appearance of TDP2 in the cytoplasm was observed during poliovirus infection of HEK-293, SK-N-SH, and MCF7 breast cancer cell lines, although the kinetics of relocalization were slower as well in HEK-293 and MCF7 cells, which displayed substantial cytoplasmic TDP2 staining starting at 6 hpi, compared to in SK-N-SH and HeLa cells, for which this occurred earlier at 4 hpi. Importantly, we demonstrate TDP2 sequestration to the cell periphery away from sites of viral encapsidation (represented by the capsid protein, VP1), which was shown in (185) and proposed to be a mechanism to regulate VPg unlinkase activity, appears to be a HeLa-specific phenomenon. This suggests that sequestration of TDP2 may not be a general mechanism used by picornaviruses to modulate TDP2 enzymatic activity during infection. Additionally, we show for the first time that VP1 enters the nucleus of MCF7 cells, but not of HeLa cells, and colocalizes with TDP2 in the nucleus. Thus, while TDP2 relocalization away from encapsidation sites in the cytoplasm at late times post-infection appears to be HeLa-specific, TDP2 might have interactions with VP1 in the nucleus which could have implications for virus infection and how TDP2 activity might be regulated throughout the infection time course.

Introduction

Picornaviruses, like other positive-sense RNA viruses, replicate exclusively in the cell cytoplasm. Despite this fact, these viruses also have extensive interactions with the host nucleus (50). Picornavirus alterations to host RNA nuclear import and export pathways have been well-described in the literature, a task that is carried out by the virus in order to hijack RNA binding proteins for their replication cycles. Central to this process is the proteinase, $2A^{pro}$, encoded by members of the *Enterovirus* genus. $2A^{pro}$ has been shown to cleave components of the nuclear pore complex (NPC), specifically Nup98, Nup153, and Nup62 (29, 74) leading to a bi-directional increase in nuclear envelop permeability (15). Additionally, members of the *Cardiovirus* genus have also been demonstrated to block nuclear export, but through a different mechanism. The 2A peptide of cardioviruses does not possess proteolytic activity. Instead, these viruses express what is known as the L or Leader protein, which causes alterations to the NPC via hyper-phosphorylation of several Nups (141, 142) including Nup 98 (149).

In a recent report (49), Flather *et al*. elegantly demonstrated that nuclear-cytoplasmic trafficking is disrupted during HRV16 infection of HeLa cells, leading to the retention of an extensive set of RNA binding proteins in the cytoplasm at mid-times of infection. Mass spectrometry analysis of the relocalized peptides identified a novel host factor that participates in HRV16 replication called SFPQ (49), or splicing factor proline and glutamine-rich. In the same study, the authors observed nuclear localization of the protein precursor, 3CD, a result that corroborates earlier findings demonstrating that either 3CD, or the mature form of the protein, $3D^{pol}$, translocates to the nucleus during infection with select picornaviruses (194). In particular, $3D^{pol}$ of EV71 was shown to relocalize to the nucleus during viral infection and interact with human pre-mRNA splicing factor 8, a core component of the human spliceosome complex (108). Importantly, this result was also observed for

poliovirus $3D^{pol}$ but not for the RdRps of the closely related picornaviruses CVB3 or HRV16, demonstrating a virus-specific effect in the disruption mRNA splicing mediated by a nuclear-localized viral protein. Other studies have reported divergent effects of the proteinase activity of $2A^{pro}$, specifically that different strains of HRV preferentially target either nuclear export (HRVC15) or import (HRVB04 and HRVB52) pathways (193). The authors of this latter study suggest that this differential proteolytic activity of $2A^{pro}$ on the NPC may have implications for the diversity of disease phenotypes elicited by HRV infections.

Another virus-specific effect on nuclear-cytoplasmic trafficking has been observed during infection with CVB3. This virus has been shown to induce the translocation of the VP1 structural protein to the nucleus (191), which has been demonstrated to mediate the arrest of the cell cycle in the G1 phase to promote CVB3 replication (47). The effect was shown to be mediated by VP1-induced upregulation of the heat shock protein, Hsp70 (192). The nuclear localization of poliovirus VP1 has also been demonstrated in HEp2 (human epithelial type 2) cells (18), but whether this extends to other cell types is unknown.

In the landmark study identifying the nuclear DNA repair enzyme, TDP2, as VPg unlinkase for picornaviruses (185), the authors noted that poliovirus relocalizes TDP2 from the nucleus to the cytoplasm at mid-times of infection in HeLa cells. Furthermore, TDP2 was demonstrated to form a distinctive pattern, whereby the protein is localized to the cell periphery and is adjacent to, but does not co-localize with, a marker of viral replication complexes (viral protein 3A) or viral encapsidation sites (viral capsid protein VP1) suggesting that TDP2 may be excluded from these complexes at late times of infection. TDP2 unlinkase activity levels do not change throughout the course of the replication cycle in both HeLa cells (154) and hRPE-1 cells (**Chapter 2**); however, the virus must establish a dynamic balance between the pool of VPg-linked vs. unlinked RNA throughout the course of infection. Specifically, the virus must shift from an RNA synthesis-dominant mode of replication at mid-

times of infection, to an encapsidation-dominant mode, in which the majority of the nascent, positive-sense, VPg-linked RNA synthesized is packaged instead of being used as a template further rounds of RNA synthesis. Therefore, it is logical to hypothesize that sequestration of TDP2 away from nascent VPg-linked RNA in replication complexes could act as the regulatory mechanism of VPg unlinkase activity during virus infection. If relocalization is a general mechanism that picornaviruses use to modulate TDP2, then the expectation is that the pattern of TDP2 localization should be consistent across multiple picornavirus species and in different cell types. Whether this is the case, however, remains to be determined.

Given that there are species-specific differences in the mechanisms by which nuclear-cytoplasmic trafficking pathways are altered by picornaviruses, in addition to the differential effect of TDP2 VPg unlinkase on virus replication ((111) and **Chapter 2**) we set out to characterize the pattern of TDP2 localization during picornavirus infections. Specifically, we wanted to determine if the distinctive pattern of TDP2 expression observed during poliovirus infection of HeLa cells is consistent across multiple cell types and for other picornaviruses. To do this, we determined TDP2 localization relative to that of either 3A or VP1 in multiple human cell lines. We hypothesize that different picornaviruses may utilize divergent mechanisms to regulate TDP2 VPg unlinkase activity based on the degree to which they rely on the enzyme for efficient replication and that TDP2 sequestration away from sites of virus encapsidation might be cell type-specific.

Results

TDP2 is re-localized to the cell periphery in poliovirus-infected HeLa cells at 4 and 6 hpi

Although encapsidated picornavirus RNA is VPg-linked, while viral mRNA in presence of VPg unlinkase is not, the mechanism by which unlinkase activity is regulated in order to achieve this difference remains unknown. As mentioned previously, Virgen-Slane *et al*. noted an intriguing pattern of TDP2 localization at late time during poliovirus infection of HeLa cells, wherein the protein appeared to be concentrated at the cell periphery, separate from sites where viral replication and encapsidation should be occurring. This was determined by confocal immunofluorescence (IF) microscopy using the replication complex-associated protein, 3A, and capsid protein, VP1, as markers of RNA synthesis and packaging sites, respectively (185). However, prior to the present study, TDP2 re-localization to sites distinct from RNA replication and encapsidation had not been demonstrated in poliovirus infection of cell lines other than HeLa or during other picornavirus infections. At the outset of the current project, we decided to repeat the previous microscopy experiments carried out in (185), in an effort to confirm these results. We infected HeLa cells with poliovirus and fixed cells at 0, 2, 4, or 6, hpi. We then carried out IF assays on the fixed cells, probing for TDP2 and 3A or VP1, and imaged them using confocal fluorescence microscopy. As demonstrated in **Figure 3.1, A and B**, the pattern of TDP2 localization identified in (185) can be observed, in which the protein has been moved to the cell periphery, adjacent to the 3A or VPI proteins. This observation was the most prominent at 6 hpi. A magnified image of TDP2 at the periphery is depicted in **Figure 3.1, C**. We also quantified the number of cells displaying the pattern (detectable starting at 4 hpi) which is shown in **Figure 3.1, D**. TDP2 localization to the cell periphery is not uniform, however, and is present in only ~40% of infected cells at 4 hpi and in ~50% at 6 hpi.

Figure 3.1 TDP2 is re-localized to the cell periphery in poliovirus-infected HeLa cells at 4 and 6 hpi. HeLa cells were seeded onto coverslips placed into a 6-well plate. Cells were plated at a density of $5x10^5$ cells/well. Seeded cells were then infected with poliovirus at a MOI of 20 and fixed in 3.7% formaldehyde at the indicated times post-infection. Fixed cells were permeabilized, blocked in 1% BSA, and incubated sequentially with a rabbit anti-TDP2 (Bethyl, 1:200) and A) mouse anti-pan enterovirus VP1 (1:200) or B) mouse anti-3A (1:500) (3A was generously provided by George Belov, University of Maryland). Cells were counterstained with DAPI to visualize nuclei. Coverslips were mounted onto microscope slides and imaged with a Zeiss LSM 700 microscope at 63x magnification. C) 4x magnified version of the 6 hpi time point depicted in A) and B). TDP2 localization to the cell periphery is indicated with white arrows. D) Quantification of the percentage of infected cells displaying TDP2 localization to the periphery at 4 and 6 hpi. 100 cells were counted per experiment. Statistical error is represented as the standard deviation of the results from three separate experiments.

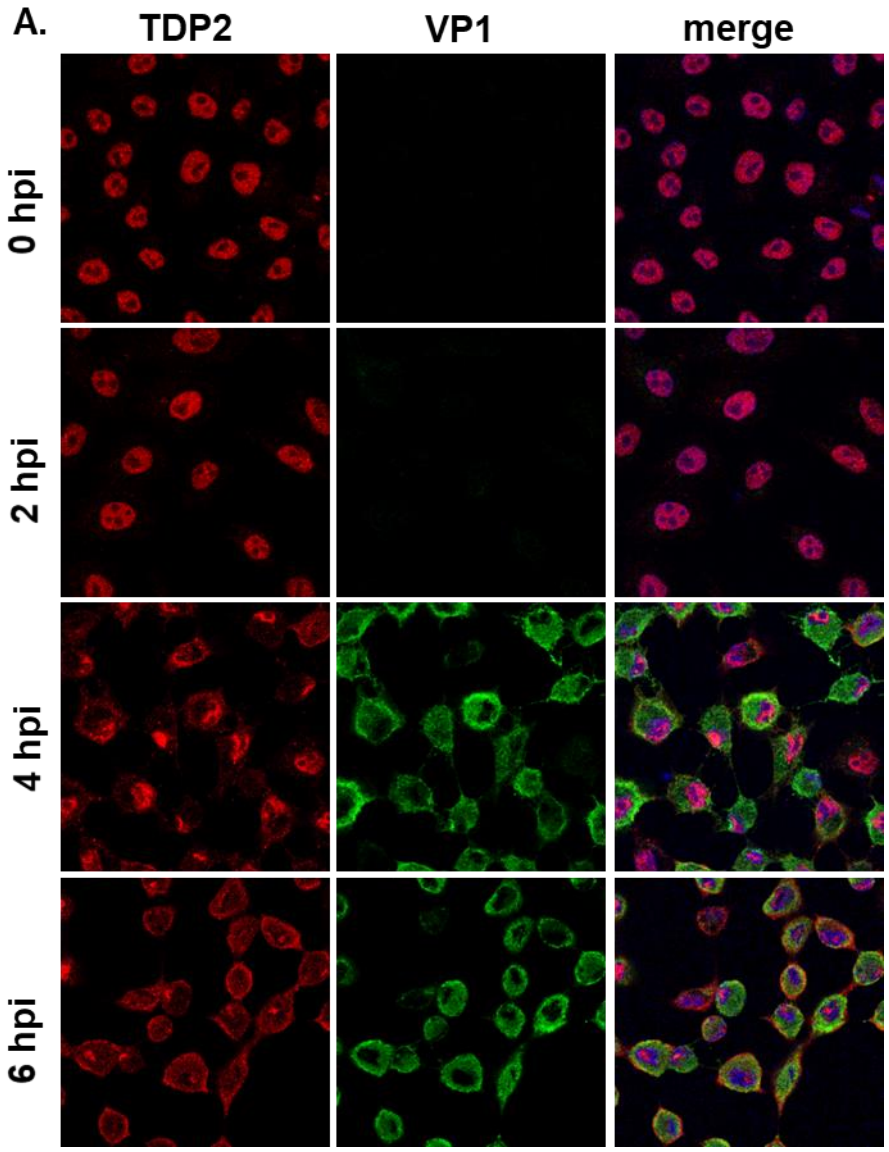
A.
TDP2
VP1
merge
0 hpi
2 hpi
4 hpi
6 hpi

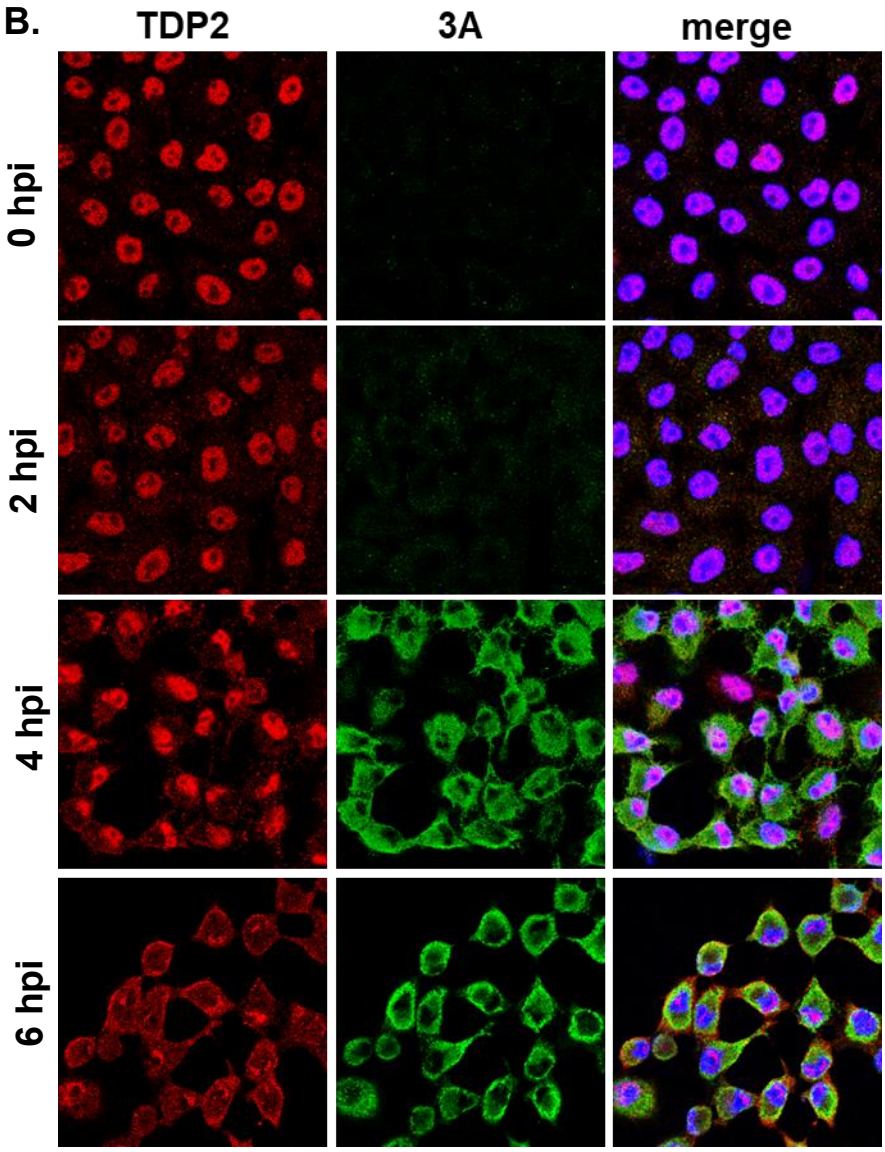
B.
TDP2
3A
merge
0 hpi
2 hpi
4 hpi
6 hpi

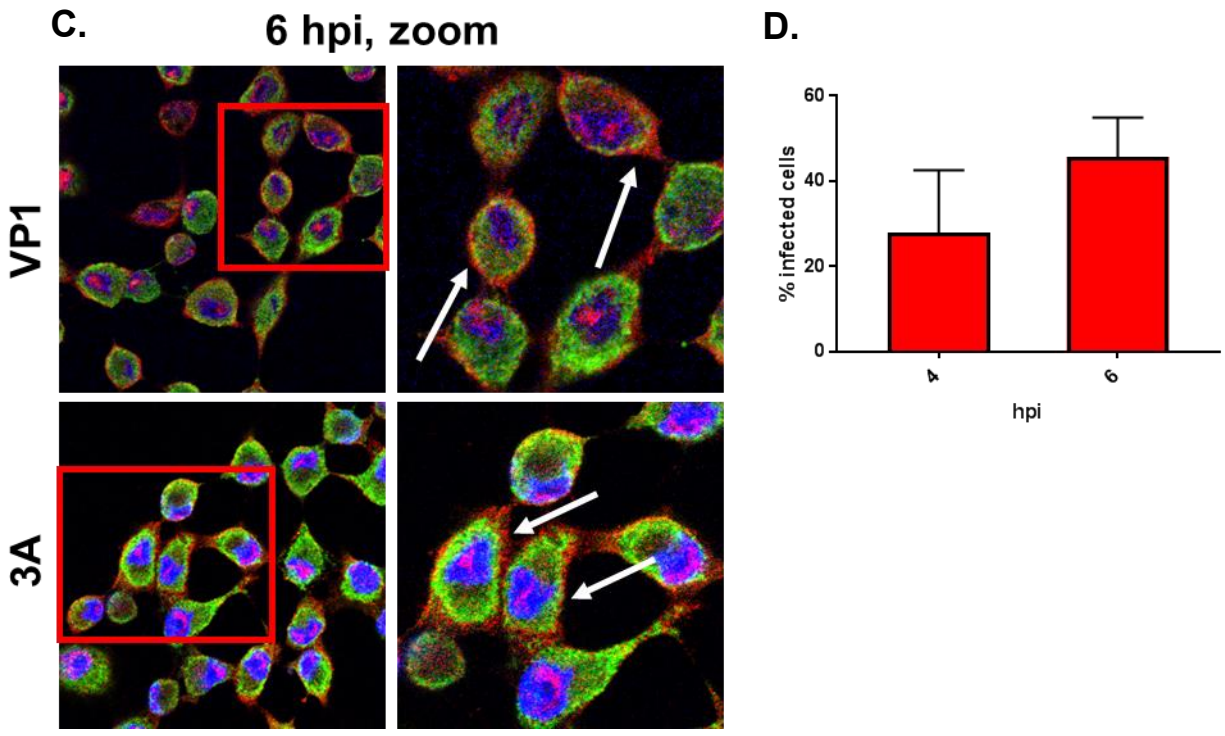
C.
6 hpi, zoom
VP1
3A
D.
% infected cells
60
40
20
0
4
6
hpi

TDP2 colocalizes with plasma membrane marker, PVR, at the cell periphery in poliovirus-infected HeLa cells at 6 hpi

We next wanted to determine the specific region where TDP2 is localized at the cell periphery late during infection. To do this, we carried out IF assays in poliovirus-infected cells wherein we probed for both TDP2 and the poliovirus receptor (PVR) (as a marker for the plasma membrane), which we hypothesized to be a site for relocalized TDP2. As demonstrated in **Figure 3.2, A and B**, TDP2 partially co-localizes with PVR at 6 hpi, which we confirmed by Z-stack analysis, suggesting that the virus does sequester a portion of cytoplasmic TDP2 to the plasma membrane at late times of infection in HeLa cells.

TDP2 does not relocalize to the cell periphery during poliovirus infection of HEK-293 cells

To determine if the pattern of TDP2 localization observed during poliovirus infection of HeLa cells is consistent across multiple cell types, we infected another human cell line permissive to poliovirus infection, HEK-293, and carried out IF assays. These results are depicted in **Figure 3.3, A**, with a magnification of the image in **Figure 3.3 B**. TDP2 is re-localized from the nucleus to the cytoplasm in poliovirus infection of HEK-293 cells, as was observed in poliovirus-infected HeLa cells. However, in contrast to infection of HeLa cells, TDP2 does not appear to be sequestered to a specific cellular location and is evenly distributed throughout the cytoplasm of HEK-293 cells. Notably, TDP2 partially co-localizes with VP1 at 6 hpi, which also contrasts with what we observed in HeLa cells. This suggests that there are cell type-specific differences that might influence how the virus relocalizes (and perhaps modulates) TDP2.

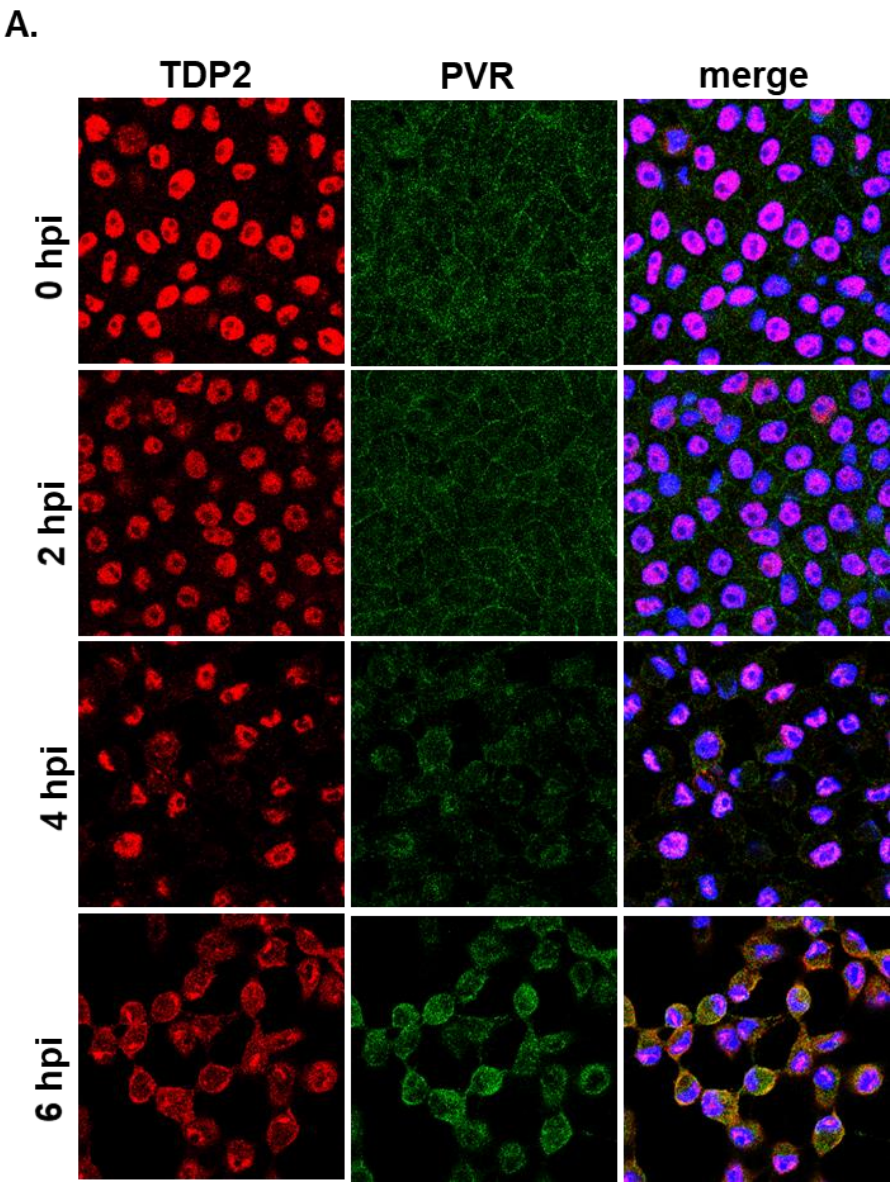

Figure 3.2 TDP2 colocalizes with plasma membrane marker, PVR, at the cell periphery in poliovirus-infected HeLa cells at 6 hpi. A) HeLa cells were infected with poliovirus at a MOI of 20, fixed at the indicated time points, and immunofluorescence assay was carried out as in the legend to Figure 3.1. Mouse anti-PVR (Abcam) antibody was used at a concentration of 1:200. PVR displays localization to the plasma membrane and partially colocalizes with TDP2 at 6 hpi. B) 4x magnified image of 6 hpi time point shown in A). Areas of colocalization between TDP2 and PVR are indicated by white arrows.

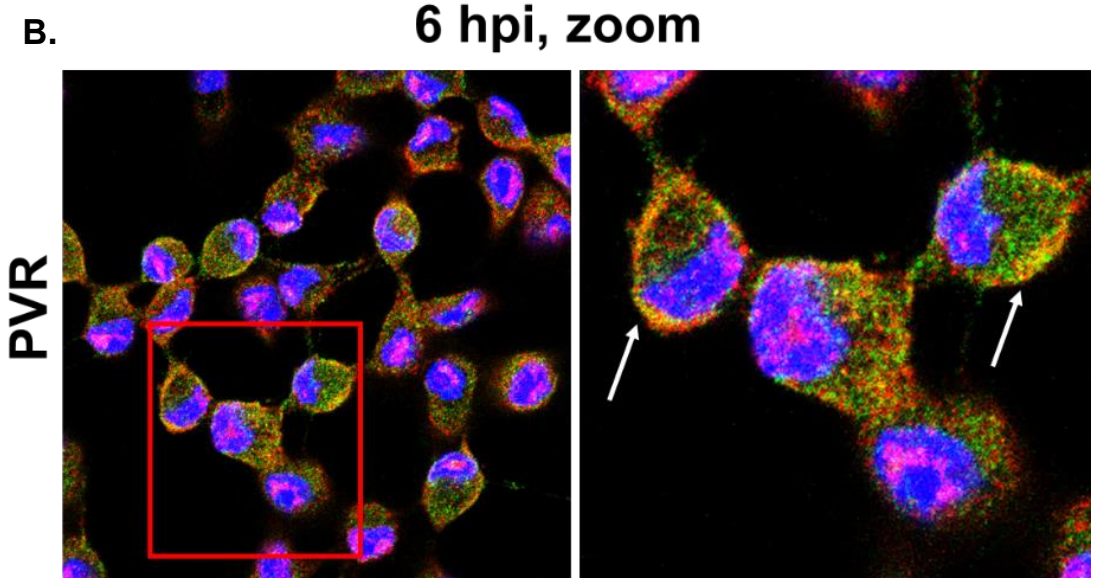
B.
6 hpi, zoom
PVR

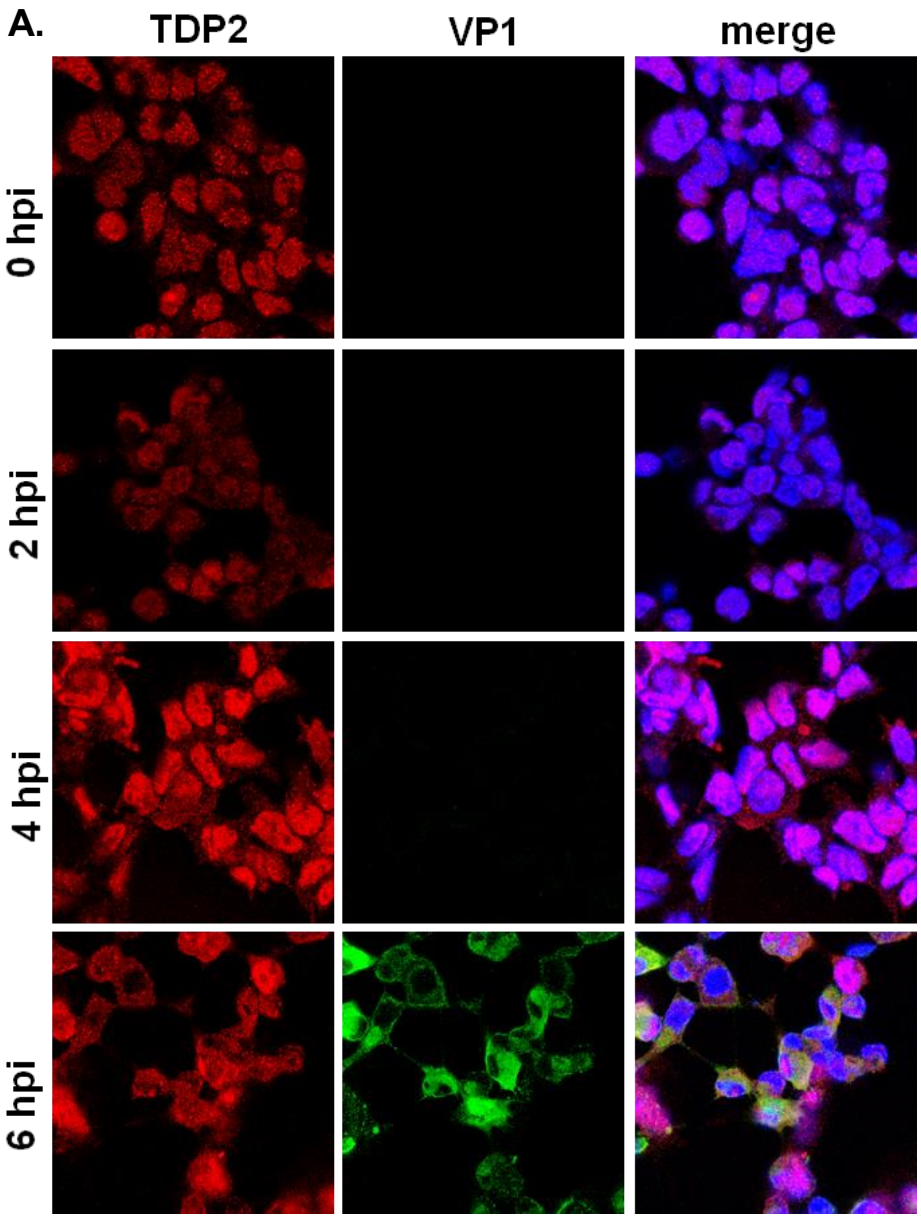

Figure 3.3 TDP2 partially colocalizes with poliovirus VP1 but does not relocalize to the cell periphery during infection of HEK-293 cells. A) HEK-293 cells were seeded at a density of $2.5x10^5$ cells/well onto coverslips placed into 6-well plates. Cells were infected with poliovirus at MOI of 20 and fixed in 3.7% formaldehyde. Immunofluorescence assays were carried out as described in Figure 3.1. B) 4x magnified image of 6 hpi time point depicted in A). TDP2 relocalizes from the nucleus to the cytoplasm starting at 4 hpi with complete cytoplasmic localization at 6 hpi.

B.

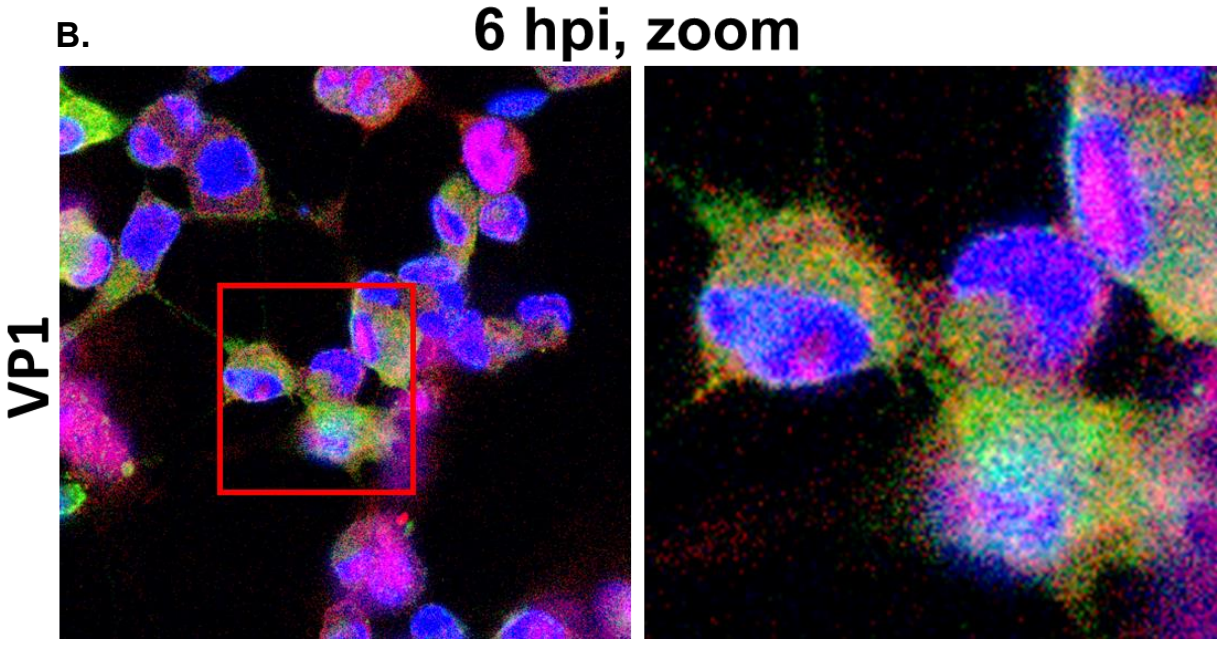

TDP2 forms cytoplasmic aggregates but does not relocalize to the cell periphery during poliovirus infection of SK-N-SH cells

Having observed that there is a divergence in how TDP2 is localized in HeLa vs. HEK-293 cells, we aimed to further examine this phenomenon using a cell line that is closer to the natural tropism for our viruses of interest. To this end, we chose SK-N-SH neuroblastoma cells. We infected cells with poliovirus, fixed cells at 0, 2, 4, and 6 hpi, and carried out IF assays on the fixed cells, probing for TDP2 and viral capsid. Consistent with the data obtained from the other cell lines, TDP2 is relocalized from the nucleus to the cytoplasm starting at 4 hpi (**Figure 3.4 A and B**). Interestingly, in contrast to infection of HeLa and HEK-293, TDP2 forms a punctate staining pattern in neuroblastoma cells in the cytoplasm. This is noteworthy given that TDP2 has been shown to localize to cytoplasmic aggregates in the brains of Parkinson's disease patients upon post-mortem analysis (184). This highlights a potential link between TDP2's role in neural maintenance and picornavirus neuropathogenesis. Importantly, however, for the current study, we found that the enzyme is also evenly distributed throughout the cytoplasm and is not sequestered to the cell periphery, similar to what we observed in HEK-293 cells. This suggests that relocalization of TDP2 to the plasma membrane is not a consistent feature of picornavirus infections and may be specific to a cell subset typified by HeLa cells.

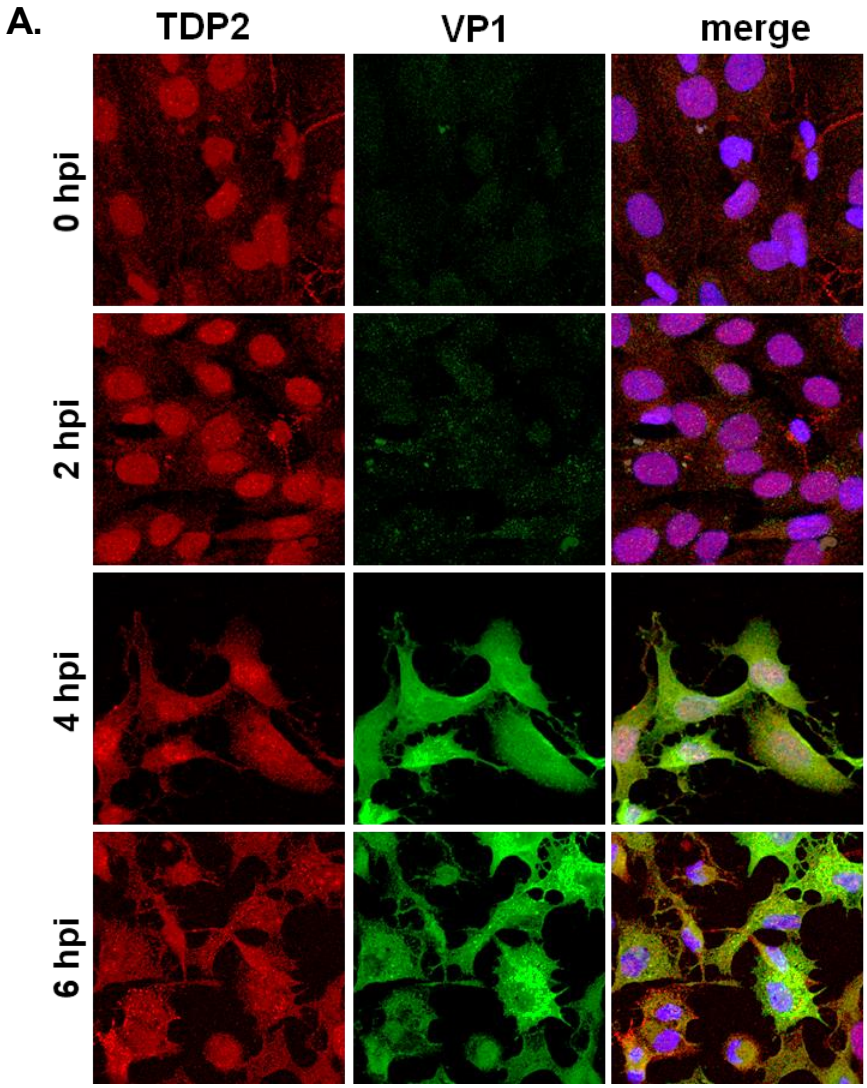

Figure 3.4 TDP2 forms cytoplasmic aggregates but does not relocalize to the cell periphery during poliovirus infection of SK-N-SH cells. A) SK-N-SH neuroblastoma cells were seeded onto coverslips placed into 6-well plates (density = $2.5x10^5$ cells/well). Cells were infected with poliovirus at MOI of 20 and fixed in 3.7% formaldehyde. Immunofluorescence assays were carried out as described in Figure 3.1. B) 4x magnified image of 6 hpi time point depicted in A). TDP2 forms cytoplasmic puncta and partially colocalizes with poliovirus VP1 at 6 hpi. Nuclear-cytoplasmic relocalization of TDP2 begins at 4 hpi. TDP2 has a mostly cytoplasmic distribution by 6 hpi.

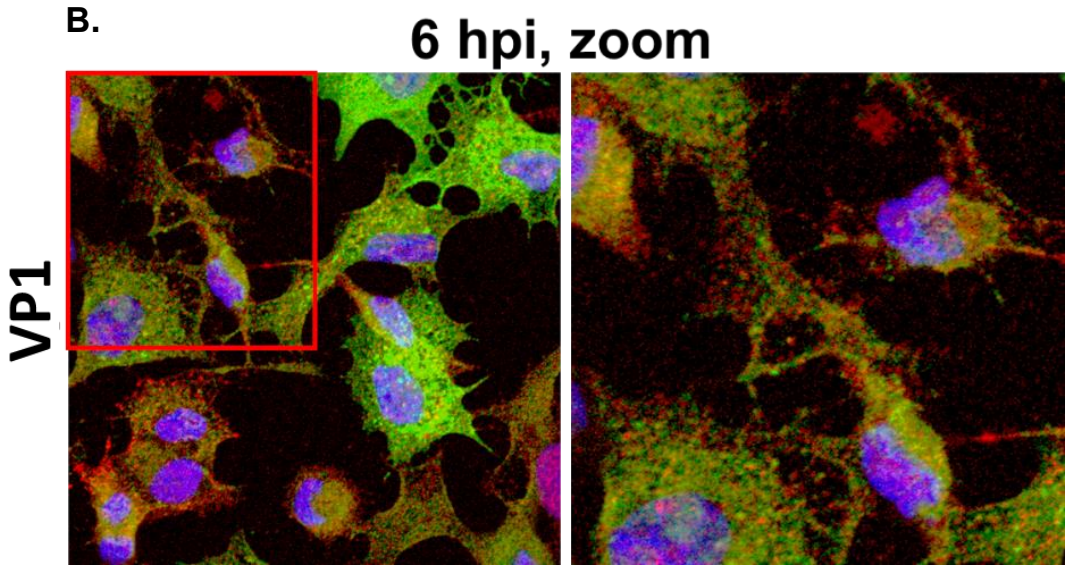
B.
6 hpi, zoom
VP1

Poliovirus and CVB3 VP1 translocates to the nucleus and colocalizes with TDP2 in MCF7 and HeLa cells, respectively

To test if the exclusion of TDP2 from putative replication and encapsidation sites extends beyond poliovirus infection, we infected HeLa cells with CVB3 and carried out IF assays on infected cells that were fixed at 0, 2, 4, or 6 hpi. As observed in **Figure 3.5, A**, CVB3 infection does not appear to elicit the same localization pattern of TDP2 as does poliovirus. The kinetics of relocalization of TDP2 to the cytoplasm are slower, and the protein is still mostly nuclear at 7 hpi. This is likely due, in part, to the fact that growth kinetics for CVB3 overall are slower than those of poliovirus (by about 1-1.5 hours). Furthermore, TDP2 staining is diffuse throughout the cytoplasmic during infection with CVB3. These results further suggest that TDP2 sequestration to the cell periphery at late times of infection in HeLa cells is likely a cell type- and virus-specific phenomenon, and not a general mechanism used by picornaviruses to modulate VPg uninkase activity.

As mentioned in the Introduction, the CVB3 structural protein, VP1, has been shown to possess a nuclear localization signal and can be visualized in the nucleus of transfected cells (191). This activity results in the arrest of the cell cycle, which contributes to virus replication (47, 192). Corroborating these results, we also observed VP1 staining in the nucleus by confocal fluorescence microscopy during CVB3 infection of HeLa cells starting at 5 hpi (**Figure 3.5, A**). To confirm the localization of VP1 to the nucleus, we infected HeLa cells with CVB3 and harvested the infected cells every hour from 0-7 hpi. We then utilized a commercially available kit (NE-PER, Invitrogen) to perform nuclear-cytoplasmic fractionation assays on the cell lysates. Finally, we carried out Western blot analysis on the fractions, probing for VP1. Interestingly, VP1 appeared in the nuclear fraction (at 5 hpi) before appearing in the cytoplasm, which did not occur until 6 hpi (**Figure 3.5, B**). This suggests that VP1 is likely translocated to the nucleus immediately after it is synthesized, a phenomenon

that has not been previously reported before for the protein during infection. Moreover, we also observed that CVB3 VP1 colocalizes with TDP2 in the nucleus (**Figure 3.5, C**), suggesting a putative interaction.

Nevertheless, CVB3 is currently the only picornavirus described in the literature to localize a structural protein to the nucleus. However, in our studies to determine if TDP2 localization to the cell periphery is generalizable across multiple cell types, we made the observation that poliovirus also induces translocation of VP1 to the nucleus during infection of MCF7 breast cancer cell lines, where the protein also colocalizes with TDP2 (**Figure 3.5 D**), a finding similar to what was observed during CVB3 infection. Notably, the kinetics of TDP2 relocalization to the cytoplasm in poliovirus-infected MCF7 cells are also similar to those in CVB3 infection of HeLa cells, whereby most of the staining for TDP2 is nuclear at 4 hpi. This, again, contrasts with the data obtained from poliovirus infection of HeLa and SK-N-SH cells, in which TDP2 noticeably begins to relocalize at 4 hpi (**Figure 3.1 A and B, and Figure 3.4 A**). Altogether, the data suggest the following: 1) there is likely an alternative mechanism other than TDP2 sequestration to the cell periphery at work to modulate VPg unlinkase activity during virus infection; 2) the kinetics of TDP2 nuclear-cytoplasmic relocalization during poliovirus infection are cell-type specific; 3) VP1 nuclear localization is both specific to the virus and host cell type.

Figure 3.5 Poliovirus and CVB3 VP1 translocates to the nucleus and colocalizes with TDP2 in MCF7 and HeLa cells, respectively. HeLa A) or MCF7 C) cells were seeded onto coverslips (density=2.5x10^5) and infected with CVB3 (HeLa) or poliovirus (MCF7) at a MOI of 20. Cells were fixed in 3.7% formaldehyde. Immunofluorescence assays were carried out as described in Figure 3.1. B) Western blot analysis of CVB3-infected HeLa cells that were subjected to nuclear-cytoplasmic fractionation assays using the NE-PER Nuclear and Cytoplasmic Fractionation Reagents (Thermo Scientific). 50 µg of protein from each fraction was loaded onto an SDS-PAGE gel. Protein bands were resolved for 2 hours at 200 V. Proteins were transferred onto a PVDF membrane overnight. Membrane was subsequently blocked in 5% milk and incubated with mouse anti-pan enterovirus VP1 (1:2000), rabbit anti-Lamin A (Bethyl, 1:1000) rabbit anti-PKM2 (Bethyl, 1:1000) and subsequent goat anti-mouse or rabbit horse radish peroxidase-conjugated secondary antibodies. Lamin A and PKM2 denote the nuclear (N) and cytoplasmic (C) fractions, respectively. Western blots of the 6 and 7 hpi time points and mock-infected sample was carried out on the same day but was loaded onto a different gel due to lane number constraints. Images of these data were spliced onto the image showing the data from the 0-5 hpi time points as depicted. (D) 4x magnified image of 6 hpi time point depicted in A) and C) showing TDP2 colocalization with CVB3 and poliovirus VP1 proteins in the nucleus. Image is the merge of VP1 (green) and TDP2 (red) staining. Colocalization was confirmed by Z-stack analysis.

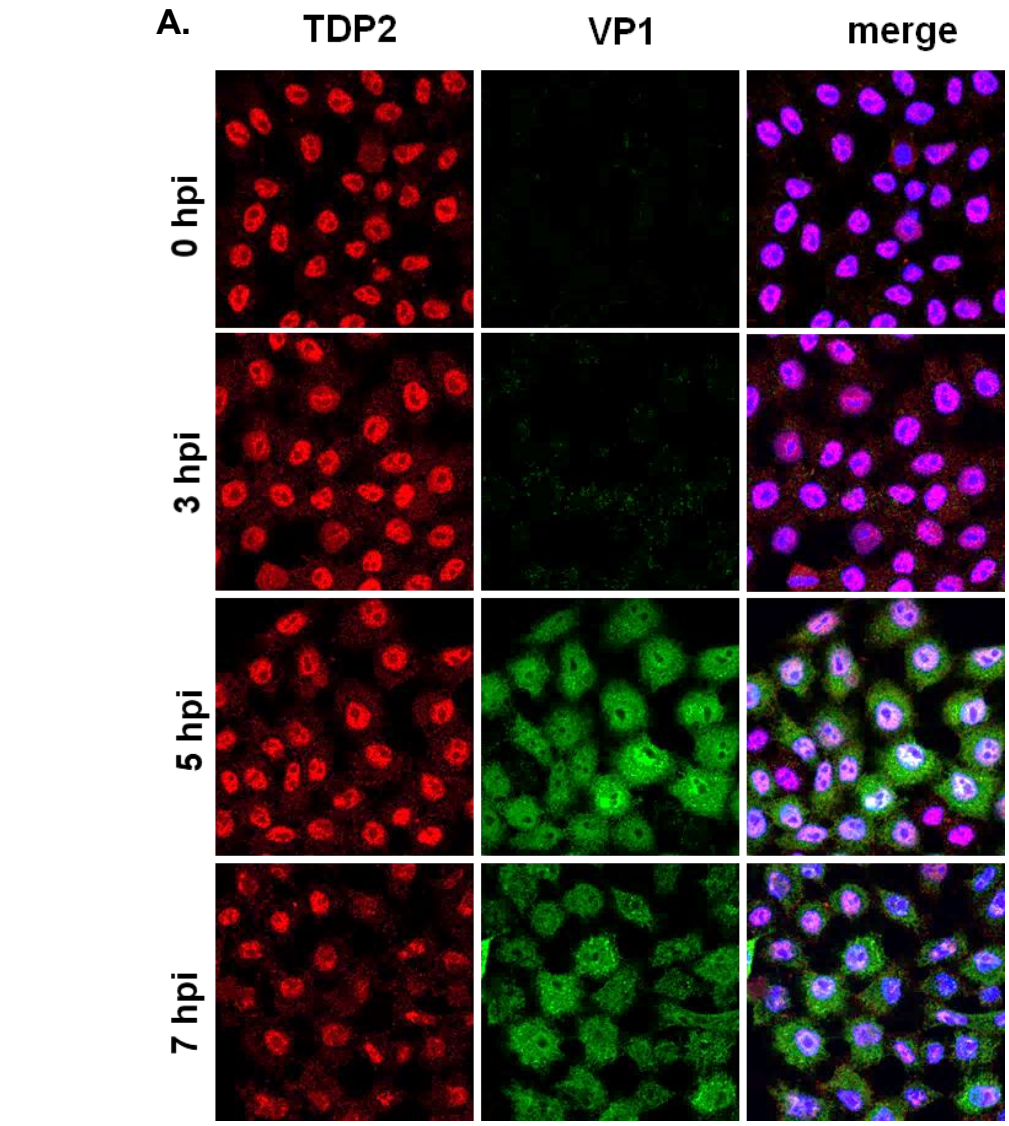
A.
TDP2
VP1
merge
0 hpi
3 hpi
5 hpi
7 hpi

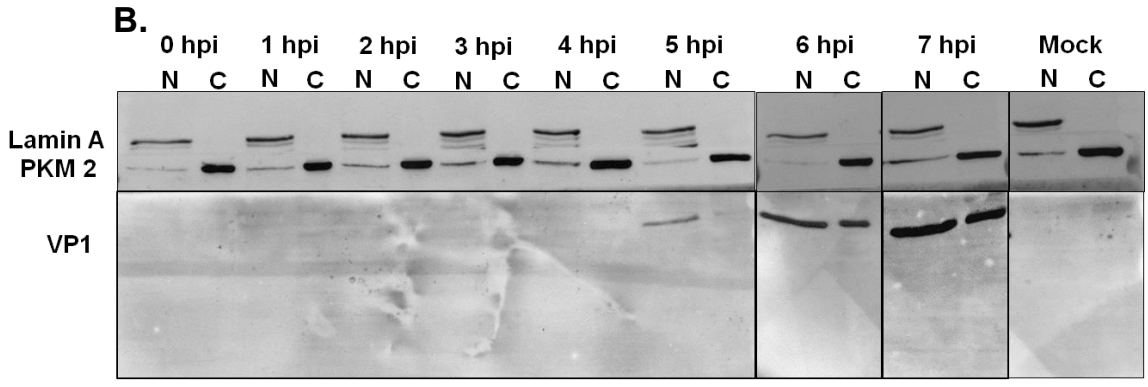
B.
0 hpi
1 hpi
2 hpi
3 hpi
4 hpi
5 hpi
6 hpi
7 hpi
Mock
N C
Lamin A
PKM 2
VP1

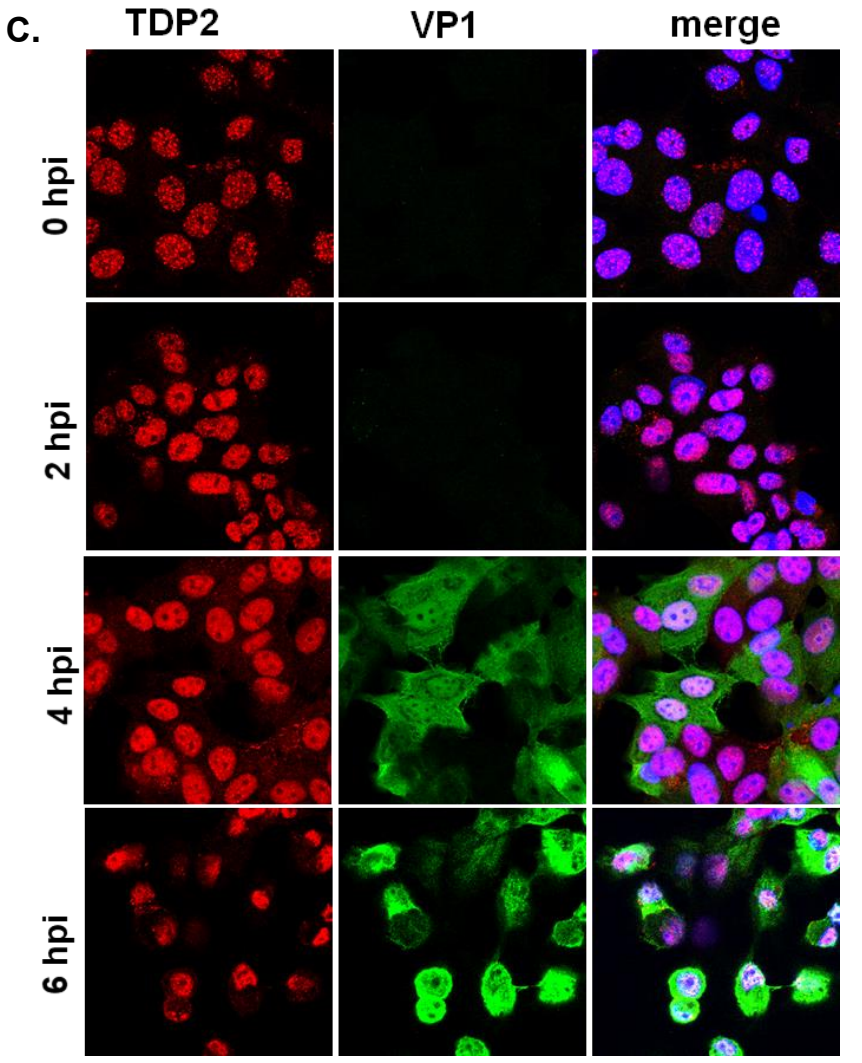
C.
TDP2
VP1
merge
0 hpi
2 hpi
4 hpi
6 hpi

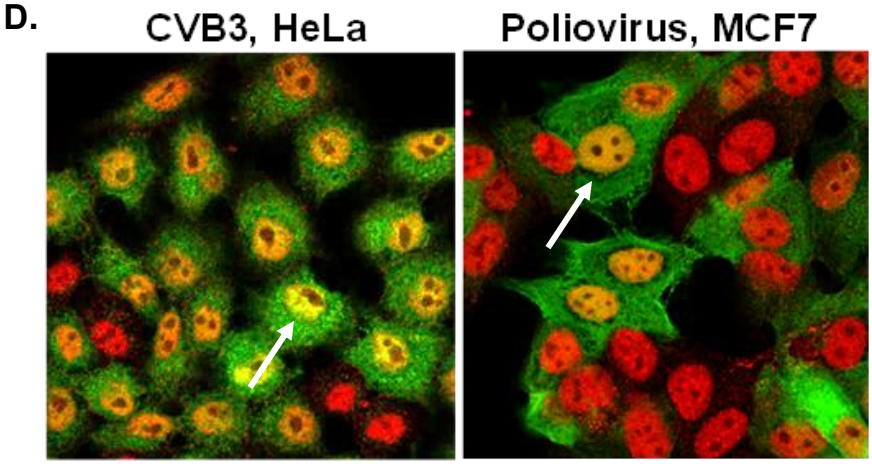
D.
CVB3, HeLa
Poliovirus, MCF7

Discussion

In this chapter, we demonstrated that two picornaviruses of the *Enterovirus* genus, poliovirus and CVB3, elicit divergent effects on the subcellular localization of the DNA repair enzyme, TDP2. Furthermore, we determined that while nuclear-cytoplasmic relocalization of TDP2 is consistent across cell types for both viruses tested, unambiguous sequestration to sites in the cell away from replication and RNA packaging organelles at late times of infection in cell lines other than HeLa cells could not be detected. Finally, we showed for the first time that poliovirus VP1 is able to enter the nucleus of MCF7 breast cancer cells, but not during poliovirus infection of HeLa cells, suggesting that cell type-specific factors influence how picornaviruses are able to modulate nuclear-cytoplasmic trafficking. The results are summarized in Table 1.

Given that our data suggest TDP2 relocalization to the cell periphery is not likely a general feature of picornavirus infections, in the absence of an apparent change in VPg unlinkase activity level throughout virus infection, what then, is the mechanism by which the virus modulates TDP2? One possibility is via protein-protein interactions. We observed that TDP2 partially colocalizes with poliovirus VP1 in HEK-293 and SK-N-SH cells at late times of infection (**Figures 3.3 and 3.4**), which could indicate that it is the interaction *between* replication complex proteins and TDP2 that blocks TDP2 from accessing nascent, VPg-linked RNA *within* the replication organelle late during the infection. Perhaps the dramatic exclusion of TDP2 from putative sites of replication and encapsidation observed during poliovirus infection of HeLa cells is not necessary to shield the phosphotyrosyl linkage from TDP2 hydrolysis, and simply a “rearrangement” of factors within the complex may be sufficient. This could be tested by isolating membranous replication complexes (41) and probing for interactions among the proteins present. It is also important to note, however, that the subcellular location in which TDP2 removes VPg from the RNA has not yet been identified,

so it is an *a priori* assumption that TDP2 is in the replication complex at all. Removal of VPg occurs prior to polysome formation in the presence of VPg unlinkase (126) and translation and replication have been shown to be functionally, but not necessarily spatially coupled (127). Thus, it is possible that unlinkase acts at a location other than the replication complex and the unlinked RNA is subsequently transported to the complex. This would suggest that TDP2 does not need to be relocalized from the complex at all.

Another caveat to consider is that our assay may not be sensitive enough to detect small fluctuations in VPg unlinkase activity. Moreover, while global VPg unlinkase activity may be unchanged during infection, there could be local differences in the activity level at the replication complex which we would not be able to detect in our assay given that it uses whole cell lysate preparations and not fractionated cells. It is possible that by specifically isolating replication complexes at different times during early, mid, and late infection (provided that TDP2 is present in them), and using these as the source of VPg unlinkase activity in the assay, a clearer picture of time-dependent activity levels may emerge. Finally, although we demonstrated that poliovirus can use all isoforms of TDP2 *individually* to efficiently carry out its replication cycle (**Figure 2.7**), the possibility remains that TDP2 preferentially uses one isoform over the other when all three of the isoforms are present in the same cell. If this is the case, the virus may modulate the enzymatic activity of the *specific* isoform that it preferentially utilizes, but overall VPg unlinkase activity may appear unchanged in the assay given that all three isoforms possess unlinkase activity (**Figure 2.7**).

We observed differential effects on the nuclear localization of the picornavirus structural protein, VP1. Confocal fluorescence microscopy revealed that CVB3 and poliovirus localize VP1 to the nucleus in HeLa cells and MCF7 cells, respectively, but not in other cell types. One possibility to account for this is that components of the NPC have been shown to vary in their expression between cell types (169). Moreover, as mentioned previously,

different strains of HRV (193) as well as the Mahoney strain of poliovirus (131) have been demonstrated to differentially alter nuclear-cytoplasmic trafficking pathways. It is possible that there are certain NPC proteins which are expressed in HeLa or MCF7 cells that either CVB3 or poliovirus cleaves in order to translocate their VP1 into the nucleus which are not expressed in the other cell types tested. An alternative possibility is that the NLS of VP1 may get cleaved or modified such that it is no longer functional; however we have not observed (nor has it been reported) the formation of VP1 cleavage products in Western blot analysis during virus infection. It is possible that the cleavage fragment may be too small to detect with the percentage of polyacrylamide that we routinely use in our SDS-PAGE. Nevertheless, these results imply that nuclear import of VP1 might be important for picornavirus replication only in certain cellular contexts.

Divergent nuclear localization of viral proteins between highly related viruses has been described for a number of RNA virus families. For example, the non-structural protein, NS5, of dengue virus (DENV) has been shown to vary in its subcellular localization in a serotype-specific manner (75). While the NS5 proteins of DENV-2 and -3 localize to the nucleus, NS5 of DENV-1 and -4 accumulate almost exclusively in the cytoplasm (75). The authors of this study concluded that NS5 nuclear localization is likely not required for virus replication but might act in an auxiliary manner (75). Given that picornaviruses generate a molar excess of viral proteins during virus replication, a certain proportion of VP1 could also be dedicated to acting in a supplementary fashion, in addition to being used in its structural role to encapsidate nascent VPg-linked RNA. Furthermore, several influenza virus strains also exhibit differential localization of the nucleocapsid protein from the nucleus (the compartment in which these viruses replicate their genomic RNA), to the cytoplasm, which influences cell tropism and *in vivo* pathogenicity, via an increase in polymerase activity (101). Whether

divergent nuclear localization of VP1 has any bearing on picornavirus pathogenicity remains an open question in the field.

Cell line	Virus infection	TDP2 nuclear-cytoplasmic re-localization?	TDP2 at the cell periphery?	Co-localization with capsid protein or 3A?	VP1 nuclear localization?
HeLa	Polio, CVB3	Yes	Yes	No	Yes (CVB3) No (Polio)
HEK-293	Polio	Yes	No	Yes	No
SK-N-SH neuroblastoma	Polio	Yes	No	Yes (weakly)	No
MCF7	Polio	Yes	No	Yes	Yes (Polio)

Table 3.1 Summary of TDP2 and VP1 localization patterns observed during either poliovirus or CVB3 infection of multiple human cell lines.

Materials and Methods

Cell culture and virus stocks

MCF7 breast cancer cell lines were kindly provided by Keith Caldecott at the University of Sussex. HeLa, MCF7, HEK-293, and SK-N-SH neuroblastoma cells were grown in Dulbecco's modified Eagle's medium containing 10% fetal bovine serum (FBS) (HEK-293 and MCF7), 20% FBS (SK-N-SH), or 8% newborn calf serum (HeLa). Poliovirus type 1 (Mahoney strain) was used to infect HeLa, HEK-293, and SK-N-HSH cells. Coxsackievirus B3-0 strain was used to infect HeLa cells. Infected cells were harvested or fixed at the indicated time points.

Immunofluorescence assays

HeLa, MCF7, HEK-293, or SK-N-SH cells were seeded onto coverslips placed into 6-well plates. Cells were infected with poliovirus or CVB3 as indicated and fixed in 3.7% formaldehyde at room temperature at the indicated time points for 10 minutes. Formaldehyde was removed and fixed cells were washed twice in 1x PBS and subsequently stored at 4°C. The cells were subsequently permeabilized in 0.5% NP-40 in PBS for 5 min and were then washed 3 times with 1% NCS in 1X PBS. Cells were blocked in 1% donkey serum in 200 µl of 1% bovine serum albumin (BSA) for 30 minutes at room temperature. The cells were washed again 3 times with 1% NCS and incubated with the primary rabbit anti-TDP2 antibody (Bethyl) and either anti-PVR (Abcam), mouse monoclonal antibody against poliovirus 3A, or mouse monoclonal anti-pan-enterovirus VP1 antibody for 2 hours at a concentration of 1:200. The primary antibodies were diluted in 1% BSA. 3A antibody was kindly provided by George Belov, University of Maryland. After incubation, the coverslips were washed 3 times with 1% NCS and then incubated with the fluorescent secondary anti-mouse (Dylight 488, Bethyl) or anti-rabbit (DyLight 594, Bethyl). Coverslips were then washed 3 times with 1% NCS and counterstained with DAPI to label nuclei. Coverslips were mounted onto microscope slides

using Fluoro-gel (Electron Microscopy Sciences) and imaged using a Zeiss LSM700 confocal fluorescence microscope at 63x magnification. Co-localization was confirmed by Z-stack analysis.

Preparation of lysates from uninfected and infected cells and nuclear cytoplasmic fractionation

Cells were collected and centrifugated at 15,000 RPM in 1.5 ml Eppendorf tubes. The cell pellet was washed once with 1X PBS. Nuclear-cytoplasmic fractionation was carried out using the NE-PER Nuclear and Cytoplasmic Extraction Reagents (Thermo Scientific). Protein concentration was determined by Bradford assay. Fractions were stored at -80°C until use. For Western blot analysis, fractions were thawed on ice and 50 µg of protein was loaded onto an SDS-containing, 12.5% polyacrylamide gel, subjected to electrophoresis, and transferred onto a PVDF membrane. The membrane was blocked in 5% milk for 1 hour and incubated with the primary and secondary antibodies for 1 hour or 45 minutes, respectively. Membrane was washed 4 times in 0.01% PBS-tween in between primary and secondary antibody incubations. Anti-pan enterovirus VP1 antibody was used at a dilution of 1:1000 Anti-PKM2 (Bethyl) was used at a concentration of 1:5000 to detect endogenous PKM2 as protein a loading control. Anti-mouse or -rabbit HRP-conjugated secondary antibodies were used to detect the primary antibodies. Protein bands were visualized by ECL Western Blotting Substrate (Life Technologies).

CHAPTER 4

Final conclusions and overall significance

Picornaviruses employ a distinct mechanism to replicate their genome involving the protein primer, VPg. This results in the formation of a unique RNA-protein 5' phosphotyrosyl bond during infection. The bond is subsequently cleaved by the DNA repair enzyme, TDP2, (alias: VPg unlinkase), but deciphering the biological underpinnings for this cleavage has been elusive. In this dissertation, we present evidence which sheds light on the functional significance of TDP2-mediated hydrolysis of VPg from picornavirus genomic RNA. Furthermore, given that different forms of the viral RNA possess a differential linkage to VPg (46, 125), we further clarify potential mechanisms to account for the modulation of TDP2/VPg unlinkase activity during the virus infection.

In **Chapter 2**, we determined that both poliovirus and CVB3 infectious particle production is delayed in the absence of TDP2 in a human cell model of infection, but this defect is recovered at the end of the infectious cycle. We also showed that the growth delay phenotype is both dependent on the MOI and on the 5' phosphodiesterase activity of TDP2. This indicates that: 1) it is the presence of VPg on the RNA (and not a secondary function of TDP2) responsible for the delay; and 2) once the number of genome copies reaches a certain threshold in the infected cell, the defect brought about by not removing VPg becomes negligible. Our data suggest that the defect is intrinsic to virus replication and can be self-corrected as the infection proceeds. We also considered the alternative possibility that a redundant 5' phosphodiesterase activity becomes activated in the absence of TDP2 at late times of infection to account for the recovery of virus production. However, we found that no such activity could be detected (**Figure 2.6**).

We then went on to examine the steps of the replication cycle which would most likely be affected by the presence of VPg on the viral RNA: translation and/or RNA synthesis. Since

we observed that ribosomes can still load efficiently onto viral RNA in the absence of TDP2, but total RNA levels are diminished, this points to RNA synthesis being affected. One counterpoint to this observation, is that the polysome analysis does not take into account the fact that ribosome recycling might be affected by the presence of VPg on the RNA, which could also result in a growth delay. That is, while the RNA might appear to be translating efficiently because the read-out being used is its association with the polysome fraction, it is possible that the RNA being detected cannot *reinitiate* translation efficiently, and polysomes could end up effectively "stuck" on VPg-linked RNA.

Given that circularization of picornavirus RNA has been proposed to play a role in both RNA synthesis (78) and translation (19, 130), once the ribosome reaches the stop codon of the polyprotein, the 5' and 3' ends would be positioned such that the presence of VPg might impede the access of translation release factors to the ribosome. If this were the case, one would expect there to be an excess of ribosomes on the RNA, leading to a larger proportion of viral RNA found in the higher polysome fraction. To some extent, this can be observed in poliovirus-infected TDP2 KO cells (**Figure 2.10, B**), in which the amount of RNA found in the heaviest fraction (9-10) is slightly higher than that of WT TDP2 cells. However, the pattern of polysome association is virtually identical at 4 hpi in the two cell types (**Figure 2.10 D-E**). Virus growth and RNA production is still not recovered until late during the infection time course, suggesting that an impairment in ribosome recycling is likely not responsible for the growth defect.

In support of the proposition that RNA synthesis is the step that is negatively affected by the presence of VPg on the viral RNA, we observed that dsRNA production, which is indicative of the formation of RNA synthesis intermediates, is diminished in poliovirus-infected TDP2 KO cells compared to in WT TDP2 cells. We also determined that premature RNA packaging could not account for the observed phenotype. Finally, we observed the trend that

proteinase K-treatment of viral RNA (resulting in the degradation of VPg), can partially rescue both positive and negative-strand RNA synthesis, suggesting that the release of VPg does play a part in the ensuring that these activities proceed efficiently. If this is the case, how might the presence of VPg on the viral RNA make RNA synthesis inefficient? As mentioned previously, it is known that the formation of a ternary complex consisting of the host proteins PCBP1/2, the viral protein precursor, 3CD, and the 5' cloverleaf structure of poliovirus RNA is critical for the initiation of both positive and negative strand RNA synthesis (11, 132, 175, 186) as well as stabilization of the viral RNA (11). PCBP2 has specifically been shown to directly engage the RNA via its first K-homologous (KH) domain (163, 188), an interaction which is largely mediated by Van der Waals forces and hydrophobic interactions (179). However, VPg has been described to exist as two charged forms during virus infection (148); a basic form which is found on virion RNA, and an acidic form which is found in RF. A fairly straightforward explanation is that the presence of a charged VPg at the 5' end might act to disrupt the hydrophobic interactions which direct the binding of PCBP2. One way to test this directly is to carry out *in vitro* pull-down assays using either VPg-linked or unlinked 5' cloverleaf RNA as the bait to determine if the latter binds PCBP2 more efficiently. Importantly, 5' cloverleaf RNA by itself, as opposed to full length RNA, would have to be used in this experiment to eliminate the potential contribution of the viral IRES to the pull-down of PCBP2, since the protein has been shown to bind to the IRES as well (19, 20).

It has been shown that the RNA structure of the 5' cloverleaf itself is also important for the initiation of RNA synthesis (11). Structural analyses have not yet been carried out to determine if the cloverleaf adopts a different conformation in the presence or absence of VPg. Therefore, it is also possible that removal of VPg allows the 5' cloverleaf to adopt a "replication competent" conformation. This could be tested by doing SHAPE analysis (167, 197) on VPg-linked and unlinked cloverleaf RNA. Altogether, our working model (**Figure 4.1**) proposes that

the presence of VPg on the viral RNA may preclude the binding of the critical host factor, PCBP2 either by directly disrupting the binding of the protein or by preventing the RNA from folding into the appropriate structure to be competent to initiate RNA synthesis.

Another more provocative possibility that arises from our data is that the 5' phsophotyrosyl bond linking VPg and the viral RNA might act as a novel signal for innate immune sensors. We observed that although positive and negative-sense viral RNA levels appear to be stable across the 4- and 5-hour time points in WT TDP2 cells transfected with either proteinase K-treated or mock-treated virion RNA (**Figure 2.15, A and B**), viral RNA levels in KO TDP2 cells were reduced and did not begin to recover until 6 hpt (**Figure 2.15, B and 6**). The recovery was modestly enhanced by proteinase K- treatment of the RNA. This raises the possibility that the presence of VPg on the viral RNA, and specifically the 5' phosphotyrosyl linkage could be recognized and activate the innate immune response, leading to an antiviral state in the KO cells that would account for the diminished viral RNA levels observed during the early to mid-phase of the infection.

While we do not have sufficient evidence that the above scenario occurs, the hypothesis is based on the following: it is known that DNA damage and the genome instability that follows precipitates the formation of cytoplasmic micronuclei; small, nuclear envelop-enclosed vesicles that contain chromosomal fragments (202). One form of DNA damage that induces micronuclei formation is DNA double-stranded breaks, which, as mentioned in the introduction can arise from stalled TOP2 cleavage complexes (64). Ultimately, due to the hyperinstability of the DNA fragments within micronuclei (202) the envelope of these foci ruptures, leading the DNA contents to be exposed and recognized by the cytoplasmic DNA sensor, cGAS, which then activates the type I interferon pathway (113, 170). cGAS binds double-stranded DNA in a sequence-independent, but length-dependent manner (5) and has not been shown to recognize 5' phosphotyrosyl linkages. Additionally, it is not known if

micronuclei specifically contain DNA which possess the 5' phosphotyrosyl-DNA linkage; however, it has been demonstrated that γH2AX foci (often used as a marker for double-stranded breaks) can be detected within micronuclei that are associated with KO of TDP2 (64). Therefore, since the linkage itself, in addition to the double-stranded DNA, is also misplaced by virtue of it being exposed in the cytoplasm, this could potentially act as a trigger for innate immune sensors as well. If this is the case, it would make sense that the virus should hydrolyze the bond and remove VPg from the RNA to mask this facet of its replication cycle.

Inherent to this proposition is that KO of TDP2 in and of itself could cause the secondary effect of cGAS activation, leading to an indirect effect on virus infection which is also *dependent* on TDP2 phosphodiesterase activity. However, Gomez-Herreros and colleagues found that TDP2 KO cells do not contain increased numbers of endogenous γH2AX foci, and it is only until the cell is perturbed with exogenous stimuli of DNA damage (i.e., etoposide or UV radiation) that the number of DNA double-stranded breaks increases (63). This suggests that KO of TDP2 alone is likely insufficient to induce DNA damage such that it activates the innate immune response. This does not rule out the possibility that the 5' phosphotyrosyl linage between VPg and the viral RNA could act effectively as "DNA damage" in the infected cell. A simple way to begin testing for this is to determine if IRF3 phosphorylation (a downstream target of cGAS) is increased during infection of TDP2 KO cells compared to WT.

In addition to the mechanisms which underlie the functional consequences of VPg removal, in **Chapter 3** of this dissertation we provided evidence demonstrating that sequestration of TDP2 to the cell periphery is a HeLa-specific phenomenon and is likely not the mechanism by which picornaviruses regulate VPg unlinkase activity. Moreover, we demonstrated for the first time that poliovirus VP1 enters the nucleus of MCF7 cells and

colocalizes with TDP2. While the significance of this observation is unclear, among the cell lines tested, VP1 appeared in the nucleus of infected cells in which the kinetics of TDP2 nuclear-cytoplasmic relocalization were slower than for those in which VP1 remained cytoplasmic (for reference, compare **Figures 3.1 and 3.5**). Moreover, it is known that VP1 acts to disrupt the cell cycle during CVB3 infection, but whether this is the case for poliovirus remains to be determined. It would be interesting to determine the virus- and cell type-specific effects of VP1 nuclear localization and how colocalization with TDP2 might play a role.

If cytoplasmic redistribution of TDP2 is not the mechanism by which picornaviruses modulate VPg unlinkase activity, what is? One possibility, as mentioned in **Chapter 3**, is that one isoform of TDP2 might be preferentially used when all three are expressed together in the cell, an occurrence that would not be captured by the experiments we carried out using cell lines which express each isoform individually. Another possibility is that our assay might not be sensitive enough to detect small differences in VPg unlinkase activity, even though the virus is still regulating the enzyme to its advantage. If this is the case, post-translational modifications of TDP2 could be a potential way that the virus modulates VPg unlinkase activity, as it is known that ERK3 phosphorylation of TDP2 enhances its 5' phosphodiesterase activity (17). In any case, it is clear that picornaviruses do require a way to regulate VPg unlinkase activity to achieve the differential linkage to VPg that has been long recognized in the field (46, 125, 126).

The data presented in this dissertation provide a framework to clarify the significance of VPg removal from picornavirus RNA. Ultimately, given that blocking hydrolysis of VPg from the RNA results in a growth defect, this opens the possibility of harnessing it for the development of novel, anti-viral therapeutics. To do so effectively, it is crucial to understand the nuanced differences between the viral VPg-RNA linkage and the similar TOP2-DNA linkage that forms on host cell DNA to minimize off-target effects. Overall, by understanding

the basic mechanisms of picornavirus replication, not only does this enhance our knowledge of RNA virus biology, but it also allows us to more effectively translate these findings into clinical applications. This in turn, allows us to fine tune the ways in which we target the virus, coming ever closer to winning the perennial battle between virus and host.

Figure 4.1 Model of viral RNA synthesis in the presence and absence of VPg. In WT TDP2 cells, VPg is removed allowing the association of the host and viral factors PCBP2 and 3CD to proceed normally to initiate (-) and (+) strand synthesis (represented by thick red arrows). In TDP2 KO cells, VPg remains on the RNA and acts as an impediment to PCBP2/3CD binding, either by acting as a steric hindrance or disrupting hydrophobic interactions between PCBP2 and the viral RNA, thereby making the initiation of RNA synthesis inefficient (dashed arrows). This leads to a reduction in the number of (+) sense templates produced and an overall delay in viral growth. However, the exponential amplification of (+) sense RNA on the (-) strand template can eventually compensate for the inefficiency.

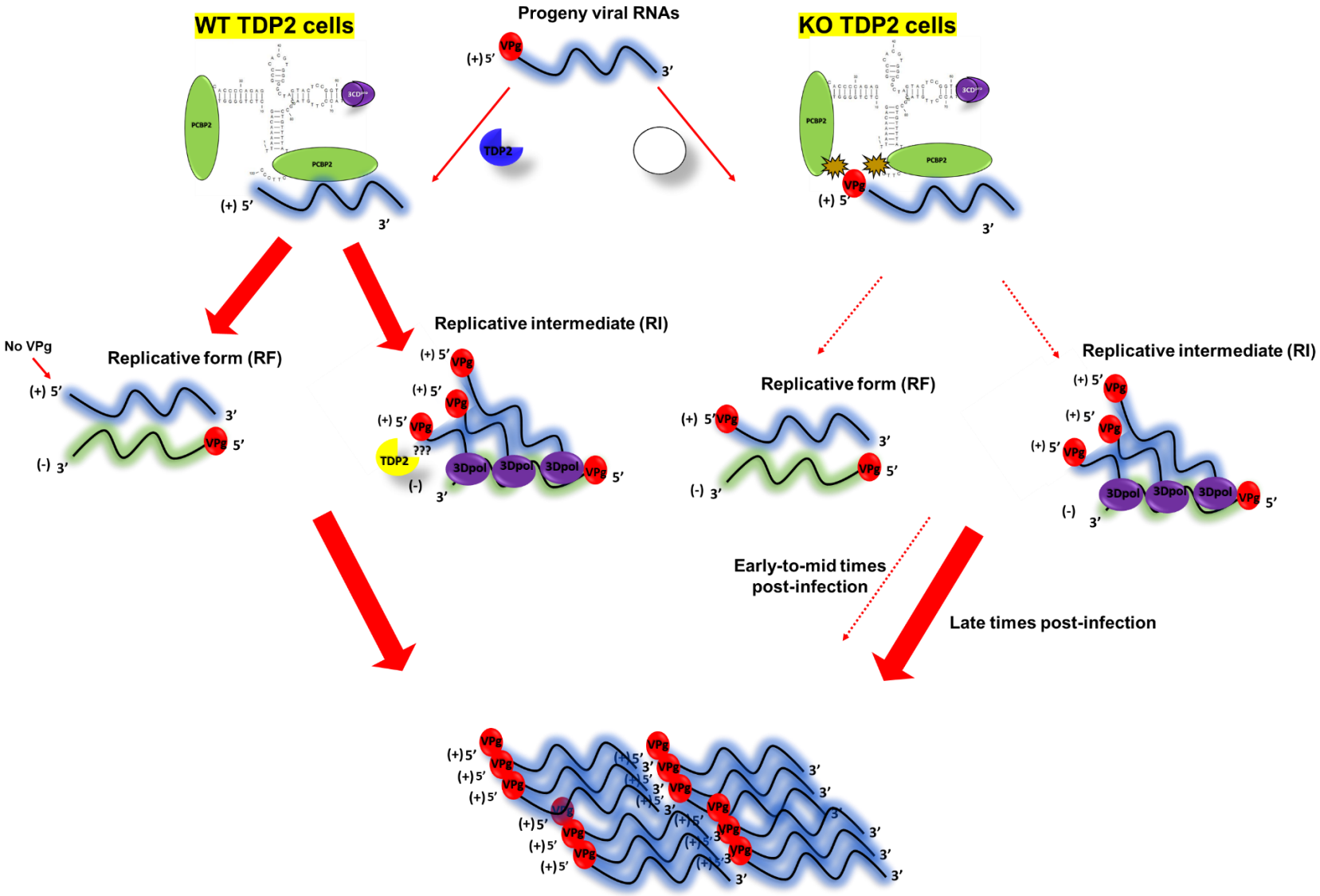
WT TDP2 cells
Progeny viral RNAs
KO TDP2 cells
PCBP2
3CDpro
(+) 5′
3′
VPg
TDP2
No VPg
Replicative form (RF)
Replicative intermediate (RI)
(-) 3′
5′
???
3Dpol
Early-to-mid times post-infection
Late times post-infection

REFERENCES

1. **Ambros, V., and D. Baltimore.** 1978. Protein is linked to the 5' end of poliovirus RNA by a phosphodiester linkage to tyrosine. J Biol Chem **253:**5263-5266.
2. **Ambros, V., R. F. Pettersson, and D. Baltimore.** 1978. An enzymatic activity in uninfected cells that cleaves the linkage between poliovirion RNA and the 5' terminal protein. Cell **15:**1439-1446.
3. **Anczukow, O., and A. R. Krainer.** 2016. Splicing-factor alterations in cancers. RNA **22:**1285-1301.
4. **Andino, R., G. E. Rieckhof, and D. Baltimore.** 1990. A functional ribonucleoprotein complex forms around the 5' end of poliovirus RNA. Cell **63:**369-380.
5. **Andreeva, L., B. Hiller, D. Kostrewa, C. Lassig, C. C. de Oliveira Mann, D. Jan Drexler, A. Maiser, M. Gaidt, H. Leonhardt, V. Hornung, and K. P. Hopfner.** 2017. cGAS senses long and HMGB/TFAM-bound U-turn DNA by forming protein-DNA ladders. Nature **549:**394-398.
6. **Arden, K. E., and I. M. Mackay.** 2009. Human rhinoviruses: coming in from the cold. Genome Med **1:**44.
7. **Asare, E., J. Mugavero, P. Jiang, E. Wimmer, and A. V. Paul.** 2016. A Single Amino Acid Substitution in Poliovirus Nonstructural Protein 2CATPase Causes Conditional Defects in Encapsidation and Uncoating. J Virol **90:**6174-6186.
8. **Austin, C. A., K. C. Lee, R. L. Swan, M. M. Khazeem, C. M. Manville, P. Cridland, A. Treumann, A. Porter, N. J. Morris, and I. G. Cowell.** 2018. TOP2B: The First Thirty Years. Int J Mol Sci **19**.
9. **Bao, J. L., and L. Lin.** 2014. MiR-155 and miR-148a reduce cardiac injury by inhibiting NF-kappaB pathway during acute viral myocarditis. Eur Rev Med Pharmacol Sci **18:**2349-2356.
10. **Barton, D. J., B. J. Morasco, and J. B. Flanegan.** 1999. Translating ribosomes inhibit poliovirus negative-strand RNA synthesis. J Virol **73:**10104-10112.
11. **Barton, D. J., B. J. O'Donnell, and J. B. Flanegan.** 2001. 5' cloverleaf in poliovirus RNA is a cis-acting replication element required for negative-strand synthesis. EMBO J **20:**1439-1448.
12. **Bedard, K. M., and B. L. Semler.** 2004. Regulation of picornavirus gene expression. Microbes Infect **6:**702-713.
13. **Beigelman, A., and L. B. Bacharier.** 2016. Early-life respiratory infections and asthma development: role in disease pathogenesis and potential targets for disease prevention. Curr Opin Allergy Clin Immunol **16:**172-178.
14. **Bejjani, F., E. Evanno, K. Zibara, M. Piechaczyk, and I. Jariel-Encontre.** 2019. The AP-1 transcriptional complex: Local switch or remote command? Biochim Biophys Acta Rev Cancer **1872:**11-23.
15. **Belov, G. A., P. V. Lidsky, O. V. Mikitas, D. Egger, K. A. Lukyanov, K. Bienz, and V. I. Agol.** 2004. Bidirectional increase in permeability of nuclear envelope upon poliovirus infection and accompanying alterations of nuclear pores. J Virol **78:**10166-10177.
16. **Belov, G. A., V. Nair, B. T. Hansen, F. H. Hoyt, E. R. Fischer, and E. Ehrenfeld.** 2012. Complex dynamic development of poliovirus membranous replication complexes. J Virol **86:**302-312.
17. **Bian, K., N. R. Muppani, L. Elkhadragy, W. Wang, C. Zhang, T. Chen, S. Jung, O. M. Seternes, and W. Long.** 2016. ERK3 regulates TDP2-mediated DNA damage response and chemoresistance in lung cancer cells. Oncotarget **7:**6665-6675.

18. **Bienz, K., D. Egger, Y. Rasser, and W. Bossart.** 1982. Accumulation of poliovirus proteins in the host cell nucleus. Intervirology **18:**189-196.
19. **Blyn, L. B., K. M. Swiderek, O. Richards, D. C. Stahl, B. L. Semler, and E. Ehrenfeld.** 1996. Poly(rC) binding protein 2 binds to stem-loop IV of the poliovirus RNA 5' noncoding region: identification by automated liquid chromatography-tandem mass spectrometry. Proc Natl Acad Sci U S A **93:**11115-11120.
20. **Blyn, L. B., J. S. Towner, B. L. Semler, and E. Ehrenfeld.** 1997. Requirement of poly(rC) binding protein 2 for translation of poliovirus RNA. J Virol **71:**6243-6246.
21. **Bonin, M., J. Oberstrass, N. Lukacs, K. Ewert, E. Oesterschulze, R. Kassing, and W. Nellen.** 2000. Determination of preferential binding sites for anti-dsRNA antibodies on double-stranded RNA by scanning force microscopy. RNA **6:**563-570.
22. **Bramley, T. J., D. Lerner, and M. Sames.** 2002. Productivity losses related to the common cold. J Occup Environ Med **44:**822-829.
23. **Brown, M. C., J. D. Bryant, E. Y. Dobrikova, M. Shveygert, S. S. Bradrick, V. Chandramohan, D. D. Bigner, and M. Gromeier.** 2014. Induction of viral, 7-methyl-guanosine cap-independent translation and oncolysis by mitogen-activated protein kinase-interacting kinase-mediated effects on the serine/arginine-rich protein kinase. J Virol **88:**13135-13148.
24. **Brown, M. C., E. K. Holl, D. Boczkowski, E. Dobrikova, M. Mosaheb, V. Chandramohan, D. D. Bigner, M. Gromeier, and S. K. Nair.** 2017. Cancer immunotherapy with recombinant poliovirus induces IFN-dominant activation of dendritic cells and tumor antigen-specific CTLs. Sci Transl Med **9**.
25. **Brunner, J. E., K. J. Ertel, J. M. Rozovics, and B. L. Semler.** 2010. Delayed kinetics of poliovirus RNA synthesis in a human cell line with reduced levels of hnRNP C proteins. Virology **400:**240-247.
26. **Brunner, J. E., J. H. Nguyen, H. H. Roehl, T. V. Ho, K. M. Swiderek, and B. L. Semler.** 2005. Functional interaction of heterogeneous nuclear ribonucleoprotein C with poliovirus RNA synthesis initiation complexes. J Virol **79:**3254-3266.
27. **Cappadocia, L., A. Pichler, and C. D. Lima.** 2015. Structural basis for catalytic activation by the human ZNF451 SUMO E3 ligase. Nat Struct Mol Biol **22:**968-975.
28. **Castello, A., E. Alvarez, and L. Carrasco.** 2011. The multifaceted poliovirus 2A protease: regulation of gene expression by picornavirus proteases. J Biomed Biotechnol **2011:**369648.
29. **Castello, A., J. M. Izquierdo, E. Welnowska, and L. Carrasco.** 2009. RNA nuclear export is blocked by poliovirus 2A protease and is concomitant with nucleoporin cleavage. J Cell Sci **122:**3799-3809.
30. **Chase, A. J., S. Daijogo, and B. L. Semler.** 2014. Inhibition of poliovirus-induced cleavage of cellular protein PCBP2 reduces the levels of viral RNA replication. J Virol **88:**3192-3201.
31. **Chen, I. J., S. C. Hu, K. L. Hung, and C. W. Lo.** 2018. Acute flaccid myelitis associated with enterovirus D68 infection: A case report. Medicine (Baltimore) **97:**e11831.
32. **Chen, Z. G., H. Liu, J. B. Zhang, S. L. Zhang, L. H. Zhao, and W. Q. Liang.** 2015. Upregulated microRNA-214 enhances cardiac injury by targeting ITCH during coxsackievirus infection. Mol Med Rep **12:**1258-1264.
33. **Chesne, J., F. Braza, G. Mahay, S. Brouard, M. Aronica, and A. Magnan.** 2014. IL-17 in severe asthma. Where do we stand? Am J Respir Crit Care Med **190:**1094-1101.

34. **Chou, A. C., A. Aslanian, H. Sun, and T. Hunter.** 2019. An internal ribosome entry site in the coding region of tyrosyl-DNA phosphodiesterase 2 drives alternative translation start. J Biol Chem **294:**2665-2677.
35. **Corsten, M. F., A. Papageorgiou, W. Verhesen, P. Carai, M. Lindow, S. Obad, G. Summer, S. L. Coort, M. Hazebroek, R. van Leeuwen, M. J. Gijbels, E. Wijnands, E. A. Biessen, M. P. De Winther, F. R. Stassen, P. Carmeliet, S. Kauppinen, B. Schroen, and S. Heymans.** 2012. MicroRNA profiling identifies microRNA-155 as an adverse mediator of cardiac injury and dysfunction during acute viral myocarditis. Circ Res **111:**415-425.
36. **Cortes Ledesma, F., S. F. El Khamisy, M. C. Zuma, K. Osborn, and K. W. Caldecott.** 2009. A human 5'-tyrosyl DNA phosphodiesterase that repairs topoisomerase-mediated DNA damage. Nature **461:**674-678.
37. **Desjardins, A., M. Gromeier, J. E. Herndon, 2nd, N. Beaubier, D. P. Bolognesi, A. H. Friedman, H. S. Friedman, F. McSherry, A. M. Muscat, S. Nair, K. B. Peters, D. Randazzo, J. H. Sampson, G. Vlahovic, W. T. Harrison, R. E. McLendon, D. Ashley, and D. D. Bigner.** 2018. Recurrent Glioblastoma Treated with Recombinant Poliovirus. N Engl J Med **379:**150-161.
38. **Dougherty, J. D., J. P. White, and R. E. Lloyd.** 2011. Poliovirus-mediated disruption of cytoplasmic processing bodies. J Virol **85:**64-75.
39. **Du, X., Y. Zhang, J. Zou, Z. Yuan, and Z. Yi.** 2018. Replicase-mediated shielding of the poliovirus replicative double-stranded RNA to avoid recognition by MDA5. J Gen Virol **99:**1199-1209.
40. **Dyda, A., S. Stelzer-Braid, D. Adam, A. A. Chughtai, and C. R. MacIntyre.** 2018. The association between acute flaccid myelitis (AFM) and Enterovirus D68 (EV-D68) - what is the evidence for causation? Euro Surveill **23**.
41. **Egger, D., N. Teterina, E. Ehrenfeld, and K. Bienz.** 2000. Formation of the poliovirus replication complex requires coupled viral translation, vesicle production, and viral RNA synthesis. J Virol **74:**6570-6580.
42. **Engelmann, I., E. K. Alidjinou, A. Bertin, J. Bossu, C. Villenet, M. Figeac, F. Sane, and D. Hober.** 2017. Persistent coxsackievirus B4 infection induces microRNA dysregulation in human pancreatic cells. Cell Mol Life Sci **74:**3851-3861.
43. **Ertel, K. J., J. E. Brunner, and B. L. Semler.** 2010. Mechanistic consequences of hnRNP C binding to both RNA termini of poliovirus negative-strand RNA intermediates. J Virol **84:**4229-4242.
44. **Fehrenbach, H., C. Wagner, and M. Wegmann.** 2017. Airway remodeling in asthma: what really matters. Cell Tissue Res **367:**551-569.
45. **Feldman, A. S., Y. He, M. L. Moore, M. B. Hershenson, and T. V. Hartert.** 2015. Toward primary prevention of asthma. Reviewing the evidence for early-life respiratory viral infections as modifiable risk factors to prevent childhood asthma. Am J Respir Crit Care Med **191:**34-44.
46. **Fernandez-Munoz, R., and J. E. Darnell.** 1976. Structural difference between the 5' termini of viral and cellular mRNA in poliovirus-infected cells: possible basis for the inhibition of host protein synthesis. J Virol **18:**719-726.
47. **Feuer, R., I. Mena, R. Pagarigan, M. K. Slifka, and J. L. Whitton.** 2002. Cell cycle status affects coxsackievirus replication, persistence, and reactivation in vitro. J Virol **76:**4430-4440.
48. **Fitzgerald, K. D., and B. L. Semler.** 2011. Re-localization of cellular protein SRp20 during poliovirus infection: bridging a viral IRES to the host cell translation apparatus. PLoS Pathog **7:**e1002127.

49. **Flather, D., J. H. C. Nguyen, B. L. Semler, and P. D. Gershon.** 2018. Exploitation of nuclear functions by human rhinovirus, a cytoplasmic RNA virus. PLoS Pathog **14:**e1007277.
50. **Flather, D., and B. L. Semler.** 2015. Picornaviruses and nuclear functions: targeting a cellular compartment distinct from the replication site of a positive-strand RNA virus. Front Microbiol **6:**594.
51. **Foster, C. B., R. Coelho, P. M. Brown, A. Wadhwa, A. Dossul, B. E. Gonzalez, S. Cardenas, C. Sabella, D. Kohn, S. Vogel, B. Yen-Lieberman, and G. Piedimonte.** 2017. A comparison of hospitalized children with enterovirus D68 to those with rhinovirus. Pediatr Pulmonol **52:**827-832.
52. **Franco, D., H. B. Pathak, C. E. Cameron, B. Rombaut, E. Wimmer, and A. V. Paul.** 2005. Stimulation of poliovirus RNA synthesis and virus maturation in a HeLa cell-free in vitro translation-RNA replication system by viral protein 3CDpro. Virol J **2:**86.
53. **Franco, D., H. B. Pathak, C. E. Cameron, B. Rombaut, E. Wimmer, and A. V. Paul.** 2005. Stimulation of poliovirus synthesis in a HeLa cell-free in vitro translation-RNA replication system by viral protein 3CDpro. J Virol **79:**6358-6367.
54. **Gamarnik, A. V., and R. Andino.** 2000. Interactions of viral protein 3CD and poly(rC) binding protein with the 5' untranslated region of the poliovirus genome. J Virol **74:**2219-2226.
55. **Gamarnik, A. V., and R. Andino.** 1998. Switch from translation to RNA replication in a positive-stranded RNA virus. Genes Dev **12:**2293-2304.
56. **Gamarnik, A. V., and R. Andino.** 1997. Two functional complexes formed by KH domain containing proteins with the 5' noncoding region of poliovirus RNA. RNA **3:**882-892.
57. **Gao, M., H. Duan, J. Liu, H. Zhang, X. Wang, M. Zhu, J. Guo, Z. Zhao, L. Meng, and Y. Peng.** 2014. The multi-targeted kinase inhibitor sorafenib inhibits enterovirus 71 replication by regulating IRES-dependent translation of viral proteins. Antiviral Res **106:**80-85.
58. **Gao, R., M. J. Schellenberg, S. Y. Huang, M. Abdelmalak, C. Marchand, K. C. Nitiss, J. L. Nitiss, R. S. Williams, and Y. Pommier.** 2014. Proteolytic degradation of topoisomerase II (Top2) enables the processing of Top2.DNA and Top2.RNA covalent complexes by tyrosyl-DNA-phosphodiesterase 2 (TDP2). J Biol Chem **289:**17960-17969.
59. **Gerber, K., E. Wimmer, and A. V. Paul.** 2001. Biochemical and genetic studies of the initiation of human rhinovirus 2 RNA replication: identification of a cis-replicating element in the coding sequence of 2A(pro). J Virol **75:**10979-10990.
60. **Glanville, N., and S. L. Johnston.** 2015. Challenges in developing a cross-serotype rhinovirus vaccine. Curr Opin Virol **11:**83-88.
61. **Goetz, C., R. G. Everson, L. C. Zhang, and M. Gromeier.** 2010. MAPK signal-integrating kinase controls cap-independent translation and cell type-specific cytotoxicity of an oncolytic poliovirus. Mol Ther **18:**1937-1946.
62. **Golini, F., B. L. Semler, A. J. Dorner, and E. Wimmer.** 1980. Protein-linked RNA of poliovirus is competent to form an initiation complex of translation in vitro. Nature **287:**600-603.
63. **Gomez-Herreros, F., J. H. Schuurs-Hoeijmakers, M. McCormack, M. T. Greally, S. Rulten, R. Romero-Granados, T. J. Counihan, E. Chaila, J. Conroy, S. Ennis, N. Delanty, F. Cortes-Ledesma, A. P. de Brouwer, G. L. Cavalleri, S. F. El-Khamisy, B. B. de Vries, and K. W. Caldecott.** 2014. TDP2 protects transcription

from abortive topoisomerase activity and is required for normal neural function. Nat Genet **46:**516-521.

64. **Gomez-Herreros, F., G. Zagnoli-Vieira, I. Ntai, M. I. Martinez-Macias, R. M. Anderson, A. Herrero-Ruiz, and K. W. Caldecott.** 2017. TDP2 suppresses chromosomal translocations induced by DNA topoisomerase II during gene transcription. Nat Commun **8:**233.
65. **Goodfellow, I.** 2011. The genome-linked protein VPg of vertebrate viruses - a multifaceted protein. Curr Opin Virol **1:**355-362.
66. **Goodfellow, I., Y. Chaudhry, A. Richardson, J. Meredith, J. W. Almond, W. Barclay, and D. J. Evans.** 2000. Identification of a cis-acting replication element within the poliovirus coding region. J Virol **74:**4590-4600.
67. **Goodfellow, I. G., C. Polacek, R. Andino, and D. J. Evans.** 2003. The poliovirus 2C cis-acting replication element-mediated uridylylation of VPg is not required for synthesis of negative-sense genomes. J Gen Virol **84:**2359-2363.
68. **Gradi, A., Y. V. Svitkin, H. Imataka, and N. Sonenberg.** 1998. Proteolysis of human eukaryotic translation initiation factor eIF4GII, but not eIF4GI, coincides with the shutoff of host protein synthesis after poliovirus infection. Proc Natl Acad Sci U S A **95:**11089-11094.
69. **Gromeier, M., L. Alexander, and E. Wimmer.** 1996. Internal ribosomal entry site substitution eliminates neurovirulence in intergeneric poliovirus recombinants. Proc Natl Acad Sci U S A **93:**2370-2375.
70. **Gromeier, M., B. Bossert, M. Arita, A. Nomoto, and E. Wimmer.** 1999. Dual stem loops within the poliovirus internal ribosomal entry site control neurovirulence. J Virol **73:**958-964.
71. **Gromeier, M., S. Lachmann, M. R. Rosenfeld, P. H. Gutin, and E. Wimmer.** 2000. Intergeneric poliovirus recombinants for the treatment of malignant glioma. Proc Natl Acad Sci U S A **97:**6803-6808.
72. **Guest, S., E. Pilipenko, K. Sharma, K. Chumakov, and R. P. Roos.** 2004. Molecular mechanisms of attenuation of the Sabin strain of poliovirus type 3. J Virol **78:**11097-11107.
73. **Gulevich, A. Y., R. A. Yusupova, and Y. F. Drygin.** 2002. VPg unlinkase, the phosphodiesterase that hydrolyzes the bond between VPg and picornavirus RNA: a minimal nucleic moiety of the substrate. Biochemistry (Mosc) **67:**615-621.
74. **Gustin, K. E., and P. Sarnow.** 2001. Effects of poliovirus infection on nucleo-cytoplasmic trafficking and nuclear pore complex composition. EMBO J **20:**240-249.
75. **Hannemann, H., P. Y. Sung, H. C. Chiu, A. Yousuf, J. Bird, S. P. Lim, and A. D. Davidson.** 2013. Serotype-specific differences in dengue virus non-structural protein 5 nuclear localization. J Biol Chem **288:**22621-22635.
76. **Hellgren, J., A. Cervin, S. Nordling, A. Bergman, and L. O. Cardell.** 2010. Allergic rhinitis and the common cold--high cost to society. Allergy **65:**776-783.
77. **Herold, J., and R. Andino.** 2000. Poliovirus requires a precise 5' end for efficient positive-strand RNA synthesis. J Virol **74:**6394-6400.
78. **Herold, J., and R. Andino.** 2001. Poliovirus RNA replication requires genome circularization through a protein-protein bridge. Mol Cell **7:**581-591.
79. **Hewlett, M. J., J. K. Rose, and D. Baltimore.** 1976. 5'-terminal structure of poliovirus polyribosomal RNA is pUp. Proc Natl Acad Sci U S A **73:**327-330.
80. **Ho, B. C., I. S. Yu, L. F. Lu, A. Rudensky, H. Y. Chen, C. W. Tsai, Y. L. Chang, C. T. Wu, L. Y. Chang, S. R. Shih, S. W. Lin, C. N. Lee, P. C. Yang, and S. L. Yu.** 2014.

Inhibition of miR-146a prevents enterovirus-induced death by restoring the production of type I interferon. Nat Commun **5:**3344.

81. **Hoa, N. N., T. Shimizu, Z. W. Zhou, Z. Q. Wang, R. A. Deshpande, T. T. Paull, S. Akter, M. Tsuda, R. Furuta, K. Tsutsui, S. Takeda, and H. Sasanuma.** 2016. Mre11 Is Essential for the Removal of Lethal Topoisomerase 2 Covalent Cleavage Complexes. Mol Cell **64:**1010.
82. **Hober, D., and P. Sauter.** 2010. Pathogenesis of type 1 diabetes mellitus: interplay between enterovirus and host. Nat Rev Endocrinol **6:**279-289.
83. **Holl, E. K., M. C. Brown, D. Boczkowski, M. A. McNamara, D. J. George, D. D. Bigner, M. Gromeier, and S. K. Nair.** 2016. Recombinant oncolytic poliovirus, PVSRIPO, has potent cytotoxic and innate inflammatory effects, mediating therapy in human breast and prostate cancer xenograft models. Oncotarget **7:**79828-79841.
84. **Hornung, V., J. Ellegast, S. Kim, K. Brzozka, A. Jung, H. Kato, H. Poeck, S. Akira, K. K. Conzelmann, M. Schlee, S. Endres, and G. Hartmann.** 2006. 5'-Triphosphate RNA is the ligand for RIG-I. Science **314:**994-997.
85. **Hsu, N. Y., O. Ilnytska, G. Belov, M. Santiana, Y. H. Chen, P. M. Takvorian, C. Pau, H. van der Schaar, N. Kaushik-Basu, T. Balla, C. E. Cameron, E. Ehrenfeld, F. J. van Kuppeveld, and N. Altan-Bonnet.** 2010. Viral reorganization of the secretory pathway generates distinct organelles for RNA replication. Cell **141:**799-811.
86. **Hu, Q., R. Chen, T. Teesalu, E. Ruoslahti, and D. O. Clegg.** 2014. Reprogramming human retinal pigmented epithelial cells to neurons using recombinant proteins. Stem Cells Transl Med **3:**1526-1534.
87. **Huang, S. N., I. Dalla Rosa, S. A. Michaels, D. V. Tulumello, K. Agama, S. Khiati, S. R. Jean, S. A. Baechler, V. M. Factor, S. Varma, J. Murai, L. M. Miller Jenkins, S. O. Kelley, and Y. Pommier.** 2018. Mitochondrial tyrosyl-DNA phosphodiesterase 2 and its TDP2(S) short isoform. EMBO Rep **19**.
88. **Imamura, T., and H. Oshitani.** 2015. Global reemergence of enterovirus D68 as an important pathogen for acute respiratory infections. Rev Med Virol **25:**102-114.
89. **Jackson, D. J., M. D. Evans, R. E. Gangnon, C. J. Tisler, T. E. Pappas, W. M. Lee, J. E. Gern, and R. F. Lemanske, Jr.** 2012. Evidence for a causal relationship between allergic sensitization and rhinovirus wheezing in early life. Am J Respir Crit Care Med **185:**281-285.
90. **Jahan, N., E. Wimmer, and S. Mueller.** 2013. Polypyrimidine tract binding protein-1 (PTB1) is a determinant of the tissue and host tropism of a human rhinovirus/poliovirus chimera PV1(RIPO). PLoS One **8:**e60791.
91. **Kametani, Y., C. Takahata, T. Narita, K. Tanaka, S. Iwai, and I. Kuraoka.** 2016. FEN1 participates in repair of the 5'-phosphotyrosyl terminus of DNA single-strand breaks. Carcinogenesis **37:**56-62.
92. **Kempf, B. J., and D. J. Barton.** 2008. Poly(rC) binding proteins and the 5' cloverleaf of uncapped poliovirus mRNA function during de novo assembly of polysomes. J Virol **82:**5835-5846.
93. **Kim, K. W., A. Ho, A. Alshabee-Akil, A. A. Hardikar, T. W. Kay, W. D. Rawlinson, and M. E. Craig.** 2016. Coxsackievirus B5 Infection Induces Dysregulation of microRNAs Predicted to Target Known Type 1 Diabetes Risk Genes in Human Pancreatic Islets. Diabetes **65:**996-1003.
94. **Kuhn, R. J., H. Tada, M. F. Ypma-Wong, B. L. Semler, and E. Wimmer.** 1988. Mutational analysis of the genome-linked protein VPg of poliovirus. J Virol **62:**4207-4215.

95. **Langereis, M. A., Q. Feng, F. H. Nelissen, R. Virgen-Slane, G. J. van der Heden van Noort, S. Maciejewski, D. V. Filippov, B. L. Semler, F. L. van Delft, and F. J. van Kuppeveld.** 2014. Modification of picornavirus genomic RNA using 'click' chemistry shows that unlinking of the VPg peptide is dispensable for translation and replication of the incoming viral RNA. Nucleic Acids Res **42:**2473-2482.
96. **Lee, K. Y.** 2016. Enterovirus 71 infection and neurological complications. Korean J Pediatr **59:**395-401.
97. **Lehmann, G. L., I. Benedicto, N. J. Philp, and E. Rodriguez-Boulan.** 2014. Plasma membrane protein polarity and trafficking in RPE cells: past, present and future. Exp Eye Res **126:**5-15.
98. **Leigh, R., W. Oyelusi, S. Wiehler, R. Koetzler, R. S. Zaheer, R. Newton, and D. Proud.** 2008. Human rhinovirus infection enhances airway epithelial cell production of growth factors involved in airway remodeling. J Allergy Clin Immunol **121:**1238-1245 e1234.
99. **Li, C., S. Fan, T. K. Owonikoko, F. R. Khuri, S. Y. Sun, and R. Li.** 2011. Oncogenic role of EAPII in lung cancer development and its activation of the MAPK-ERK pathway. Oncogene **30:**3802-3812.
100. **Li, C., S. Y. Sun, F. R. Khuri, and R. Li.** 2011. Pleiotropic functions of EAPII/TTRAP/TDP2: cancer development, chemoresistance and beyond. Cell Cycle **10:**3274-3283.
101. **Li, J., W. Zheng, L. Hou, C. Chen, W. Fan, H. Qu, J. Jiang, J. Liu, G. F. Gao, J. Zhou, L. Sun, and W. Liu.** 2017. Differential nucleocytoplasmic shuttling of the nucleoprotein of influenza a viruses and association with host tropism. Cell Microbiol **19**.
102. **Li, Q., Z. Zheng, Y. Liu, Z. Zhang, Q. Liu, J. Meng, X. Ke, Q. Hu, and H. Wang.** 2016. 2C Proteins of Enteroviruses Suppress IKKbeta Phosphorylation by Recruiting Protein Phosphatase 1. J Virol **90:**5141-5151.
103. **Li, X., W. Ma, Y. Zhuo, R. T. Yan, and S. Z. Wang.** 2010. Using neurogenin to reprogram chick RPE to produce photoreceptor-like neurons. Invest Ophthalmol Vis Sci **51:**516-525.
104. **Li, X., and J. W. Wilson.** 1997. Increased vascularity of the bronchial mucosa in mild asthma. Am J Respir Crit Care Med **156:**229-233.
105. **Lim, B. K., J. H. Nam, C. O. Gil, S. H. Yun, J. H. Choi, D. K. Kim, and E. S. Jeon.** 2005. Coxsackievirus B3 replication is related to activation of the late extracellular signal-regulated kinase (ERK) signal. Virus Res **113:**153-157.
106. **Lin, J. Y., M. L. Li, P. N. Huang, K. Y. Chien, J. T. Horng, and S. R. Shih.** 2008. Heterogeneous nuclear ribonuclear protein K interacts with the enterovirus 71 5' untranslated region and participates in virus replication. J Gen Virol **89:**2540-2549.
107. **Liu, T., Y. Liu, M. Miller, L. Cao, J. Zhao, J. Wu, J. Wang, L. Liu, S. Li, M. Zou, J. Xu, D. H. Broide, and L. Dong.** 2017. Autophagy plays a role in FSTL1-induced epithelial mesenchymal transition and airway remodeling in asthma. Am J Physiol Lung Cell Mol Physiol **313:**L27-L40.
108. **Liu, Y. C., R. L. Kuo, J. Y. Lin, P. N. Huang, Y. Huang, H. Liu, J. J. Arnold, S. J. Chen, R. Y. Wang, C. E. Cameron, and S. R. Shih.** 2014. Cytoplasmic viral RNA-dependent RNA polymerase disrupts the intracellular splicing machinery by entering the nucleus and interfering with Prp8. PLoS Pathog **10:**e1004199.
109. **Liu, Y. L., W. Wu, Y. Xue, M. Gao, Y. Yan, Q. Kong, Y. Pang, and F. Yang.** 2013. MicroRNA-21 and -146b are involved in the pathogenesis of murine viral myocarditis by regulating TH-17 differentiation. Arch Virol **158:**1953-1963.

110. **Luo, H., B. Yanagawa, J. Zhang, Z. Luo, M. Zhang, M. Esfandiarei, C. Carthy, J. E. Wilson, D. Yang, and B. M. McManus.** 2002. Coxsackievirus B3 replication is reduced by inhibition of the extracellular signal-regulated kinase (ERK) signaling pathway. J Virol **76:**3365-3373.
111. **Maciejewski, S., J. H. Nguyen, F. Gomez-Herreros, F. Cortes-Ledesma, K. W. Caldecott, and B. L. Semler.** 2015. Divergent Requirement for a DNA Repair Enzyme during Enterovirus Infections. MBio **7:**e01931-01915.
112. **Maciejewski, S., W. Ullmer, and B. L. Semler.** 2018. VPg unlinkase/TDP2 in cardiovirus infected cells: Re-localization and proteolytic cleavage. Virology **516:**139-146.
113. **Mackenzie, K. J., P. Carroll, C. A. Martin, O. Murina, A. Fluteau, D. J. Simpson, N. Olova, H. Sutcliffe, J. K. Rainger, A. Leitch, R. T. Osborn, A. P. Wheeler, M. Nowotny, N. Gilbert, T. Chandra, M. A. M. Reijns, and A. P. Jackson.** 2017. cGAS surveillance of micronuclei links genome instability to innate immunity. Nature **548:**461-465.
114. **Makeyev, A. V., and S. A. Liebhaber.** 2002. The poly(C)-binding proteins: a multiplicity of functions and a search for mechanisms. RNA **8:**265-278.
115. **Mao, Y., S. D. Desai, C. Y. Ting, J. Hwang, and L. F. Liu.** 2001. 26 S proteasome-mediated degradation of topoisomerase II cleavable complexes. J Biol Chem **276:**40652-40658.
116. **Mason, P. W., S. V. Bezborodova, and T. M. Henry.** 2002. Identification and characterization of a cis-acting replication element (cre) adjacent to the internal ribosome entry site of foot-and-mouth disease virus. J Virol **76:**9686-9694.
117. **McKnight, K. L., and S. M. Lemon.** 1998. The rhinovirus type 14 genome contains an internally located RNA structure that is required for viral replication. RNA **4:**1569-1584.
118. **Merrill, M. K., E. Y. Dobrikova, and M. Gromeier.** 2006. Cell-type-specific repression of internal ribosome entry site activity by double-stranded RNA-binding protein 76. J Virol **80:**3147-3156.
119. **Messacar, K., M. J. Abzug, and S. R. Dominguez.** 2016. The Emergence of Enterovirus-D68. Microbiol Spectr **4**.
120. **Midgley, C. M., J. T. Watson, W. A. Nix, A. T. Curns, S. L. Rogers, B. A. Brown, C. Conover, S. R. Dominguez, D. R. Feikin, S. Gray, F. Hassan, S. Hoferka, M. A. Jackson, D. Johnson, E. Leshem, L. Miller, J. B. Nichols, A. C. Nyquist, E. Obringer, A. Patel, M. Patel, B. Rha, E. Schneider, J. E. Schuster, R. Selvarangan, J. F. Seward, G. Turabelidze, M. S. Oberste, M. A. Pallansch, and S. I. Gerber.** 2015. Severe respiratory illness associated with a nationwide outbreak of enterovirus D68 in the USA (2014): a descriptive epidemiological investigation. Lancet Respir Med **3:**879-887.
121. **Minor, D. M., and D. Proud.** 2017. Role of human rhinovirus in triggering human airway epithelial-mesenchymal transition. Respir Res **18:**110.
122. **Murray, K. E., and D. J. Barton.** 2003. Poliovirus CRE-dependent VPg uridylylation is required for positive-strand RNA synthesis but not for negative-strand RNA synthesis. J Virol **77:**4739-4750.
123. **Murray, K. E., A. W. Roberts, and D. J. Barton.** 2001. Poly(rC) binding proteins mediate poliovirus mRNA stability. RNA **7:**1126-1141.
124. **Neznanov, N., K. M. Chumakov, L. Neznanova, A. Almasan, A. K. Banerjee, and A. V. Gudkov.** 2005. Proteolytic cleavage of the p65-RelA subunit of NF-kappaB during poliovirus infection. J Biol Chem **280:**24153-24158.

125. **Nomoto, A., N. Kitamura, F. Golini, and E. Wimmer.** 1977. The 5'-terminal structures of poliovirion RNA and poliovirus mRNA differ only in the genome-linked protein VPg. Proc Natl Acad Sci U S A **74:**5345-5349.
126. **Nomoto, A., Y. F. Lee, and E. Wimmer.** 1976. The 5' end of poliovirus mRNA is not capped with m7G(5')ppp(5')Np. Proc Natl Acad Sci U S A **73:**375-380.
127. **Novak, J. E., and K. Kirkegaard.** 1994. Coupling between genome translation and replication in an RNA virus. Genes Dev **8:**1726-1737.
128. **Nugent, C. I., K. L. Johnson, P. Sarnow, and K. Kirkegaard.** 1999. Functional coupling between replication and packaging of poliovirus replicon RNA. J Virol **73:**427-435.
129. **Ogram, S. A., and J. B. Flanegan.** 2011. Non-template functions of viral RNA in picornavirus replication. Curr Opin Virol **1:**339-346.
130. **Ogram, S. A., A. Spear, N. Sharma, and J. B. Flanegan.** 2010. The 5'CL-PCBP RNP complex, 3' poly(A) tail and 2A(pro) are required for optimal translation of poliovirus RNA. Virology **397:**14-22.
131. **Park, N., P. Katikaneni, T. Skern, and K. E. Gustin.** 2008. Differential targeting of nuclear pore complex proteins in poliovirus-infected cells. J Virol **82:**1647-1655.
132. **Parsley, T. B., J. S. Towner, L. B. Blyn, E. Ehrenfeld, and B. L. Semler.** 1997. Poly (rC) binding protein 2 forms a ternary complex with the 5'-terminal sequences of poliovirus RNA and the viral 3CD proteinase. RNA **3:**1124-1134.
133. **Paul, A. V., J. Peters, J. Mugavero, J. Yin, J. H. van Boom, and E. Wimmer.** 2003. Biochemical and genetic studies of the VPg uridylylation reaction catalyzed by the RNA polymerase of poliovirus. J Virol **77:**891-904.
134. **Paul, A. V., J. H. van Boom, D. Filippov, and E. Wimmer.** 1998. Protein-primed RNA synthesis by purified poliovirus RNA polymerase. Nature **393:**280-284.
135. **Paul, A. V., and E. Wimmer.** 2015. Initiation of protein-primed picornavirus RNA synthesis. Virus Res **206:**12-26.
136. **Paul, A. V., J. Yin, J. Mugavero, E. Rieder, Y. Liu, and E. Wimmer.** 2003. A "slide-back" mechanism for the initiation of protein-primed RNA synthesis by the RNA polymerase of poliovirus. J Biol Chem **278:**43951-43960.
137. **Pei, H., J. S. Yordy, Q. Leng, Q. Zhao, D. K. Watson, and R. Li.** 2003. EAPII interacts with ETS1 and modulates its transcriptional function. Oncogene **22:**2699-2709.
138. **Perera, R., S. Daijogo, B. L. Walter, J. H. Nguyen, and B. L. Semler.** 2007. Cellular protein modification by poliovirus: the two faces of poly(rC)-binding protein. J Virol **81:**8919-8932.
139. **Pilipenko, E. V., E. G. Viktorova, S. T. Guest, V. I. Agol, and R. P. Roos.** 2001. Cell-specific proteins regulate viral RNA translation and virus-induced disease. EMBO J **20:**6899-6908.
140. **Pommier, Y., S. Y. Huang, R. Gao, B. B. Das, J. Murai, and C. Marchand.** 2014. Tyrosyl-DNA-phosphodiesterases (TDP1 and TDP2). DNA Repair (Amst) **19:**114-129.
141. **Porter, F. W., Y. A. Bochkov, A. J. Albee, C. Wiese, and A. C. Palmenberg.** 2006. A picornavirus protein interacts with Ran-GTPase and disrupts nucleocytoplasmic transport. Proc Natl Acad Sci U S A **103:**12417-12422.
142. **Porter, F. W., and A. C. Palmenberg.** 2009. Leader-induced phosphorylation of nucleoporins correlates with nuclear trafficking inhibition by cardioviruses. J Virol **83:**1941-1951.
143. **Pype, S., W. Declercq, A. Ibrahimi, C. Michiels, J. G. Van Rietschoten, N. Dewulf, M. de Boer, P. Vandenabeele, D. Huylebroeck, and J. E. Remacle.** 2000. TTRAP,

a novel protein that associates with CD40, tumor necrosis factor (TNF) receptor-75 and TNF receptor-associated factors (TRAFs), and that inhibits nuclear factor-kappa B activation. J Biol Chem **275:**18586-18593.

144. **Rajput, C., M. Han, J. K. Bentley, J. Lei, T. Ishikawa, Q. Wu, J. L. Hinde, A. P. Callear, T. L. Stillwell, W. T. Jackson, E. T. Martin, and M. B. Hershenson.** 2018. Enterovirus D68 infection induces IL-17-dependent neutrophilic airway inflammation and hyperresponsiveness. JCI Insight **3**.
145. **Rao, T., R. Gao, S. Takada, M. Al Abo, X. Chen, K. J. Walters, Y. Pommier, and H. Aihara.** 2016. Novel TDP2-ubiquitin interactions and their importance for the repair of topoisomerase II-mediated DNA damage. Nucleic Acids Res **44:**10201-10215.
146. **Reid, C. R., A. M. Airo, and T. C. Hobman.** 2015. The Virus-Host Interplay: Biogenesis of +RNA Replication Complexes. Viruses **7:**4385-4413.
147. **Ribeiro, C. J. A., J. Kankanala, K. Shi, K. Kurahashi, E. Kiselev, A. Ravji, Y. Pommier, H. Aihara, and Z. Wang.** 2018. New fluorescence-based high-throughput screening assay for small molecule inhibitors of tyrosyl-DNA phosphodiesterase 2 (TDP2). Eur J Pharm Sci **118:**67-79.
148. **Richards, O. C., T. D. Hey, and E. Ehrenfeld.** 1981. Two forms of VPg on poliovirus RNAs. J Virol **38:**863-871.
149. **Ricour, C., S. Delhaye, S. V. Hato, T. D. Olenyik, B. Michel, F. J. van Kuppeveld, K. E. Gustin, and T. Michiels.** 2009. Inhibition of mRNA export and dimerization of interferon regulatory factor 3 by Theiler's virus leader protein. J Gen Virol **90:**177-186.
150. **Rieder, E., A. V. Paul, D. W. Kim, J. H. van Boom, and E. Wimmer.** 2000. Genetic and biochemical studies of poliovirus cis-acting replication element cre in relation to VPg uridylylation. J Virol **74:**10371-10380.
151. **Roberts, P. J., and C. J. Der.** 2007. Targeting the Raf-MEK-ERK mitogen-activated protein kinase cascade for the treatment of cancer. Oncogene **26:**3291-3310.
152. **Roehl, H. H., T. B. Parsley, T. V. Ho, and B. L. Semler.** 1997. Processing of a cellular polypeptide by 3CD proteinase is required for poliovirus ribonucleoprotein complex formation. J Virol **71:**578-585.
153. **Roehl, H. H., and B. L. Semler.** 1995. Poliovirus infection enhances the formation of two ribonucleoprotein complexes at the 3' end of viral negative-strand RNA. J Virol **69:**2954-2961.
154. **Rozovics, J. M., R. Virgen-Slane, and B. L. Semler.** 2011. Engineered picornavirus VPg-RNA substrates: analysis of a tyrosyl-RNA phosphodiesterase activity. PLoS One **6:**e16559.
155. **Rubner, F. J., D. J. Jackson, M. D. Evans, R. E. Gangnon, C. J. Tisler, T. E. Pappas, J. E. Gern, and R. F. Lemanske, Jr.** 2017. Early life rhinovirus wheezing, allergic sensitization, and asthma risk at adolescence. J Allergy Clin Immunol **139:**501-507.
156. **Schellenberg, M. J., C. D. Appel, S. Adhikari, P. D. Robertson, D. A. Ramsden, and R. S. Williams.** 2012. Mechanism of repair of 5'-topoisomerase II-DNA adducts by mammalian tyrosyl-DNA phosphodiesterase 2. Nat Struct Mol Biol **19:**1363-1371.
157. **Schellenberg, M. J., J. A. Lieberman, A. Herrero-Ruiz, L. R. Butler, J. G. Williams, A. M. Munoz-Cabello, G. A. Mueller, R. E. London, F. Cortes-Ledesma, and R. S. Williams.** 2017. ZATT (ZNF451)-mediated resolution of topoisomerase 2 DNA-protein cross-links. Science **357:**1412-1416.
158. **Sean, P., J. H. Nguyen, and B. L. Semler.** 2008. The linker domain of poly(rC) binding protein 2 is a major determinant in poliovirus cap-independent translation. Virology **378:**243-253.

159. **Shaikhibrahim, Z., and N. Wernert.** 2012. ETS transcription factors and prostate cancer: the role of the family prototype ETS-1 (review). Int J Oncol **40:**1748-1754.
160. **Shariff, S., C. Shelfoon, N. S. Holden, S. L. Traves, S. Wiehler, C. Kooi, D. Proud, and R. Leigh.** 2017. Human Rhinovirus Infection of Epithelial Cells Modulates Airway Smooth Muscle Migration. Am J Respir Cell Mol Biol **56:**796-803.
161. **Sharma, N., S. A. Ogram, B. J. Morasco, A. Spear, N. M. Chapman, and J. B. Flanegan.** 2009. Functional role of the 5' terminal cloverleaf in Coxsackievirus RNA replication. Virology **393:**238-249.
162. **Shi, K., K. Kurahashi, R. Gao, S. E. Tsutakawa, J. A. Tainer, Y. Pommier, and H. Aihara.** 2012. Structural basis for recognition of 5'-phosphotyrosine adducts by Tdp2. Nat Struct Mol Biol **19:**1372-1377.
163. **Silvera, D., A. V. Gamarnik, and R. Andino.** 1999. The N-terminal K homology domain of the poly(rC)-binding protein is a major determinant for binding to the poliovirus 5'-untranslated region and acts as an inhibitor of viral translation. J Biol Chem **274:**38163-38170.
164. **Simcock, D. E., V. Kanabar, G. W. Clarke, B. J. O'Connor, T. H. Lee, and S. J. Hirst.** 2007. Proangiogenic activity in bronchoalveolar lavage fluid from patients with asthma. Am J Respir Crit Care Med **176:**146-153.
165. **Singanayagam, A., P. V. Joshi, P. Mallia, and S. L. Johnston.** 2012. Viruses exacerbating chronic pulmonary disease: the role of immune modulation. BMC Med **10:**27.
166. **Song, J., Y. Hu, H. Li, X. Huang, H. Zheng, J. Wang, X. Jiang, J. Li, Z. Yang, H. Fan, L. Guo, H. Shi, Z. He, F. Yang, X. Wang, S. Dong, Q. Li, and L. Liu.** 2018. miR-1303 regulates BBB permeability and promotes CNS lesions following CA16 infections by directly targeting MMP9. Emerg Microbes Infect **7:**155.
167. **Spitale, R. C., P. Crisalli, R. A. Flynn, E. A. Torre, E. T. Kool, and H. Y. Chang.** 2013. RNA SHAPE analysis in living cells. Nat Chem Biol **9:**18-20.
168. **Steil, B. P., and D. J. Barton.** 2008. Poliovirus cis-acting replication element-dependent VPg Uridylylation lowers the Km of the initiating nucleoside triphosphate for viral RNA replication. J Virol **82:**9400-9408.
169. **Sun, J., Y. Shi, and E. Yildirim.** 2019. The Nuclear Pore Complex in Cell Type-Specific Chromatin Structure and Gene Regulation. Trends Genet **35:**579-588.
170. **Sun, L., J. Wu, F. Du, X. Chen, and Z. J. Chen.** 2013. Cyclic GMP-AMP synthase is a cytosolic DNA sensor that activates the type I interferon pathway. Science **339:**786-791.
171. **Sun, Y., Y. Guo, and Z. Lou.** 2014. Formation and working mechanism of the picornavirus VPg uridylylation complex. Curr Opin Virol **9:**24-30.
172. **Suresh, S., S. Forgie, and J. Robinson.** 2018. Non-polio Enterovirus detection with acute flaccid paralysis: A systematic review. J Med Virol **90:**3-7.
173. **Sweeney, T. R., I. S. Abaeva, T. V. Pestova, and C. U. Hellen.** 2014. The mechanism of translation initiation on Type 1 picornavirus IRESs. EMBO J **33:**76-92.
174. **Tijsma, A., H. J. Thibaut, D. Franco, K. Dallmeier, and J. Neyts.** 2016. Hydantoin: The mechanism of its in vitro anti-enterovirus activity revisited. Antiviral Res **133:**106-109.
175. **Toyoda, H., D. Franco, K. Fujita, A. V. Paul, and E. Wimmer.** 2007. Replication of poliovirus requires binding of the poly(rC) binding protein to the cloverleaf as well as to the adjacent C-rich spacer sequence between the cloverleaf and the internal ribosomal entry site. J Virol **81:**10017-10028.

176. **Toyoda, H., N. Koide, M. Kamiyama, K. Tobita, K. Mizumoto, and N. Imura.** 1994. Host factors required for internal initiation of translation on poliovirus RNA. Arch Virol **138:**1-15.
177. **Ullmer, W., and B. L. Semler.** 2018. Direct and Indirect Effects on Viral Translation and RNA Replication Are Required for AUF1 Restriction of Enterovirus Infections in Human Cells. MBio **9**.
178. **Ullmer, W., and B. L. Semler.** 2016. Diverse Strategies Used by Picornaviruses to Escape Host RNA Decay Pathways. Viruses **8**.
179. **Valverde, R., L. Edwards, and L. Regan.** 2008. Structure and function of KH domains. FEBS J **275:**2712-2726.
180. **van der Schaar, H. M., L. van der Linden, K. H. Lanke, J. R. Strating, G. Purstinger, E. de Vries, C. A. de Haan, J. Neyts, and F. J. van Kuppeveld.** 2012. Coxsackievirus mutants that can bypass host factor PI4KIIIbeta and the need for high levels of PI4P lipids for replication. Cell Res **22:**1576-1592.
181. **Vance, L. M., N. Moscufo, M. Chow, and B. A. Heinz.** 1997. Poliovirus 2C region functions during encapsidation of viral RNA. J Virol **71:**8759-8765.
182. **Ventoso, I., S. E. MacMillan, J. W. Hershey, and L. Carrasco.** 1998. Poliovirus 2A proteinase cleaves directly the eIF-4G subunit of eIF-4F complex. FEBS Lett **435:**79-83.
183. **Viktorova, E. G., J. A. Nchoutmboube, L. A. Ford-Siltz, E. Iverson, and G. A. Belov.** 2018. Phospholipid synthesis fueled by lipid droplets drives the structural development of poliovirus replication organelles. PLoS Pathog **14:**e1007280.
184. **Vilotti, S., M. Codrich, M. Dal Ferro, M. Pinto, I. Ferrer, L. Collavin, S. Gustincich, and S. Zucchelli.** 2012. Parkinson's disease DJ-1 L166P alters rRNA biogenesis by exclusion of TTRAP from the nucleolus and sequestration into cytoplasmic aggregates via TRAF6. PLoS One **7:**e35051.
185. **Virgen-Slane, R., J. M. Rozovics, K. D. Fitzgerald, T. Ngo, W. Chou, G. J. van der Heden van Noort, D. V. Filippov, P. D. Gershon, and B. L. Semler.** 2012. An RNA virus hijacks an incognito function of a DNA repair enzyme. Proc Natl Acad Sci U S A **109:**14634-14639.
186. **Vogt, D. A., and R. Andino.** 2010. An RNA element at the 5'-end of the poliovirus genome functions as a general promoter for RNA synthesis. PLoS Pathog **6:**e1000936.
187. **Walter, B. L., J. H. Nguyen, E. Ehrenfeld, and B. L. Semler.** 1999. Differential utilization of poly(rC) binding protein 2 in translation directed by picornavirus IRES elements. RNA **5:**1570-1585.
188. **Walter, B. L., T. B. Parsley, E. Ehrenfeld, and B. L. Semler.** 2002. Distinct poly(rC) binding protein KH domain determinants for poliovirus translation initiation and viral RNA replication. J Virol **76:**12008-12022.
189. **Walton, R. W., M. C. Brown, M. T. Sacco, and M. Gromeier.** 2018. Engineered Oncolytic Poliovirus PVSRIPO Subverts MDA5-Dependent Innate Immune Responses in Cancer Cells. J Virol **92**.
190. **Wang, S. Z., W. Ma, R. T. Yan, and W. Mao.** 2010. Generating retinal neurons by reprogramming retinal pigment epithelial cells. Expert Opin Biol Ther **10:**1227-1239.
191. **Wang, T., B. Yu, L. Lin, X. Zhai, Y. Han, Y. Qin, Z. Guo, S. Wu, X. Zhong, Y. Wang, L. Tong, F. Zhang, X. Si, W. Zhao, and Z. Zhong.** 2012. A functional nuclear localization sequence in the VP1 capsid protein of coxsackievirus B3. Virology **433:**513-521.

192. **Wang, Y., S. Zhao, Y. Chen, T. Wang, C. Dong, X. Wo, J. Zhang, Y. Dong, W. Xu, X. Feng, C. Qu, Z. Zhong, and W. Zhao.** 2019. The Capsid Protein VP1 of Coxsackievirus B Induces Cell Cycle Arrest by Up-Regulating Heat Shock Protein 70. Front Microbiol **10:**1633.
193. **Watters, K., B. Inankur, J. C. Gardiner, J. Warrick, N. M. Sherer, J. Yin, and A. C. Palmenberg.** 2017. Differential Disruption of Nucleocytoplasmic Trafficking Pathways by Rhinovirus 2A Proteases. J Virol **91**.
194. **Weidman, M. K., R. Sharma, S. Raychaudhuri, P. Kundu, W. Tsai, and A. Dasgupta.** 2003. The interaction of cytoplasmic RNA viruses with the nucleus. Virus Res **95:**75-85.
195. **Whitton, J. L., C. T. Cornell, and R. Feuer.** 2005. Host and virus determinants of picornavirus pathogenesis and tropism. Nat Rev Microbiol **3:**765-776.
196. **Wieczfinska, J., and R. Pawliczak.** 2017. Thymic stromal lymphopoietin and apocynin alter the expression of airway remodeling factors in human rhinovirus-infected cells. Immunobiology **222:**892-899.
197. **Wilkinson, K. A., E. J. Merino, and K. M. Weeks.** 2006. Selective 2'-hydroxyl acylation analyzed by primer extension (SHAPE): quantitative RNA structure analysis at single nucleotide resolution. Nat Protoc **1:**1610-1616.
198. **Williams, S. M., P. Schulz, T. L. Rosenberry, R. J. Caselli, and M. R. Sierks.** 2017. Blood-Based Oligomeric and Other Protein Variant Biomarkers to Facilitate Pre-Symptomatic Diagnosis and Staging of Alzheimer's Disease. J Alzheimers Dis **58:**23-35.
199. **Xin, L., X. Ma, Z. Xiao, H. Yao, and Z. Liu.** 2015. Coxsackievirus B3 induces autophagy in HeLa cells via the AMPK/MEK/ERK and Ras/Raf/MEK/ERK signaling pathways. Infect Genet Evol **36:**46-54.
200. **Xu, G. L., Y. K. Pan, B. Y. Wang, L. Huang, L. Tian, J. L. Xue, J. Z. Chen, and W. Jia.** 2008. TTRAP is a novel PML nuclear bodies-associated protein. Biochem Biophys Res Commun **375:**395-398.
201. **Yang, X., J. Xie, L. Jia, N. Liu, Y. Liang, F. Wu, B. Liang, Y. Li, J. Wang, C. Sheng, H. Li, H. Liu, Q. Ma, C. Yang, X. Du, S. Qiu, and H. Song.** 2017. Analysis of miRNAs Involved in Mouse Brain Damage upon Enterovirus 71 Infection. Front Cell Infect Microbiol **7:**133.
202. **Ye, C. J., Z. Sharpe, S. Alemara, S. Mackenzie, G. Liu, B. Abdallah, S. Horne, S. Regan, and H. H. Heng.** 2019. Micronuclei and Genome Chaos: Changing the System Inheritance. Genes (Basel) **10**.
203. **Yu, Y., T. R. Sweeney, P. Kafasla, R. J. Jackson, T. V. Pestova, and C. U. Hellen.** 2011. The mechanism of translation initiation on Aichivirus RNA mediated by a novel type of picornavirus IRES. EMBO J **30:**4423-4436.
204. **Zarnack, K., J. Konig, M. Tajnik, I. Martincorena, S. Eustermann, I. Stevant, A. Reyes, S. Anders, N. M. Luscombe, and J. Ule.** 2013. Direct competition between hnRNP C and U2AF65 protects the transcriptome from the exonization of Alu elements. Cell **152:**453-466.
205. **Zhang, A., Y. L. Lyu, C. P. Lin, N. Zhou, A. M. Azarova, L. M. Wood, and L. F. Liu.** 2006. A protease pathway for the repair of topoisomerase II-DNA covalent complexes. J Biol Chem **281:**35997-36003.
206. **Zhang, B., S. Seitz, Y. Kusov, R. Zell, and V. Gauss-Muller.** 2007. RNA interaction and cleavage of poly(C)-binding protein 2 by hepatitis A virus protease. Biochem Biophys Res Commun **364:**725-730.

207. **Zhang, G., J. Wang, G. Yao, and B. Shi.** 2017. Downregulation of CCL2 induced by the upregulation of microRNA-206 is associated with the severity of HEV71 encephalitis. Mol Med Rep **16:**4620-4626.
208. **Zhu, Z., G. Wang, F. Yang, W. Cao, R. Mao, X. Du, X. Zhang, C. Li, D. Li, K. Zhang, H. Shu, X. Liu, and H. Zheng.** 2016. Foot-and-Mouth Disease Virus Viroporin 2B Antagonizes RIG-I-Mediated Antiviral Effects by Inhibition of Its Protein Expression. J Virol **90:**11106-11121.
209. **Zucchelli, S., S. Vilotti, R. Calligaris, Z. S. Lavina, M. Biagioli, R. Foti, L. De Maso, M. Pinto, M. Gorza, E. Speretta, C. Casseler, G. Tell, G. Del Sal, and S. Gustincich.** 2009. Aggresome-forming TTRAP mediates pro-apoptotic properties of Parkinson's disease-associated DJ-1 missense mutations. Cell Death Differ **16:**428-438.